

# Trends in Net Delta Outflow and Other Hydrological Components in the Bay-Delta Watershed

*Prepared for:*

**State Water Contractors  
1121 L. Street, Suite 1050, Sacramento, CA 95814**

**and**

**San Luis & Delta-Mendota Water Authority  
842 6th Street, Los Baños, CA, 93635**

*Technical Representative:*

**Paul Hutton, Ph.D., P.E.  
Metropolitan Water District of Southern California  
1121 L Street, Suite 900, Sacramento CA 95814**

*Prepared by:*



**John S. Rath and Sujoy B. Roy  
Tetra Tech Inc.  
3746 Mt. Diablo Blvd., Suite 300  
Lafayette, CA 94549  
USA**

**March 21, 2016**



# TABLE OF CONTENTS

---

<b>1</b>	<b>Introduction</b> .....	<b>1-1</b>
<b>2</b>	<b>Data</b> .....	<b>2-1</b>
<b>3</b>	<b>Methods</b> .....	<b>3-1</b>
3.1	Monotonic trends: Mann-Kendall (MK) test and Sen’s slope .....	3-1
3.2	Multiple comparisons for LOD data: Kruskal-Wallis test and multiple comparisons ..	3-2
3.3	Seasonal Trend Decomposition Based on Loess (STL) .....	3-2
3.4	Flexible nonparametric mixed models: Generalized additive mixed models .....	3-3
<b>4</b>	<b>Evaluation of Delta Outflows and Inflows</b> .....	<b>4-5</b>
4.1	Historical Data .....	4-5
4.2	STL Decompositions .....	4-7
4.3	LOD Scenario Data.....	4-7
<b>5</b>	<b>Evaluation of Sacramento Valley Inflows to the Delta</b> .....	<b>5-1</b>
5.1	Historical Data .....	5-1
5.2	LOD Scenario Data.....	5-4
<b>6</b>	<b>Discussion</b> .....	<b>6-1</b>
<b>7</b>	<b>References</b> .....	<b>7-1</b>

This page intentionally left blank.

# LIST OF FIGURES

---

Figure 2-1	Schematic of inflows into and out of the Delta.....	2-4
Figure 4-1	Time series plot of net Delta outflow (DAYFLOW) with 10 year moving average (red) .....	4-9
Figure 4-2	Time series plot of net Delta outflow (DICU model-based) with 10 year moving average (red) .....	4-10
Figure 4-3	Time series plot of Delta exports (CVP + SWP + NBAQ + CCWD) with 10 year moving average (red).....	4-11
Figure 4-4	Time series plot of DAYFLOW estimates of Delta net channel depletion with 10 year moving average (red). .....	4-12
Figure 4-5	Time series plot of DICU estimates of Delta net channel depletions with 10 year moving average (red). .....	4-13
Figure 4-6	Time series plot of Sacramento Valley inflow to Delta (SAC + YOLO) with 10 year moving average (red). .....	4-14
Figure 4-7	Time series plot of Other Delta inflow (SJR + ESS) with 10 year moving average (red). .....	4-15
Figure 4-8	Time series plot of X2 position with 10 year moving average (red).....	4-16
Figure 4-9	Mann-Kendall trend evaluation for net Delta outflow (DAYFLOW) .....	4-17
Figure 4-10	Mann-Kendall trend evaluation for net Delta outflow (DICU model-based).....	4-18
Figure 4-11	Mann-Kendall trend evaluation of Delta exports (CVP + SWP + NBAQ + CCWD). .....	4-19
Figure 4-12	Mann-Kendall trend evaluation for Sacramento Valley inflow to Delta (SAC + YOLO) .....	4-20
Figure 4-13	Mann-Kendall trend evaluation for Other Delta inflow (SJR + ESS) .....	4-21
Figure 4-14	Mann-Kendall trend evaluation for X2 .....	4-22
Figure 4-15	MK trend summary for net Delta outflow (DAYFLOW).....	4-23
Figure 4-16	MK trend summary for net Delta outflow (DICU-model based estimate of net channel depletion).....	4-24
Figure 4-17	MK trend summary for Sacramento Valley inflow to Delta (SAC + YOLO). ....	4-25
Figure 4-18	MK trend summary for Other Delta inflow (SJR + ESS). .....	4-26
Figure 4-19	MK test results for X2.....	4-27
Figure 4-20	Delta water balance accounting only for total inflow. Solid black line is the 1:1 line. Dashed gray line is linear best fit, with $r^2$ value shown on upper left.....	4-28
Figure 4-21	Delta water balance accounting only for total inflow and major exports. Solid black line is the 1:1 line. Dashed gray line is linear best fit, with $r^2$ value shown on upper left. ....	4-29
Figure 4-22	Difference between DICU model and DAYFLOW net channel depletion estimates over time, and estimates of trend. ....	4-30
Figure 4-23	STL decomposition of net Delta outflow data (all units cfs), with a common y-axis for all components. ....	4-31

Figure 4-24	STL decomposition of net Delta outflow data (all units cfs). The gray bars on the right side of each panel are all the size of the smallest y-axis scale. ....	4-32
Figure 4-25	STL decomposition of net Delta outflow data (all units cfs) with a common y-axis for all components. ....	4-33
Figure 4-26	STL decomposition of net Delta outflow data using DICU model-based estimates (all units cfs). The gray bars on the right side of each panel are all the size of the smallest y-axis scale. ....	4-34
Figure 4-27	Comparison of historical and LOD scenario Net Delta Outflow. Colored bars indicate historical value and water year type. The median and 10th-90th percentiles of values from the corresponding month and water year type from the chronologically closest LOD scenario are indicated by points and error-bars.....	4-35
Figure 4-28	Comparison of historical and LOD scenario Net Delta Outflow (continued). Colored bars indicate historical value and water year type. The median and 10th-90th percentiles of values from the corresponding month and water year type from the chronologically closest LOD scenario are indicated by points and error-bars. ....	4-36
Figure 4-29	Multiple Kruskal-Wallis procedure for net Delta outflow. Boxplots filled with the same color indicate samples that were not found to differ significantly in a location by a multiple comparisons Kruskal-Wallis procedure. ....	4-37
Figure 4-30	Multiple Kruskal-Wallis procedure for Sacramento Valley inflow to Delta (SAC + YOLO). Boxplots filled with the same color indicate samples that were not found to differ significantly in a location by a multiple comparisons Kruskal-Wallis procedure. ....	4-38
Figure 4-31	Multiple Kruskal-Wallis procedure for Other Delta inflow (SJR + ESS). Boxplots filled with the same color indicate samples that were not found to differ significantly in a location by a multiple comparisons Kruskal-Wallis procedure.....	4-39
Figure 5-1	Four River inflow time series plots with 10 year moving average (red).....	5-5
Figure 5-2	Four River Index time series plots with 10 year moving average (red) .....	5-6
Figure 5-3	Eight station precipitation index time series plots with 10 year moving average (red).....	5-7
Figure 5-4	Minor Rim inflows time series plots with 10 year moving average (red).....	5-8
Figure 5-5	Sacramento River gain from groundwater time series plots with 10 year moving average (red).....	5-9
Figure 5-6	Sacramento Valley surface water diversions time series plots with 10 year moving average (red).....	5-10
Figure 5-7	Sacramento Valley groundwater pumping time series plots with 10 year moving average (red).....	5-11
Figure 5-8	Sacramento Valley floor precipitation time series plots with 10 year moving average (red) .....	5-12
Figure 5-9	Mann-Kendall trend evaluation for Four River Inflow.....	5-13
Figure 5-10	Mann-Kendall trend evaluation for Minor Rim inflows.....	5-14
Figure 5-11	MK test results for Four River inflow.....	5-15
Figure 5-12	MK test results for Four River Index.....	5-16
Figure 5-13	MK test results for Minor Rim inflows. ....	5-17

Figure 5-14	Changes in unexplained Sacramento Valley accretions/depletions considering only Four River inflow. Solid black line is the 1:1 line. Dashed gray line is linear best fit, with $r^2$ value shown on upper left. ....	5-18
Figure 5-15	Changes in unexplained Sacramento Valley accretions/depletions considering Four River inflows, Minor Rim inflows, and Trinity imports. Solid black line is the 1:1 line. Dashed gray line is linear best fit, with $r^2$ value shown on upper left. ....	5-19
Figure 5-16	Changes in unexplained Sacramento Valley accretions/depletions considering Four River inflows; Minor Rim inflows; valley floor precipitation runoff (C2VSIM input, runoff factor 0.20); gain from groundwater (C2VSIM output); runoff from groundwater pumping (C2VSIM output, runoff factor 0.10); and diversions and related runoff (C2VSIM output, runoff factor 0.20). Solid black line is the 1:1 line. Dashed gray line is linear best fit, with $r^2$ value shown on upper left. ....	5-20
Figure 5-17	Optimized runoff factors in Sacramento Valley accretion/depletion calculations. Points, thick gray lines, and thin gray lines represent posterior means, 25–75% intervals, and 10–90% intervals, respectively. ....	5-21
Figure 5-18	Changes in unexplained Sacramento Valley accretions/depletions considering Four River inflows; Minor Rim inflows; valley floor precipitation runoff (C2VSIM input, average runoff factor 0.35); gain from groundwater (C2VSIM output); runoff from groundwater pumping (C2VSIM output, runoff factor 0.10); and diversions and related runoff (C2VSIM output, runoff factor 0.36). Solid black line is the 1:1 line. Dashed gray line is linear best fit, with $r^2$ value shown on upper left. ....	5-22
Figure 5-19	Runoff flow volumes (constant factors) .....	5-23
Figure 5-20	Runoff flow volumes (optimized factors, precipitation factor varies by month) .	5-24
Figure 5-21	Time series plot of unexplained Sacramento Valley accretions/depletions considering Four River inflows; Minor Rim inflows; Trinity imports; valley floor precipitation runoff (C2VSIM input, runoff factor 0.35); gain from groundwater (C2VSIM output); runoff from groundwater pumping (C2VSIM output, runoff factor 0.10); and diversions and related runoff (C2VSIM output, runoff factor 0.36). The blue line illustrates a MK test of trend of the underlying data. ....	5-25
Figure 5-22	Trends in timing of cumulative wet season runoff (based on four-river index).	5-26
Figure 5-23	Nonparametric GAMM model of unimpaired flow arrival times. ....	5-27
Figure 5-24	Trends in timing of Four River inflow .....	5-28
Figure 5-25	Comparison of historical and LOD scenario Sacramento Valley inflow to Delta. Colored bars indicate historical value and water year type. The median and 10th-90th percentiles of values from the corresponding month and water year type from the chronologically closest LOD scenario are indicated by points and error-bars. ....	5-29
Figure 5-26	Comparison of historical and LOD scenario Sacramento Valley inflow to Delta (continued). Colored bars indicate historical value and water year type. The median and 10th-90th percentiles of values from the corresponding month and water year type from the chronologically closest LOD scenario are indicated by points and error-bars. ....	5-30
Figure 5-27	Sac Valley LOD flows by month and annually. ....	5-31
Figure 5-28	Multiple Kruskal-Wallis procedure for Four River Inflow. Boxplots filled with the same color indicate samples that were not found to differ significantly in location by a multiple comparisons Kruskal-Wallis procedure. ....	5-32

This page intentionally left blank.

# LIST OF TABLES

---

Table 1-1      Analysis methods from recent studies related to hydrological trends and change. Authors using the Mann-Kendall test of trend generally also compute the magnitude of the trend with the closely related Sen’s slope estimator (Sen, 1968). .....1-4

Table 2-1      Summary of Data (All data used are monthly averages over 1922-2009).....2-3

This page intentionally left blank.

# 1 INTRODUCTION

---

The Sacramento-San Joaquin River Delta watershed is a vital part of California's water supply and its hydrology has been the focus of measurement and study for more than a century. Stream flows and in-basin precipitation are subject to natural variability on which are overlaid multiple anthropogenic changes occurring through time, such as levee construction and channelization, storage reservoir construction, basin imports and exports, and land use change. The ambitious goal of this work is to characterize *how* and *why* freshwater inflow from the Sacramento-San Joaquin River Delta to San Francisco Bay (i.e., net Delta outflow) has changed over the past nine decades as a result of these anthropogenic and natural changes.

Water year 1922 was selected as the starting point for this work because of the availability of robust streamflow data sets that have been developed by the Department of Water Resources (DWR) for the Delta and the Bay-Delta watershed (Brush et al., 2013). Although this period of study reflects extensive change throughout the watershed – particularly construction of the State Water Project (SWP) and the Central Valley Project (CVP) – it is important to recognize that the starting point is not reflective of natural conditions as various modifications to the system had already occurred by the 1920s (Fox et al., 2015). As stated above, the goal of this analysis is to evaluate *how* and *why* Delta outflow has changed over the study period. To evaluate the *why* question, this work evaluates changes in upstream flows as well as Delta outflow. These changes are evaluated both on an annual basis as well as on a monthly basis. This work also evaluates changes in Bay-Delta salinity because of its close correspondence to Delta outflow (Hutton et al., 2015).

While some of the watershed changes over the study period have been dramatic, such as the development of major dams and conversion of extensive natural lands for agriculture and urban uses, trends in individual streamflows may nonetheless be hard to discern because of the large seasonal and inter-annual variability in precipitation in the watershed. Some of the underlying drivers of precipitation, such as sea surface temperatures, vary on decadal time-scales (Cayan et al., 1998), thus masking the streamflow trends due to watershed changes over shorter time horizons.

The characteristics of flows in the Bay-Delta watershed have been explored in previous studies. Fox et al. (1990) showed that observed flows over the period spanning water years (WYs) 1922-1986 did not show a decline despite the increase in Delta withdrawals. They attributed this finding to a variety of factors, including increasing rainfall in the upper watershed, changes in land use, water imports from other basins, and redistribution of groundwater. They observed changes on a seasonal basis with downward trends in April and May and upward trends from July to November. Knowles (2002) evaluated the effect of management and natural changes on variability in Delta outflows using data from WY 1967–1987. He reported that the effects of natural variability on flow and salinity in San Francisco Bay were much greater than the effects related to reservoir management. Dettinger and Cayan (2003) explored flow changes in multiple Sierra Nevada rivers using unimpaired flow

data from 1906–1992. These data synthetically remove the effects of reservoir storages and diversions and thus do not represent observed conditions. The authors noted changes in the hydrograph characteristics of different rivers and their individual contributions to Delta outflow. Although they found that about two-thirds of the flow variability was shared among the different river basins, the remaining variability contributed differently to flows in different seasons. Because their work did not use actual flows for analysis, time trends were not reported. Enright and Culberson (2009) explored changes in flows in the western Delta using data from 1929–2006, and compared these changes with salinity behavior at various stations. They found, in a manner similar to Knowles (2002), that the effect of natural variability was much greater than that of the water storage projects. They also found a seasonal pattern in flows similar to Fox et al. (1990) with downward trends in February through June and upward trends in July through September. Enright and Culberson (2009) explored flow patterns using non-monotonic techniques and related these to large-scale oceanic oscillations in temperature (Pacific Decadal Oscillation, PDO). Although a simple correlation between flow and PDO was not found, they observed some correspondence between these two variables on a decadal scale. Fox et al. (2015) compared computed “natural” Delta outflows with computed current level outflows, assuming a contemporary climate sequence for both scenarios, and found that long-term annual flows were similar under both scenarios. This counter-intuitive finding was explained by the occurrence of higher evapotranspirative loss in the natural system relative to the contemporary system, with this loss being of similar magnitude to the various urban and agricultural uses of today.

Long-term changes in hydrological variables are of general interest to water resources management, particularly related to the effects of anthropogenic changes to river basins as well as effects related to climatic change that has already occurred over the preceding decades. We performed a survey of recent peer-reviewed studies of hydrological trends and change from around the world to identify appropriate analytical methods. Table 1-1 provides an overview of the studies, their objectives, and the analytical tools used. The Mann-Kendall (MK) (Kendall, 1938; Mann, 1945) test is by far the most common approach among the surveyed studies to statistically test the presence of monotonic trends in discharge data. Other forms of linear regression, such as ordinary least squares or quantile regression are also occasionally used. While linear, monotonic trends are conceptually and computationally expedient, they may only approximate (and sometimes approximate poorly) the way hydrological variables are changing in reality. Several studies examine nonlinear changes, e.g., in relation to multi-decadal climate fluctuations. Statistical tools used for quantifying nonlinear changes used in these studies are smoothing methods like LOESS (from LOcal regression) including seasonal trend decomposition with LOESS (STL) or transformation of flow and climatological variables to the frequency domain. Other approaches beyond trends of monthly or annual averages include comparison of distinct periods with two-sample tests (e.g., Mann-Whitney/Wilcoxon Rank Sum, or WRS test) or examination of extremes such as flood discharges or droughts.

In this work we present an analysis of trends in streamflows across key locations in the Bay-Delta watershed and the calculated freshwater outflow from the Delta to San Francisco Bay. The analysis methods are informed by the review above and help develop an understanding of the changes that have occurred in the last nine decades. Besides the observed streamflow data, this work also utilizes the results of a parallel surface water-groundwater modeling effort using the California Central Valley Surface Water Simulation Model (C2VSIM) (Brush et al., 2013). Brush et al. (2013) modeled flow assuming a historical sequence of development. In the present work, estimates of groundwater pumping and surface water/groundwater

exchange from Brush et al. (2013) were used to compute water balances in the Central Valley. In addition, the C2VSIM modeling framework was utilized for a set of fixed development scenarios by fixing the landscape and regulatory conditions to specific years in the past, and allowing for an 88-year hydrology from WY 1922-2009 to drive the model (MWH, 2015). The scenario modeling provided estimates of the ranges of flows that would have occurred if various historical development conditions prevailed, and could be compared to observed flows over time.

The remainder of this report is organized as follows. Chapter 2 provides an overview of the data used in the analysis, including the modeled estimates. Chapter 3 describes the statistical methods used for detecting changes in the data. Chapter 4 applies these statistical methods to an evaluation of Delta outflows and inflows. Chapter 5 looks upstream and applies the same methodology to flows upstream, i.e., the flows that enter the Sacramento Valley. In both Chapter 4 and 5, trends in the observed data are compared to patterns that are observed in the modeled values. Chapter 6 presents a discussion of these results.

**Table 1-1**  
**Analysis methods from recent studies related to hydrological trends and change.**  
**Authors using the Mann-Kendall test of trend generally also compute the magnitude of the trend**  
**with the closely related Sen's slope estimator (Sen, 1968).**

Study Author(s)	Study Region	Study Focus	Methods Used
<b>Abghari et al. (2013)</b>	Western Iran	Monthly and annual trend analysis; relationship between precipitation and discharge; 1970–2009	Spearman's $\rho$ , Kendall's $\tau$ , Mann-Kendall tests.
<b>Arnell (2011)</b>	United Kingdom	Hydrological response to climate forcing	Climate and hydrological modeling
<b>Bawden et al. (2014)</b>	Athabasca River region, AB/SK, Canada	Trends and variability of twenty hydrological variables, 1966–2010	Mann-Kendall trend test, Walker's test, Regime shift test
<b>Boé and Habets (2014)</b>	France	Multidecadal variations in climate and streamflow	Numerical modeling, low-pass filtering
<b>Chen and Grasby (2009)</b>	—	Ability to detect trends in presence of century scale climate fluctuations; statistical simulations	Mann-Kendall test, generation of synthetic data
<b>Chen et al. (2014)</b>	Yangtze River, China	Annual trends of flows, temperature, and precipitation in relationship with rapid human development; 1955–2011	Mann-Kendall, Rank-sum, correlation
<b>Déry et al. (2012)</b>	Fraser River Basin, BC, Canada	Trends and variability of annual streamflow, 1911–2010	Mann-Kendall test
<b>Dettinger and Cayan (2003)</b>	California Central Valley	Covariability of Sierra Nevada streamflow with SF Bay salinity	Extended empirical orthogonal functions
<b>Enright and Culberson (2009)</b>	San Francisco Bay-Delta	Trends in salinity, outflow, and precipitation	Kendall's $\tau$ , STL
<b>Fox et al. (1990)</b>	San Francisco Bay-Delta	Trends in Delta outflow and precipitation; 1921–1986	Least squares regression, LOESS, Mann-Kendall
<b>Gudmundsson et al. (2011)</b>	Europe	Low-frequency variation in European catchments	STL, correlation analysis, spatial analysis
<b>Hannaford (2015)</b>	United Kingdom	Nationwide trends and changes in extremes, in particular their relation to climate change; variable record length	Mann-Kendall test
<b>Hannaford et al. (2013)</b>	Europe	Trends and their detectability in presence of multi-decadal climate variations; 1932–2004	LOESS, Mann-Kendall
<b>He et al. (2013)</b>	Yellow River, China	Streamflow trends; comparison of natural and observed/impaired flows; 1956–2007	Linear regression, Mann-Kendall, wavelet transform
<b>Jiang et al. (2007)</b>	Yangtze River Basin, China	Trends in precipitation amounts and frequency, streamflow averages,	Linear regression, Mann-Kendall,

Study Author(s)	Study Region	Study Focus	Methods Used
		flood discharges; 1961–2000	spatial interpolation
<b>Karlsson et al. (2014)</b>	Skjern River, Denmark	Reconstruction of streamflow from temperature and precipitation; hydrological trends; comparison with numerical model; 1875–2008	Mann-Kendall test, numerical modeling, and threshold methods
<b>Kelly and Gore (2008)</b>	Florida	Trends in relation to water withdrawal legislation and large scale climate fluctuations; records $\geq$ 60 years	Kendall's $\tau$ , Mann-Whitney
<b>Knowles (2002)</b>	San Francisco Estuary	Relationship between salinity, natural flows, and management operations	Empirical orthogonal functions, numerical modelling
<b>Lorenzo-Lacruz et al. (2012)</b>	Iberian Peninsula	Trend analysis of monthly discharge data for natural and regulated flow regimes; 1945–2005	Impoundment ratio, Mann-Kendall tests
<b>Massei and Fournier (2012)</b>	Seine River, France	Comparison of hydrological variability with large scale climate fluctuations, 1950–2008	Hilbert-Huang transform
<b>Pal et al. (2012)</b>	Bhakra Reservoir, India	Prediction of reservoir inflows from meteorological variables	Linear regression, principal components analysis, partial least squares regression
<b>Shamsudduha et al. (2009)</b>	Ganges-Brahmaputra-Meghna Delta	Trends in groundwater levels	STL, linear regression
<b>Sharif et al. (2013)</b>	Upper Indus Basin	Streamflow trends and inferences about hard-to-observe upstream changes; 1960–1998	Mann-Kendall, spring onset date, center of volume date
<b>Viviroli et al. (2012)</b>	Switzerland	Potential for misattribution of trends from pooling streamflow records	Quantile regression
<b>Zhang et al. (2011)</b>	Huai River Basin, China	Monthly/seasonal/annual trends, 1956–2000	Mann-Kendall test

This page intentionally left blank.

## 2 DATA

---

The data used for this analysis were drawn from California state and federal data sources, and included secondary sources where raw data had been compiled and cleaned for related studies. The California Department of Water Resources (DWR) maintains a digital, publicly accessible database— California Data Exchange Center (CDEC), accessible at <http://cdec.water.ca.gov>—that was the source of raw data on hydrological variables, including many of the key flows in this analysis. The U.S. Geological Survey maintains a network of stream gauges in the Bay-Delta watershed that were a source of useful information (<http://waterdata.usgs.gov/ca/nwis/nwis>). Inflows to and outflows from the Delta were obtained from DWR's DAYFLOW program (<http://www.water.ca.gov/dayflow/>), which provides a daily water budget of the Delta and a tidally averaged estimate of Delta outflow. We also draw upon some flow data used as boundary conditions in a historical run of the California Central Valley Groundwater-Surface Water Simulation Model (C2VSIM) (Brush et al. 2013). The C2VSIM boundary inflow data come primarily from data collected and published by the United States Geological Survey (USGS). This study also utilized data sets developed by DWR for C2VSIM relating to simulated groundwater pumping for irrigation and municipal use and historical surface water diversions. We used the historical C2VSIM model results, which represents the study period with changing land-use, operational and regulatory conditions, to provide data for groundwater-surface water exchange in the Sacramento Valley. All of the time series data used in the analysis were averaged over a monthly time scale.

For interpreting results, this study also makes use of data from “level of development” (LOD) modeling efforts performed by MWH (2015) utilizing the C2VSIM model. That study applied the historical WY 1922–2009 climate signal (precipitation and temperature time series) to seven scenarios of land use, water supply contracts, and regulatory requirements representative of conditions in 1900, 1920, 1940, 1960, 1980, 2000, and 2010. In contrast with the historical C2VSIM simulation identified above, where watershed and regulatory conditions are changing over the course of the simulation, the LOD scenarios assume these conditions to be fixed for the entire period of simulation. The LOD scenarios thus provide the range of hypothetical streamflows that would result for the same nine-decade long climate signal.

The main hydrological (non-tidal) components that ultimately determine the net Delta outflow are shown schematically in Figure 2-1. This analysis focuses on three main categories of flows: (1) net Delta outflow, (2) inflows to and withdrawals from the Delta, and (3) hydrological components that comprise Sacramento Valley inflow to the Delta. Variable names used here correspond to that used in DAYFLOW: SAC = Sacramento, SJR = San Joaquin River, YOLO = Yolo Bypass, CSMR = Cosumnes River, MOKE = Mokelumne River, CVP = Central Valley Project, SWP = State Water Project, NBAQ = North Bay Aqueduct, CCC = Contra Costa Canal, MISC = Miscellaneous stream flows. DAYFLOW calculates an estimate of the net Delta outflow index (NDOI) using river inflows, exports, precipitation, and net channel depletions.

In this report we drop the “index” terminology and refer simply to net Delta outflow (NDO) or more simply Delta outflow. The estimate of agricultural net channel depletions in the DAYFLOW calculations is not considered to be precise, so we also consider an alternate Delta outflow calculation with estimates of these net depletions coming from the Delta Island Consumptive Use (DICU) model (DWR 1995).

Table 2-1 presents a summary of the data used in this work and partitions these data into two categories: “Delta Flow Components” and “Sacramento Valley Components.” In addition to including net Delta Outflow estimates, the “Delta Flow Components” include Sacramento Valley inflow (SAC and YOLO); Other Delta inflow (including SJR, CSMR, MOKE, and MISC); Delta accretions/depletion estimates; and Delta exports (CVP, SWP, NBAQ, and CCC). As the Sacramento Valley inflow is the dominant natural driver of the system, we analyze that hydrological component in further detail.

The “Sacramento Valley inflow” comprises several flow data sets. The “Four River” inflow is the total observed<sup>1</sup> flow below the major reservoirs on the Sacramento, Feather, Yuba, and American rivers. Stream flows from sixteen smaller tributaries are also considered in the inflow estimate (identified as “Minor Rim inflows”). Month-to-month changes in storage volume of the major reservoirs listed above (“Change in Storage”) and basin imports (“Trinity Imports”) represent impairments or subsidies present in the Four River inflow. The “Four River Index” represents unimpaired flow from these Four Rivers. Another contributor is the valley-floor precipitation, which contributes runoff to the Sacramento Valley inflows to the Delta. Sacramento Valley accretions/depletions are defined as the Sacramento Valley inflow to the Delta minus the Four River inflow. Finally, the Northern Sierra “Eight Station Precipitation Index” is an average of precipitation observations from eight stations designed to be representative of precipitation falling in the upstream portions of the Sacramento Valley.

Freshwater outflows from the Delta strongly affect the location of the low salinity zone in San Francisco Bay. Specifically, the location or position of two parts per thousand bottom salinity – hereafter referred to as “X2” – has been correlated with the abundance of several species (Jassby et al., 1995), and is presently used for water management in the estuary. In prior work, we compiled salinity data over a period corresponding with the flow data discussed above and quantified the X2 position over this period (Hutton et al., 2015). The interpolated X2 position is an estimate of the 2.64 mS/cm isohaline derived from surface salinity observations in the Bay-Delta. Evaluation of X2 along with Delta outflows and additional flow variables allows us to compare the trends and relationships in these quantities jointly.

---

<sup>1</sup>The flows are generally averaged from observed values; a small amount of data in the earlier part of the record are estimates. See C2VSIM documentation for details (Brush et al., 2013).

**Table 2-1  
Summary of Data (All data used are monthly averages over 1922-2009)**

Variable	Data Source	Comments
<b>Delta Flow Components</b>		
Net Delta Outflow (DAYFLOW)	DAYFLOW	If not specified, the Net Delta Outflow in this document refers to this term
Net Delta Outflow (DICU model-based)	DAYFLOW; DICU	Substitute DAYFLOW Delta accretions/depletions with DICU accretions/depletions
Sacramento Valley Inflow (to Delta)	DAYFLOW	SAC+YOLO
Other Delta Inflow	DAYFLOW	SJR+CSMR+MOKE+MISC
Delta Accretions/Depletions (DAYFLOW)	DAYFLOW	
Delta Accretions/Depletions (DICU)	DICU	
Delta Exports	DAYFLOW	CVP+SWP+CCC+NBAQ
X2 Position	Hutton et al. (2015)	Interpolated from salinity data
<b>Sacramento Valley Inflow Components</b>		
Four River Inflow	C2VSIM	Primarily based on USGS observations
Minor Rim inflows	C2VSIM	Sixteen smaller streams; primarily based on USGS observations
Change in Storage	Calculated	
Trinity Imports	USGS	
Four River Index	CDEC	
Sacramento Valley Accretions/Depletions	Calculated	Sacramento Valley Inflow – Four River Inflow
Eight Station Precipitation Index	CDEC	Upper elevation stations in the Northern Sierra
Sacramento Valley Precipitation	C2VSIM	Contribution from valley floor stations; compiled for C2VSIM
Groundwater-Surface Water Exchange	C2VSIM	Modeled
Groundwater Pumping	C2VSIM	Modeled estimate
Surface Water Diversions	C2VSIM	Organized input data for historical run developed by DWR

SAC = Sacramento, SJR = San Joaquin River, YOLO = Yolo Bypass, CSMR = Cosumnes River, MOKE = Mokelumne River, CVP = Central Valley Project, SWP = State Water Project, NBAQ = North Bay Aqueduct, CCC = Contra Costa Canal.

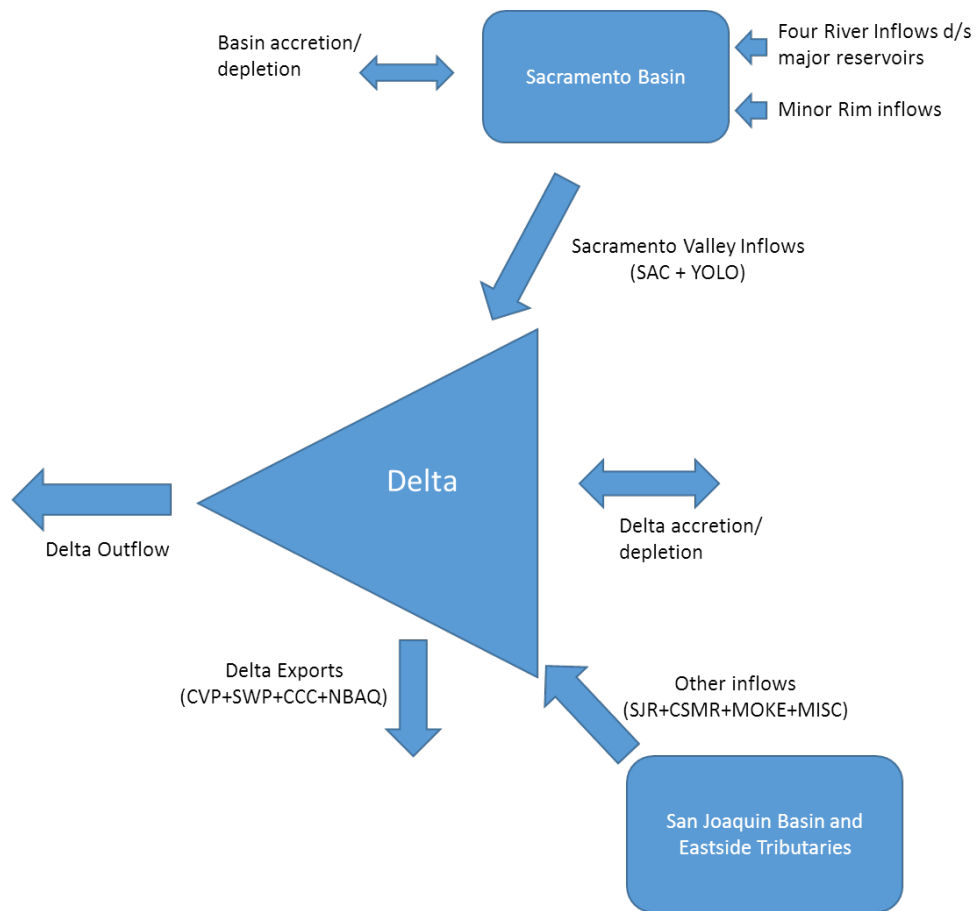


Figure 2-1 Schematic of inflows into and out of the Delta

## 3 METHODS

---

We applied a consistent set of statistical methods for analyzing each of the data time series that was informed by a review of the literature described in the Introduction. We used non-parametric tests that do not assume normality of the underlying data. A pair of tests that we use (Sen's non-parametric estimate of slope and Mann-Kendall test, described further below) has been used extensively in similar analyses to detect trends in variable data sets. The Sen slope is the median of all slopes between all possible unique pairs of individual data points in the time period being analyzed. If there are  $n$  time points, then there are a total of  $n(n-1)/2$  possible pairs of time points one could use to calculate a slope, and Sen's slope is the median of these values. The method is robust and fairly insensitive to the presence of a small fraction of outliers, non-detect, or extreme data values; thus, trend estimates based on Sen slope are not biased by the occurrence of drought in the early part of the record. Trend analyses were performed over the entire period with data (WY 1922-2012), as well as two additional intervals: Water Years 1922 to 1967 and 1968 to 2012. These intervals were selected to coincide with Enright and Culberson's (2009) "pre" and "post" water project periods, following the completion of the Central Valley Project and the State Water Projects in WY 1967. In addition to the trend analysis, for selected data categories we applied other methods that included comparison of groups of data using the Kruskal-Wallis test; exploration of trend decomposition using the seasonal trend decomposition based on loess (STL) approach; and use of generalized additive mixed models to represent some flow time series. These methods are described further below.

### 3.1 MONOTONIC TRENDS: MANN-KENDALL (MK) TEST AND SEN'S SLOPE

The Mann-Kendall (MK) test (Kendall 1938; Mann 1945) is a common nonparametric statistical procedure to determine significance of trend. It has been used extensively in previous hydrology trend studies in North America (Bawden et al. 2014; Fox et al. 1990), Europe (Déry et al. 2012; Hannaford 2015; Hannaford et al. 2013; Karlsson et al. 2014; Lorenzo-Lacruz et al. 2012), and Asia (Abghari et al. 2013; Chen and Grasby 2009; Chen et al. 2014; He et al. 2013; Jiang et al. 2007; Sharif et al. 2013). The rank-based, nonparametric MK test is useful for this purpose because streamflow data are likely to exhibit non-Gaussian residuals, contrary to what is assumed in many classical regression models. We analyze the annual flow time series (water year total) and each monthly subseries (e.g., the January subseries is all the January observations) with the MK test at the 95% confidence level.

For the analysis of annual flow trends, we summed monthly flows by water year before computing the trend using the standard MK test. This approach allowed for a consistent methodology across all data sets. An alternative approach (which we did not adopt) is to utilize a modified (i.e. seasonally corrected) version of the MK test designed to handle data with a seasonal pattern (Helsel and Hirsch 2002; Hirsch et al. 1982). This alternative approach allows for trend detection in a data series without summing to the annual level.

The “two-sided” MK test was used in this analysis, which tests the following hypothesis: “Do the data show a trend that is either increasing or decreasing over time?” Absent prior knowledge of the direction of the change anticipated (either an increase or a decrease), the two-sided test is appropriate. The “one-sided” MK test can also be applied when the test is focused on testing a single direction of change, either increase only or decrease only. For the same data set, the one-sided and two-sided tests may provide slightly different results of significance. For a subset of the data used here (i.e., X2 position), we used the one-sided MK test in prior work (Hutton et al. 2015). In that work, the MK test was performed twice; the first test was for an increasing trend and the second test was for a decreasing trend. For consistency with the analysis presented here, we use the two-sided MK test for all variables including X2, recognizing that there are some differences in the significance results from those reported in Hutton et al. (2015).

### **3.2 MULTIPLE COMPARISONS FOR LOD DATA: KRUSKAL-WALLIS TEST AND MULTIPLE COMPARISONS**

The Kruskal-Wallis (KW) test is a nonparametric version of one-way ANOVA that decides whether the center of the distribution is the same for several samples, e.g., under different treatments (Siegel and Castellan 1988). If the null hypothesis of the KW test is rejected, we can perform a post-hoc analysis of the pairwise differences between all samples. This is achieved using a rank-sum test and accounting for the multiple-comparisons inflation of  $p$ -values: when there are  $k$  samples being compared,  $k(k-1)/2$  comparisons are possible, and the test statistic for the rank-sum test must be adjusted as such (Siegel and Castellan 1988). After all pairwise comparisons have been made, a convenient way to present the results is to group all samples that have no statistically significant differences (e.g., by assigning a color to a group). For brevity, we will refer to this procedure as the “multiple-comparisons KW procedure.”

### **3.3 SEASONAL TREND DECOMPOSITION BASED ON LOESS (STL)**

Seasonal trend decomposition based on loess (STL) (Cleveland et al., 1990) is a filtering procedure for decomposing a time series into what are termed trend, remainder, and seasonal components. This approach has been used previously in hydrological studies (Enright and Culberson, 2009; Gudmundsson et al., 2011; Shamsudduha et al., 2009) to identify the presence of an underlying change that is detectable once the seasonal component is removed. This method is considered a diagnostic test for our present purpose in that the resulting “trend” is representative of an underlying change, and not a statistically significant trend as determined through the MK test described above. The STL procedure iteratively detrends data to estimate the seasonal variation, defined here over a 12-month cycle, and then removes the seasonal signal to estimate low-frequency variation and non-stationary behavior over time. The trend and seasonal components are computed using nonparametric loess smoothers. All of the variables being considered in this work are highly seasonal; therefore, by taking out a seasonal component, this procedure allows us to examine changes occurring over the longer term, i.e., over decades.

The STL approach has some advantages over the MK test. The MK test is limited to detecting monotonic trends, yet changes in flow often exhibit a more complicated pattern. Indeed, flow variables often exhibit natural variability on long time-scales, described as low frequency variability or long-term memory (Gudmundsson et al., 2011; Koutsoyiannis, 2003), which are expressed as a non-monotonic behavior, i.e., over a long period of record there may be increases as well as decreases in a certain variable. The decomposition of a time series into seasonal, long-term trend, and residual is helpful for identifying the presence of this non-

monotonic behavior and understanding whether the application of test such as MK test, which is looking for the presence of a monotonic upward or downward trend is fully appropriate. On the other hand, STL is not a hypothesis test and is meant to describe and characterize seasonal and long-term trend components rather than provide statistically significant trend results.

### **3.4 FLEXIBLE NONPARAMETRIC MIXED MODELS: GENERALIZED ADDITIVE MIXED MODELS**

In the analysis of certain flow variables (e.g., cumulative time series), explicit treatment of autocorrelation effects becomes important. Furthermore, we may wish to examine the possibility of a time trend that does not follow a specified functional form. One way to achieve these goals is to use generalized additive mixed models (GAMMs), which are an extension of both linear mixed models that would allow us to model important autocorrelations and generalized additive models that estimate fits of unknown smooth functions to data (Wood, 2006). For a selected set of analyses, relating to the cumulative outflow over the course of a water year, this method was applied to aid interpretation of changes in flows over time.

This page intentionally left blank.

# 4 EVALUATION OF DELTA OUTFLOWS AND INFLOWS

---

In this chapter, data related to the Delta flow components are presented as simple time series plots and trends are evaluated using various statistical approaches described in Chapter 3. To describe the data and plots in text, we use the following delineation of three-month seasons: September-November, fall; December-February, winter; March-May, spring; and June-August, summer.

## 4.1 HISTORICAL DATA

Time series plots for several of the important Delta flow variables are shown in Figure 4-1 through Figure 4-6. In these plots, as well as in all subsequent analysis, we show results by month and also by year. All volumetric units are reported in million acre-feet (MAF). The choice of Delta net channel depletions has a limited effect on the annual net Delta outflow calculation, but may be important during the low flow months that occur in summer and early fall. The Delta outflow was therefore presented in two ways: (1) as reported in DAYFLOW (Figure 4-1) and (2) by replacing the net channel depletion in DAYFLOW with that obtained from the DICU model (Figure 4-2). As presented in this manner, the Delta outflow shows some visible patterns despite the large inter-annual variability: flows in the summer and early fall months appear to have increased, especially in the first half of the record; flows in the late spring appear to have decreased in the middle part of the record (~1950-1980); with less distinct visual changes in the winter months and for total annual flows.

Delta exports increased steadily during the construction of the state and federal water storage projects, but diversions in April and May have decreased since 1980 (Figure 4-3). The two estimates of net channel depletion are shown in Figure 4-4 and Figure 4-5. Both estimates are of similar magnitude although there are substantial differences in certain months (e.g., October through December). In this work, both estimates are considered of equal credibility, although we acknowledge that they are not in agreement over the entire record, with the potential to influence some of the statistical analyses.

The primary inflows to the Delta from the Sacramento Valley (through the Sacramento River and Yolo Bypass) and from San Joaquin River and other east side streams are shown in Figure 4-6 and Figure 4-7. The Sacramento Valley inflows show a distinct increase in the summer and early months over the pre-Project period. This effect is present to a much weaker extent in the flows from the San Joaquin and the east side streams. Annual flows show great year-to-year variability, but not a clear visual trend for either of these two inflow categories.

Time series plots of X2, as shown in Figure 4-8, illustrate a complex pattern. From August to November, there is a decrease in X2 from the early part of the record to the mid- to late-1960s, suggesting a seaward movement of the low-salinity zone. Beyond the late-1960s, there is an increase in X2 in several months, September to December, indicative of a landward

movement of the low-salinity zone. These changes in X2 position are reflective of Delta outflow trends revealed in Figure 4-1 and Figure 4-2.

The next set of figures summarizes trend results by relying on two types of plots. The first type of plot (Figure 4-9 through Figure 4-14) presents time series plots with the trend lines overlaid; the second type of plot (Figure 4-15 through Figure 4-19) presents bar charts of the Sen slope expressed as an absolute change and as percent change.

The MK test detected several significant trends on net Delta outflow (Figure 4-9, Figure 4-10, Figure 4-15 and Figure 4-16). The pre-Project period saw significant increases in August–November flows, with August and September changes being particularly large in a relative sense. Through the post-Project period, net Delta outflows had downward trends in September–November, although the September result is not significant in the DICU model-based NDO. Over the entire period of record, using the DAYFLOW-based NDO calculation, the test suggests a nominally downward trend in October–June (significant in October, November, February, April, and May) and a significant upward trend in July and August. The results are largely similar when the outflow based on DICU model-based estimates of net channel depletion are used, with the following differences: the decrease in October is not significant, and the flow shows an upward trend from July through September.

Delta exports (sum of CVP, SWP, NBAQ, and CCWD) show a statistically significant increase over the entire period of record for all months (Figure 4-11). In the post-Project period, there is a statistically significant decrease in May, and significant increases in July through January.

Sacramento Valley inflows into the Delta show statistically significant increases over the entire period of record for July through October, and significant decreases in April through May (Figure 4-12 and Figure 4-17). San Joaquin and east side stream flows show positive trends from August through October (Figure 4-13 and Figure 4-18), although the percentage increase is smaller than for the Sacramento Valley inflows. There are significant decreases in these flows in December and June, distinct from the Sacramento Valley inflows which show a nominal, non-significant increase in these months.

The Delta outflow patterns are reflected in the X2 trends (Figure 4-14 and Figure 4-19). September through December months show opposite trends for the pre-project and post-project periods: decreases in the first part and increases in the latter part. Over the entire period of record, there are statistically significant decreases in X2 in August and September, corresponding to higher freshwater outflows. There are significant increases in X2 in November–December and April–May, indicating lower flows. January through March does not show significant changes in X2, and there are no significant trends in the annual X2 values.

The following set of figures compares inflows and outflows on a year-by-year basis, adding flow components in steps. We use this graphical approach to attribute flow changes here and in the following chapter. Figure 4-20 is an illustration of a simple Delta water balance considering only inflows and outflows and how it has changed over time, shown by varying symbol colors representing different periods. On an annual basis, Delta inflows and outflows were approximately equal in the early part of the record, with a greater separation in the latter part of the record. When evaluated monthly, a loss or depletion is apparent in the summer months, even in the earliest part of the record, but especially so in the latter part of the record. In the latter part of the record, the net annual outflow remains mostly accounted for by the inflows during the winter months, but net depletions in the summer and fall months

add up to an annual depletion of several million acre-feet. Including Delta exports into the balance (Figure 4-21) accounts for most of this depletion, but a noticeable difference remains in the summer months. Given the definition of net Delta outflow in the DAYFLOW calculation, this difference corresponds to the net channel depletions in the Delta.

Differences between the monthly and annual net channel depletion estimates from DAYFLOW and the DICU model are shown in Figure 4-22. The differences, which generally range from 0.2 to 0.4 MAF, show a trend in time (particularly between May and October). In August and September, DAYFLOW estimates of net channel depletion are higher than the DICU model-based estimates. The overall difference, although minimal on the scale of annual Delta outflows, is potentially influential during low-flow periods, as indicated by differences in the analyses of trend shown in Figure 4-15 and Figure 4-16. Sources of discrepancy between the two estimates may include the assumed Delta boundaries and the manner in which Delta precipitation is estimated. However, explaining the causes of the differences in the net channel depletion estimates is beyond the focus of the present study.

## 4.2 STL DECOMPOSITIONS

The STL decomposition provides an alternative interpretation of the underlying trends, and can be used specifically to see if there is a change in the underlying variable over a longer term periodicity (e.g. decades). This is in contrast to the MK results which test whether there is a monotonic trend over the three periods examined (pre-, post-Project, and full record). Evidence of patterns that are apparent at longer time scales from the STL approach provides additional insight into changes that may have occurred in the system that may be tied to other drivers that are yet to be explained.

The STL decomposition of net Delta outflow is presented in Figure 4-23 through Figure 4-26, shown first with constant scales and then variable scales for DAYFLOW and DICU model-based estimates of NDO. When shown using a constant scale, the figures show a reduction of the magnitude of the 12-month seasonal component, and an underlying trend that is barely visible. The residual error is of the same magnitude as the inflow series, suggesting variability that is not explained by the seasonal or trend component. When the trend is considered using a modified y-axis scale focused on a narrower range, one sees a gradual increase through around 1960 and then a gradual decrease through 2010, although the magnitude of this change is small relative to the variability. The DAYFLOW and DICU model-based NDO results are nearly indistinguishable.

## 4.3 LOD SCENARIO DATA

The LOD scenario data (MWH, 2015) and the observed historical data are structured quite differently. The historical data represents one climate realization and its interaction with the human development of the Bay-Delta watershed, whereas the LOD scenario data attempt to isolate those effects by holding climate constant while adjusting watershed development. Nevertheless, some basic comparisons are possible.

Figure 4-27 and Figure 4-28 compare the historical flow in a given month and year (shown as a colored bar, corresponding to the water year type) to the range of LOD modeled flows for the closest period for the same water year type. For example, if we look at December flow for the year 1940, the bar shows the observed flow for that month, the color indicates the water year type (below normal), and the circle with error bars shows the range of calculated flows for the 1940 LOD for all below normal years in the model period (1922-2009). These plots allow comparison of the distribution of LOD values of net Delta outflow (NDO) to

historical values. These values should be similar in the sense that the values being compared are from the LOD closest to the historical year, are from the same water year type, and are from the same month. While there is considerable agreement between the modeled values and the observed values, for most months and on an annual basis, there is one difference: The LOD scenarios significantly overestimate summer flows in the earlier part of the record.

The distributions of annual and monthly LOD data are shown in Figure 4-29 (net Delta outflow), Figure 4-30 (Sacramento Valley inflow), and Figure 4-31 (Other inflows). There are two important differences between these plots and the historical data plots: (1) the x-axis represents the scenario year, not time and (2) the ranges of possible flow values based on an 88-year hydrology are represented as box plots. Following the Kruskal-Wallis (K-W) procedure described in Chapter 3.2, the boxes are colored the same when they are not statistically significantly different from one another. For Delta outflow, the K-W test suggests a statistically significant decrease in Delta outflows with LOD scenario 1980 and beyond. This is particularly noticeable in the March through June period. There are less consistent changes in the summer outflows with LOD, somewhat contrary to observations that indicate an increase in the summer months. Sacramento Valley LOD inflows to the Delta (Figure 4-30) do not show a significant change on an annual basis, but do show increases July through October for the post 1980 LOD scenarios. Importantly, this change occurs later in the 20<sup>th</sup> century than the observations, which show increases prior to the 1960s, and few significant trends in the post-1960 period. Also, March through May inflows show a decrease beyond the 1960 LOD which is consistent with the direction of the observed patterns. Finally, Other Delta LOD inflows (Figure 4-31) show patterns different from the Sacramento Valley inflows, with a significant annual decrease and significant decreases in the summer and spring months. Both are generally consistent with the direction of the observed changes, although the observed changes are not always statistically significant.

Taken together, the LOD scenarios are a reasonable representation of Delta inflows and outflows, and the underlying system representation is considered to be useful for inferring the contributors of change. Because the climate signal is consistent across all LODs, the changes that are apparent over time are clearly attributable to development-related effects, which include reservoir construction and changes in the seasonality of streamflows, surface water diversions in the valley streams and Delta, land use change across the basin, and regulatory changes in the Delta. On an annual basis, these appear to be most significant for Delta outflows and Other Delta inflows, both of which show decreases with development. In contrast, the Sacramento Valley annual inflows do not show a significant decrease with development, but there is a redistribution of flows with greater flow volumes in summer. In this regard, the Sacramento Valley LOD flows are more aligned with the observed Delta outflows, which also show an increase in summer, than with the modeled LOD Delta outflows, which do not show such an increase.

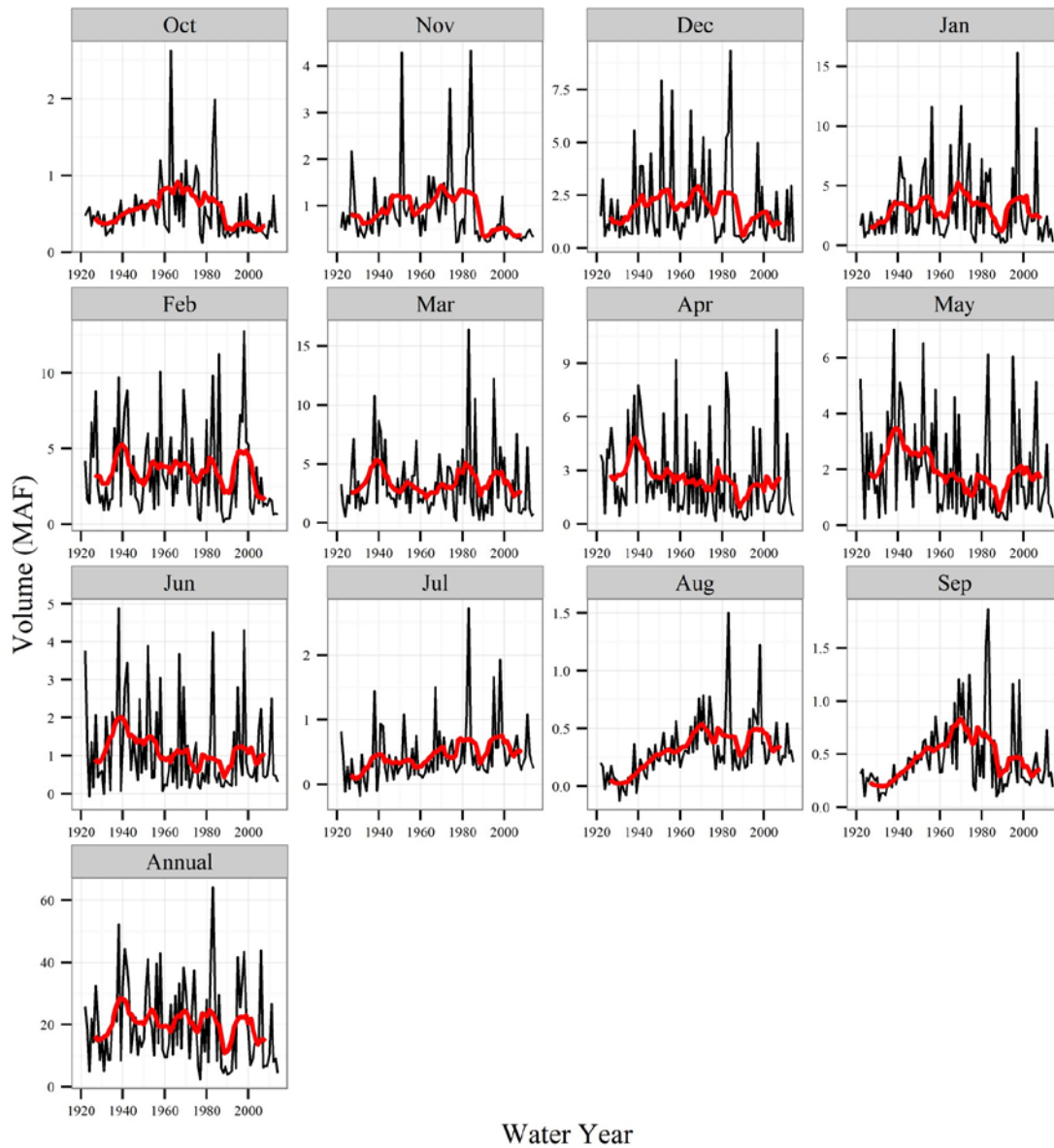


Figure 4-1 Time series plot of net Delta outflow (DAYFLOW) with 10 year moving average (red)

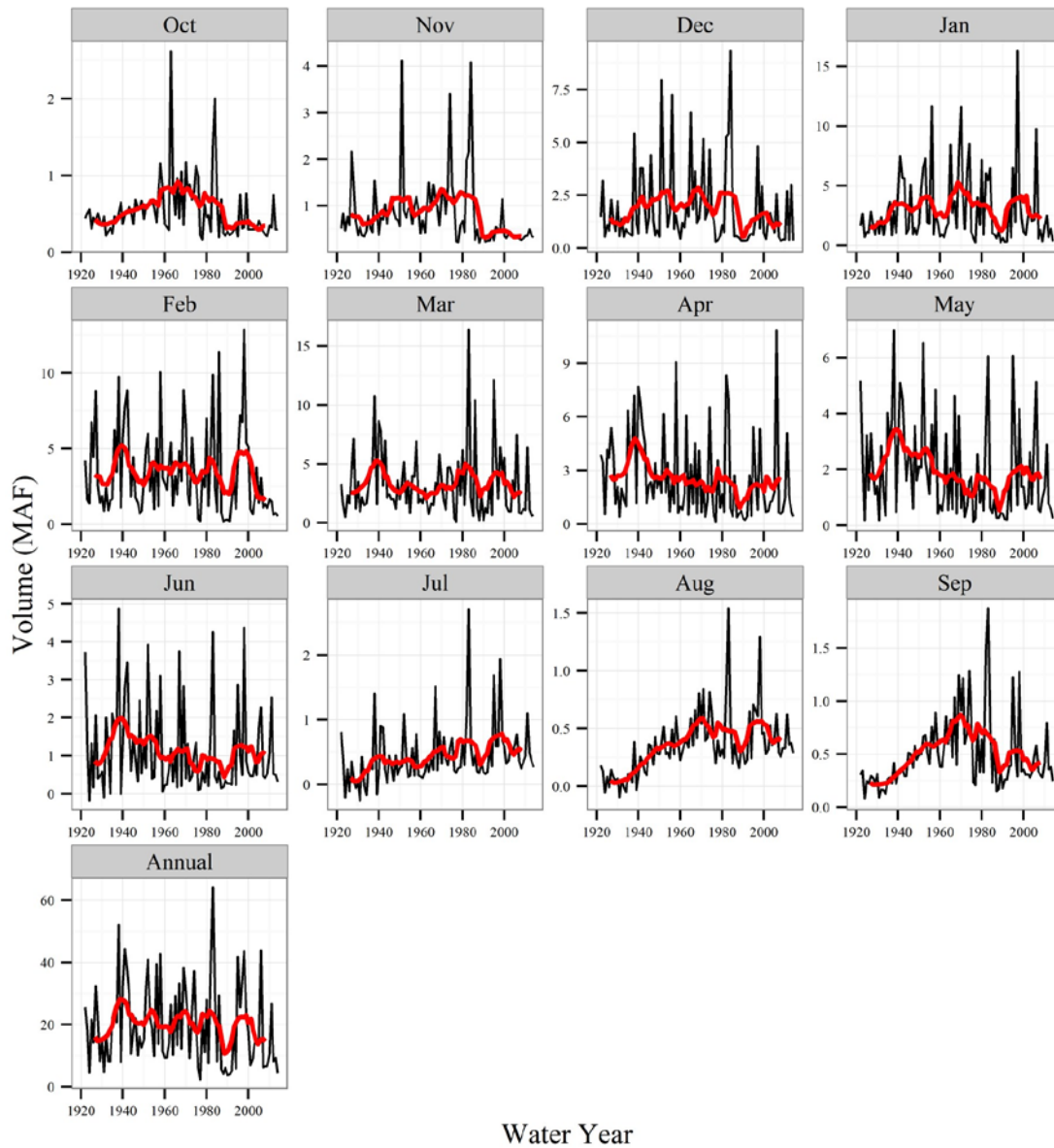


Figure 4-2 Time series plot of net Delta outflow (DICU model-based) with 10 year moving average (red)

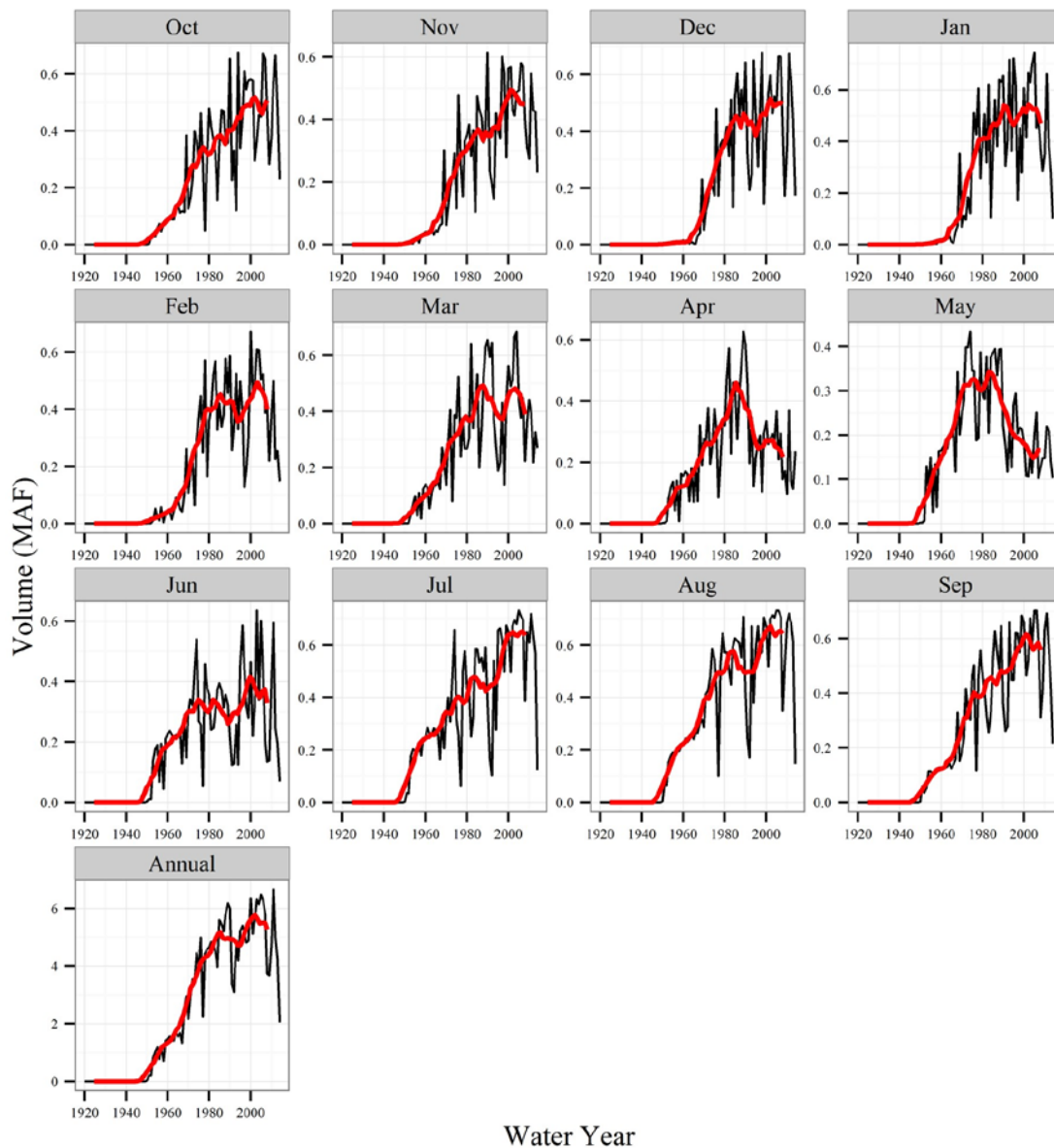


Figure 4-3 Time series plot of Delta exports (CVP + SWP + NBAQ + CCWD) with 10 year moving average (red)

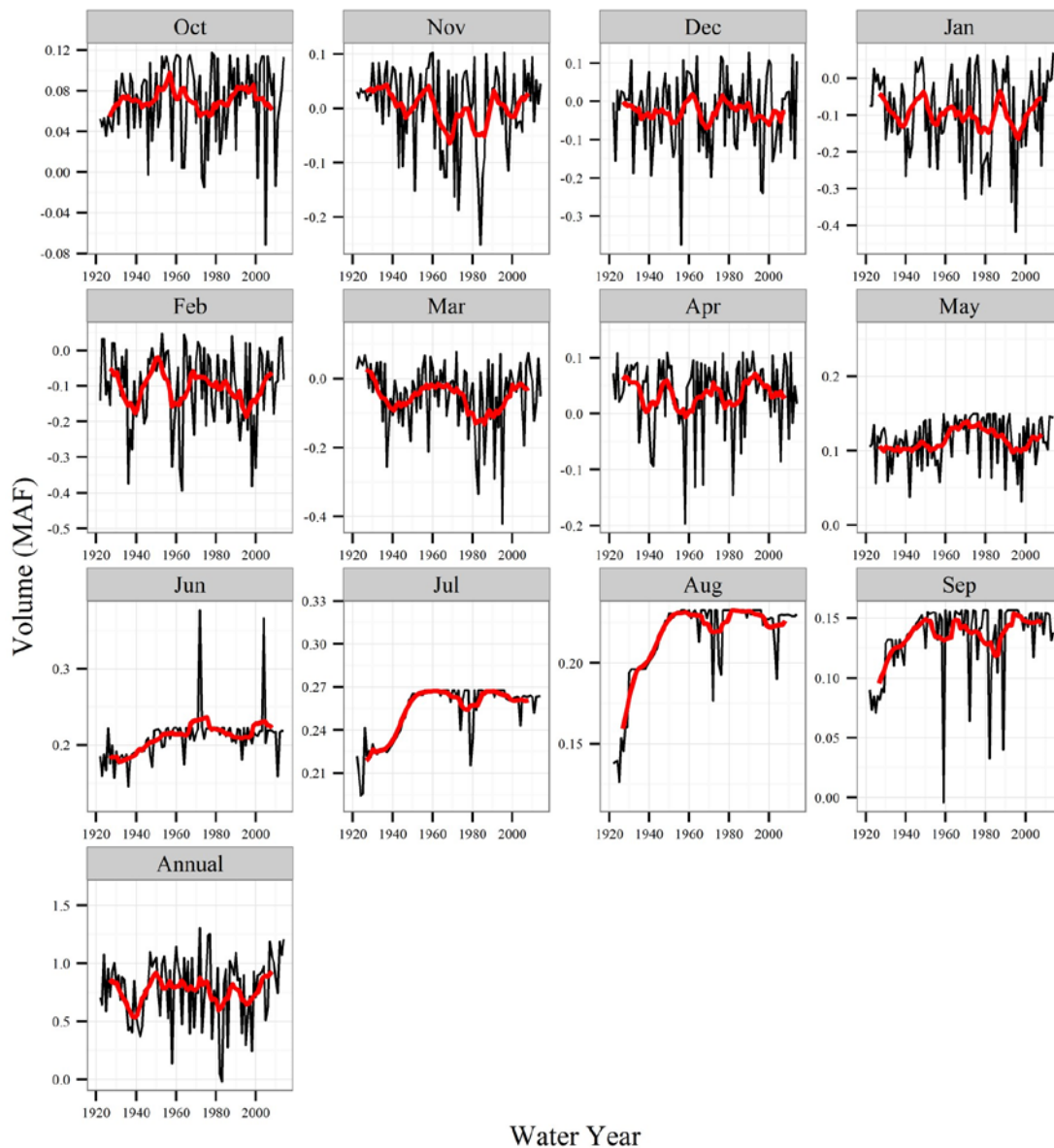


Figure 4-4 Time series plot of DAYFLOW estimates of Delta net channel depletion with 10 year moving average (red).

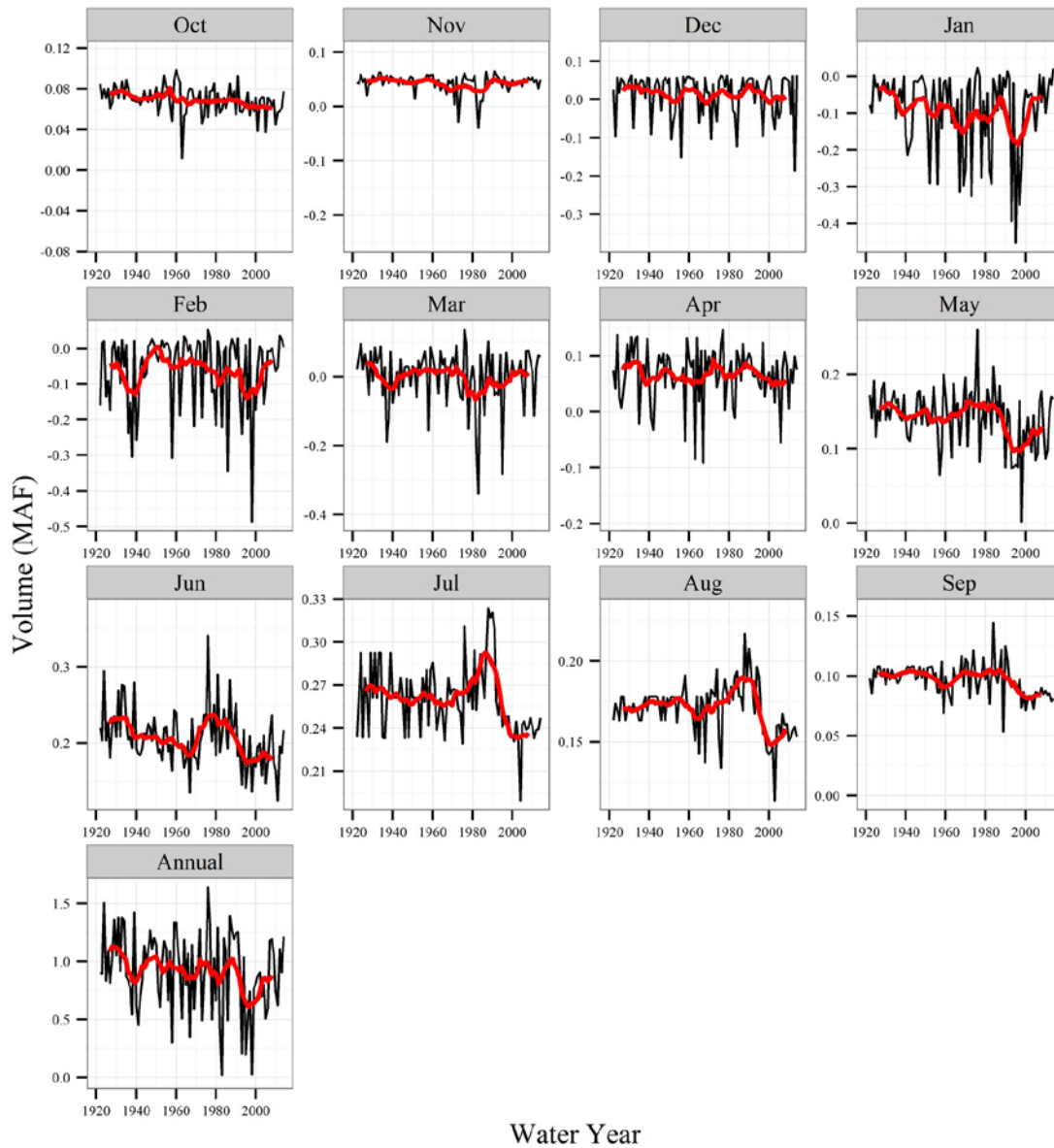


Figure 4-5 Time series plot of DICU estimates of Delta net channel depletions with 10 year moving average (red).

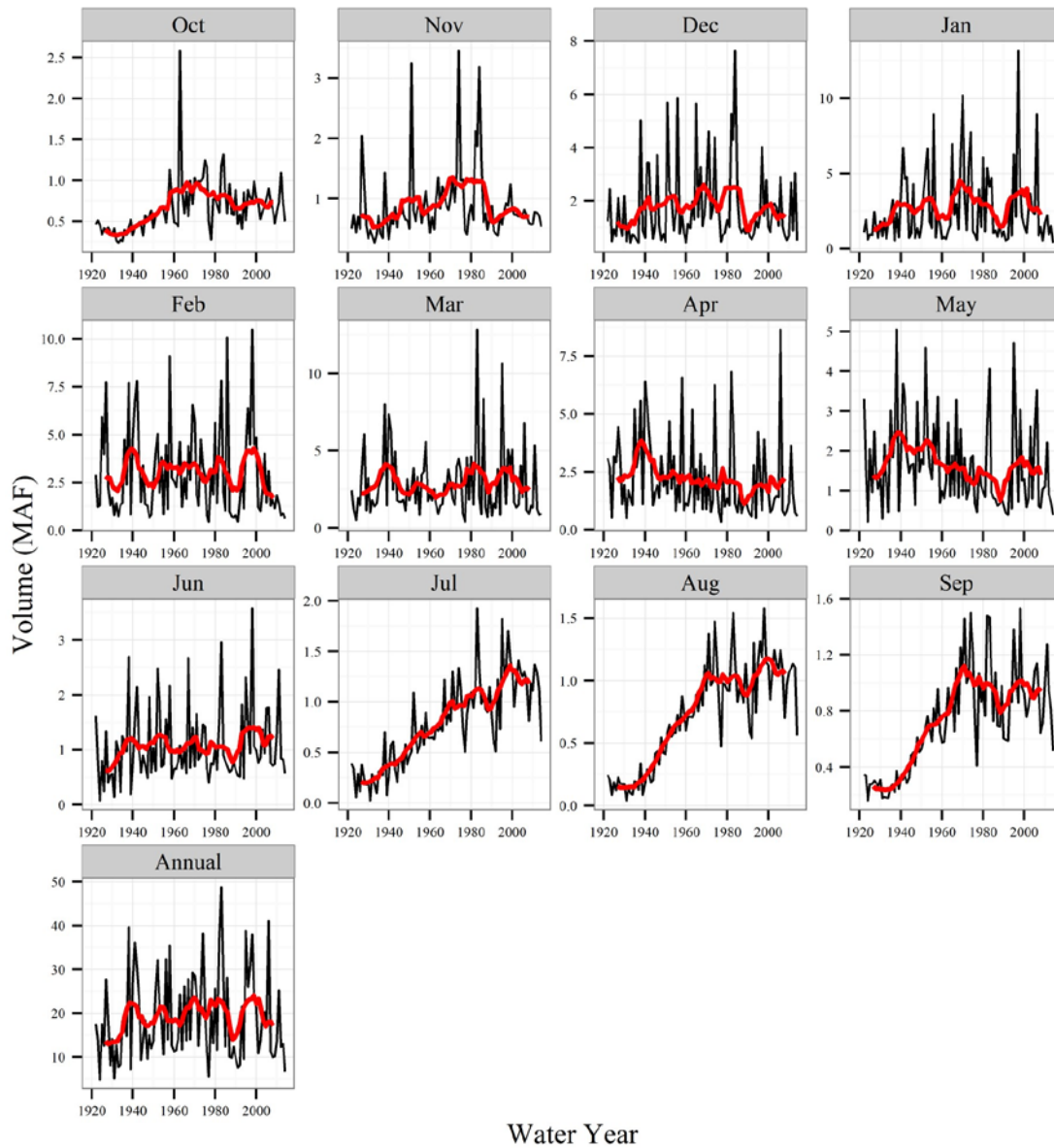


Figure 4-6 Time series plot of Sacramento Valley inflow to Delta (SAC + YOLO) with 10 year moving average (red).

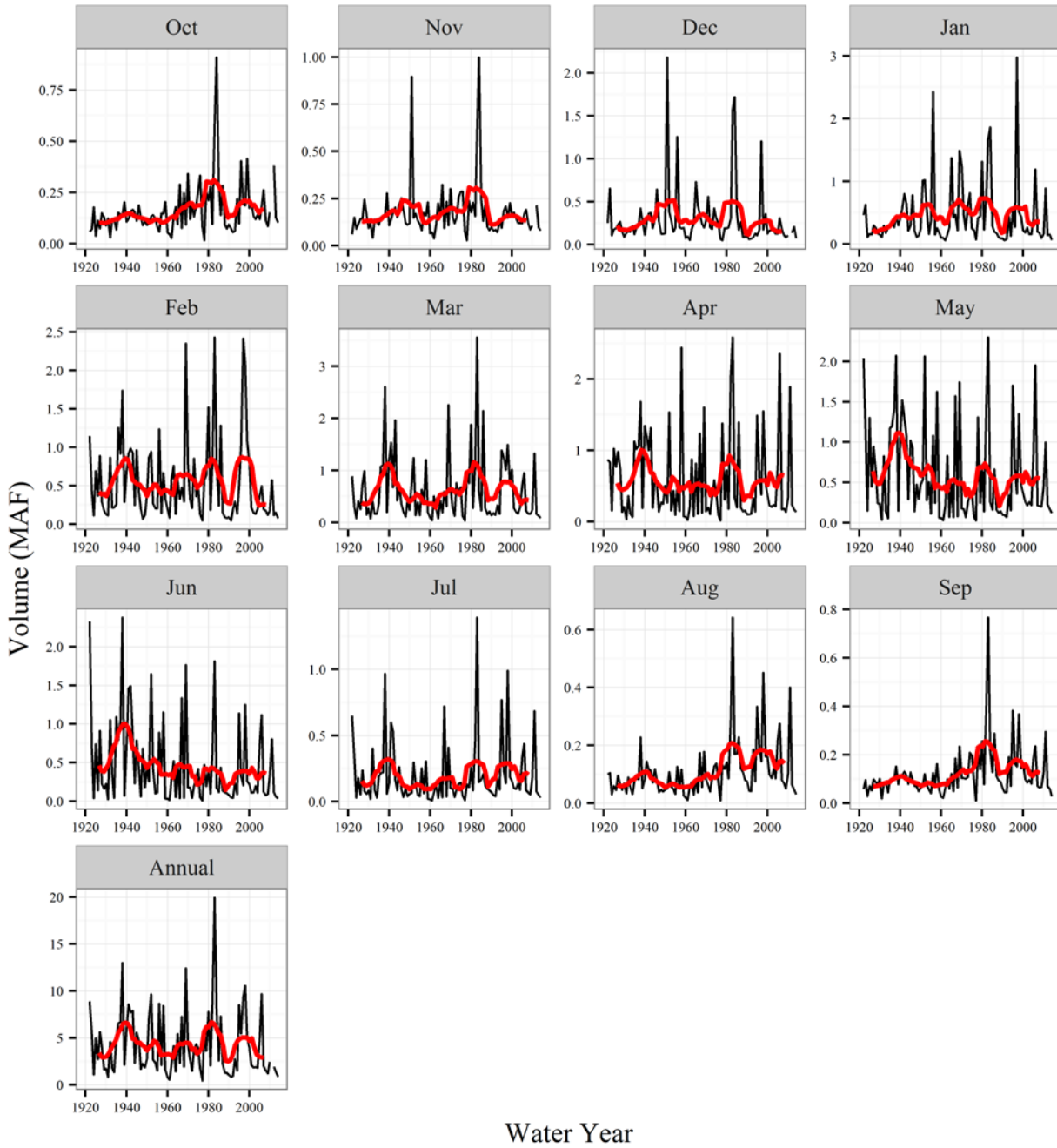


Figure 4-7 Time series plot of Other Delta inflow (SJR + ESS) with 10 year moving average (red).

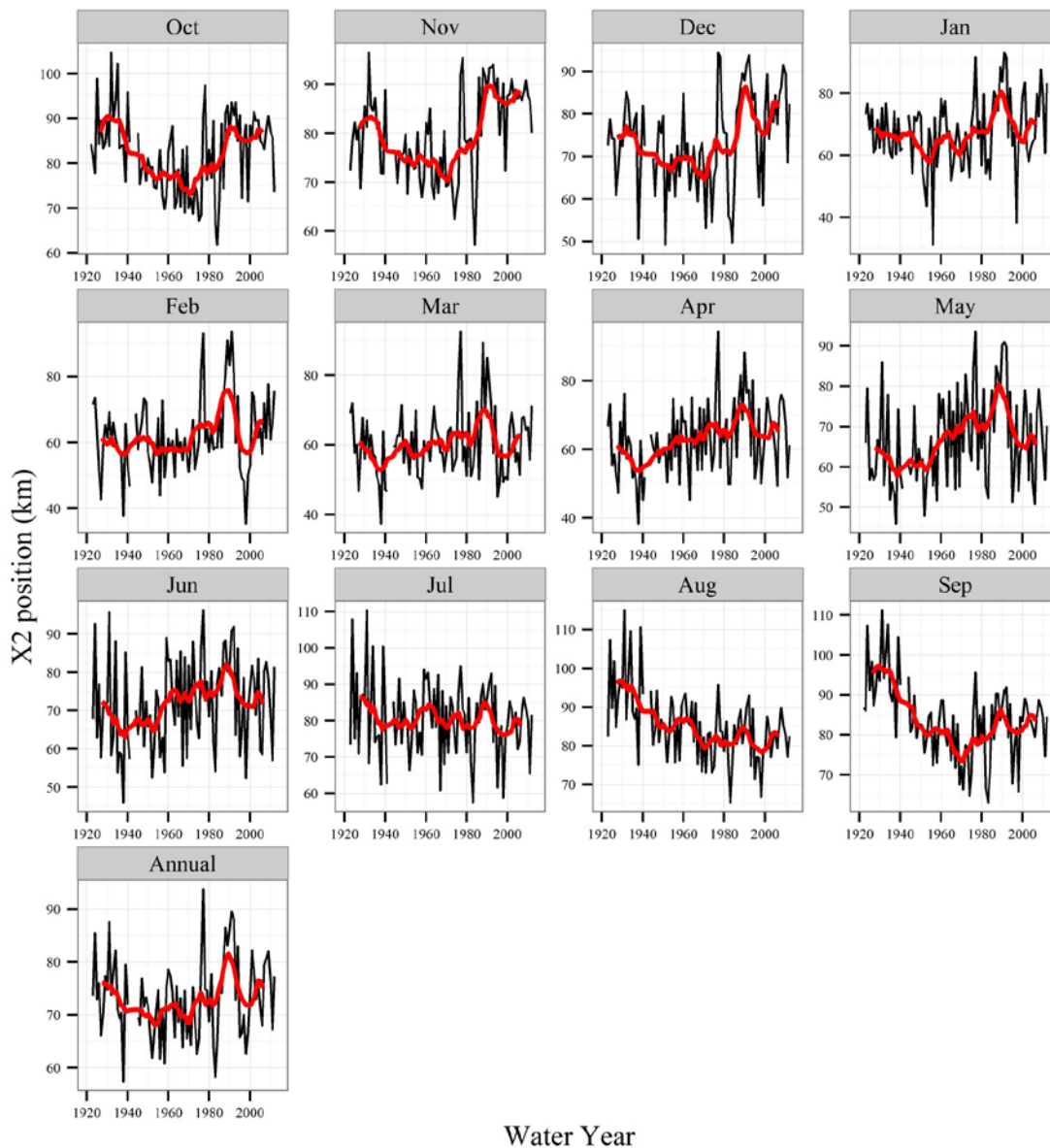


Figure 4-8 Time series plot of X2 position with 10 year moving average (red).

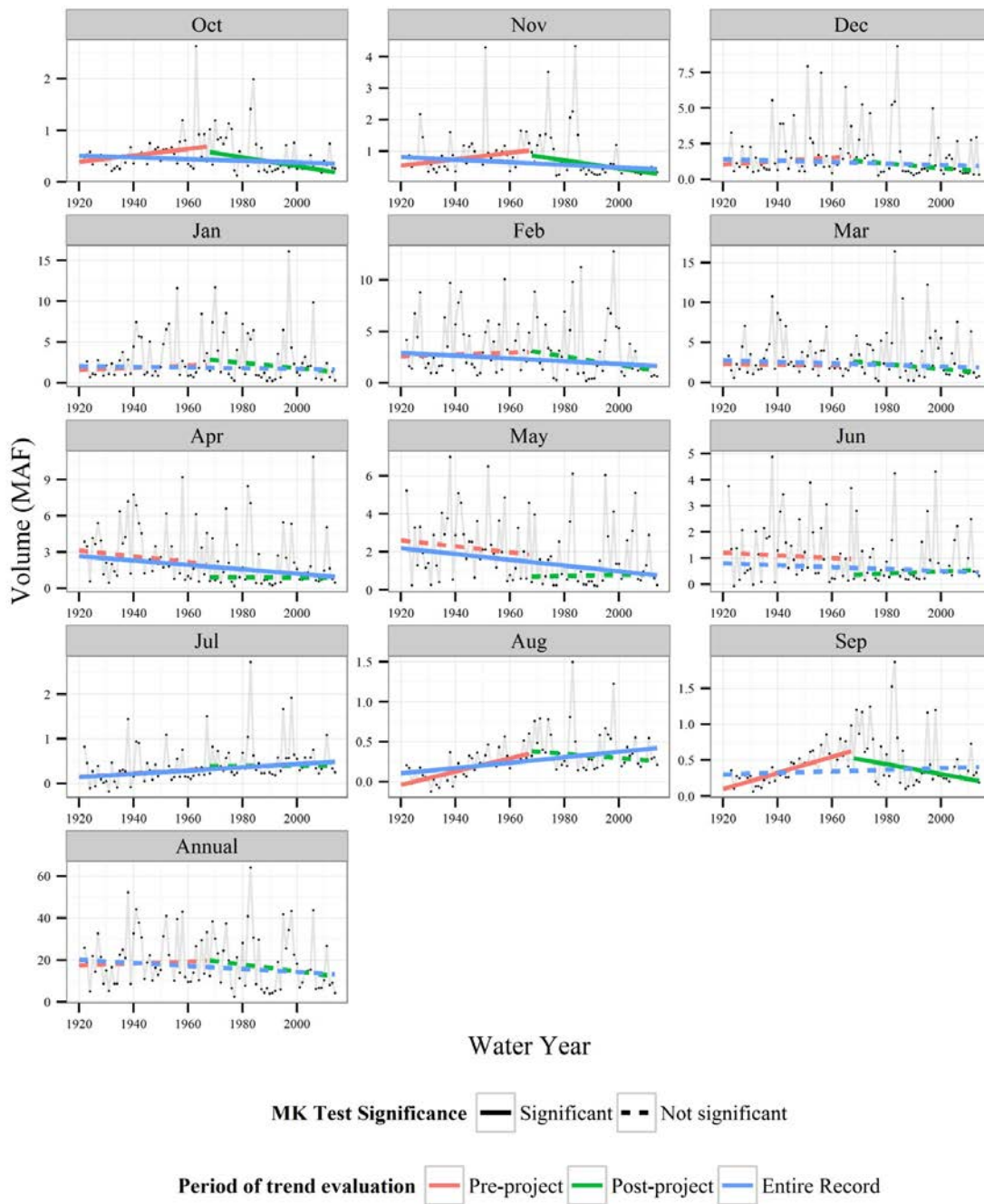


Figure 4-9 Mann-Kendall trend evaluation for net Delta outflow (DAYFLOW)

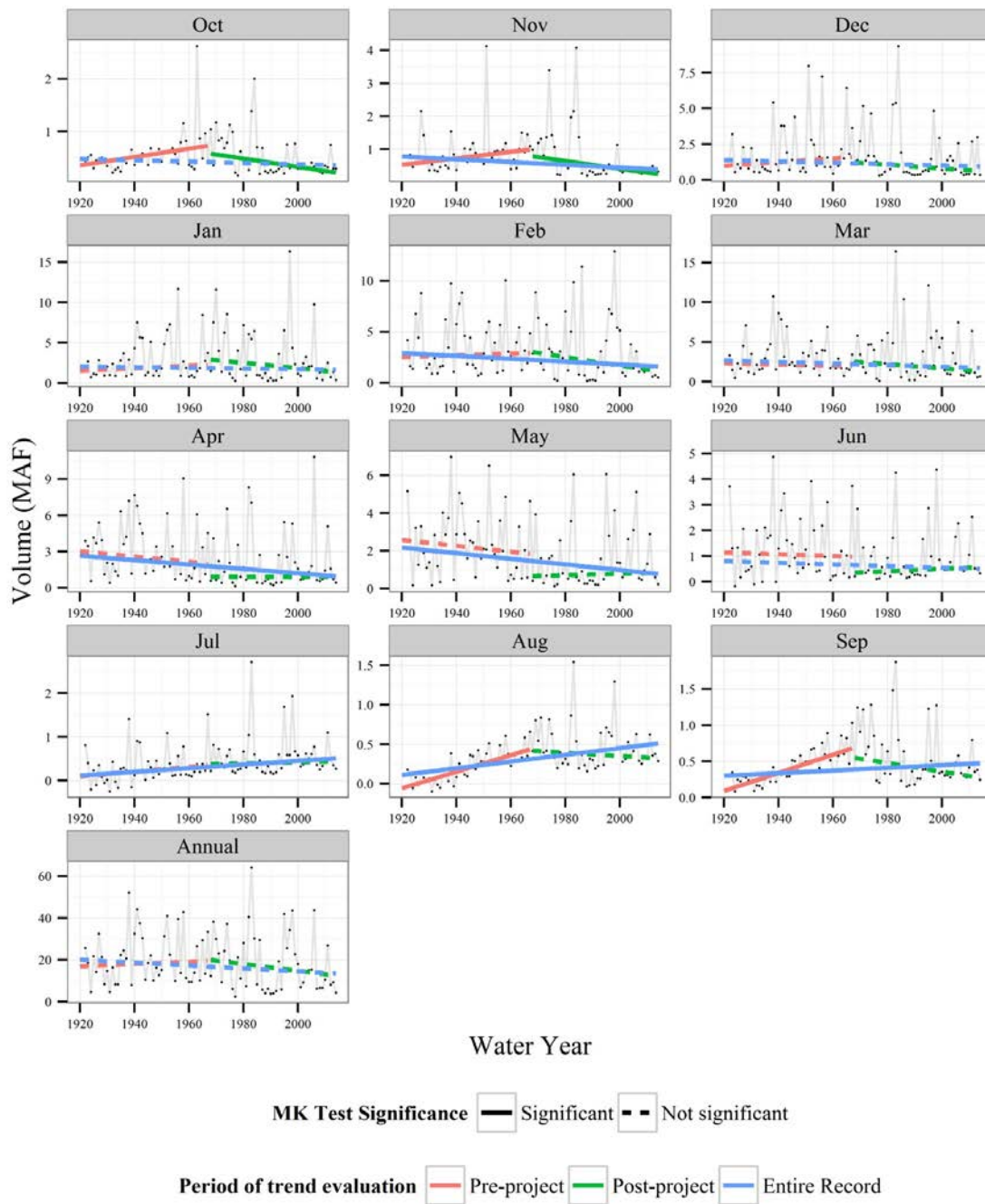


Figure 4-10 Mann-Kendall trend evaluation for net Delta outflow (DICU model-based)

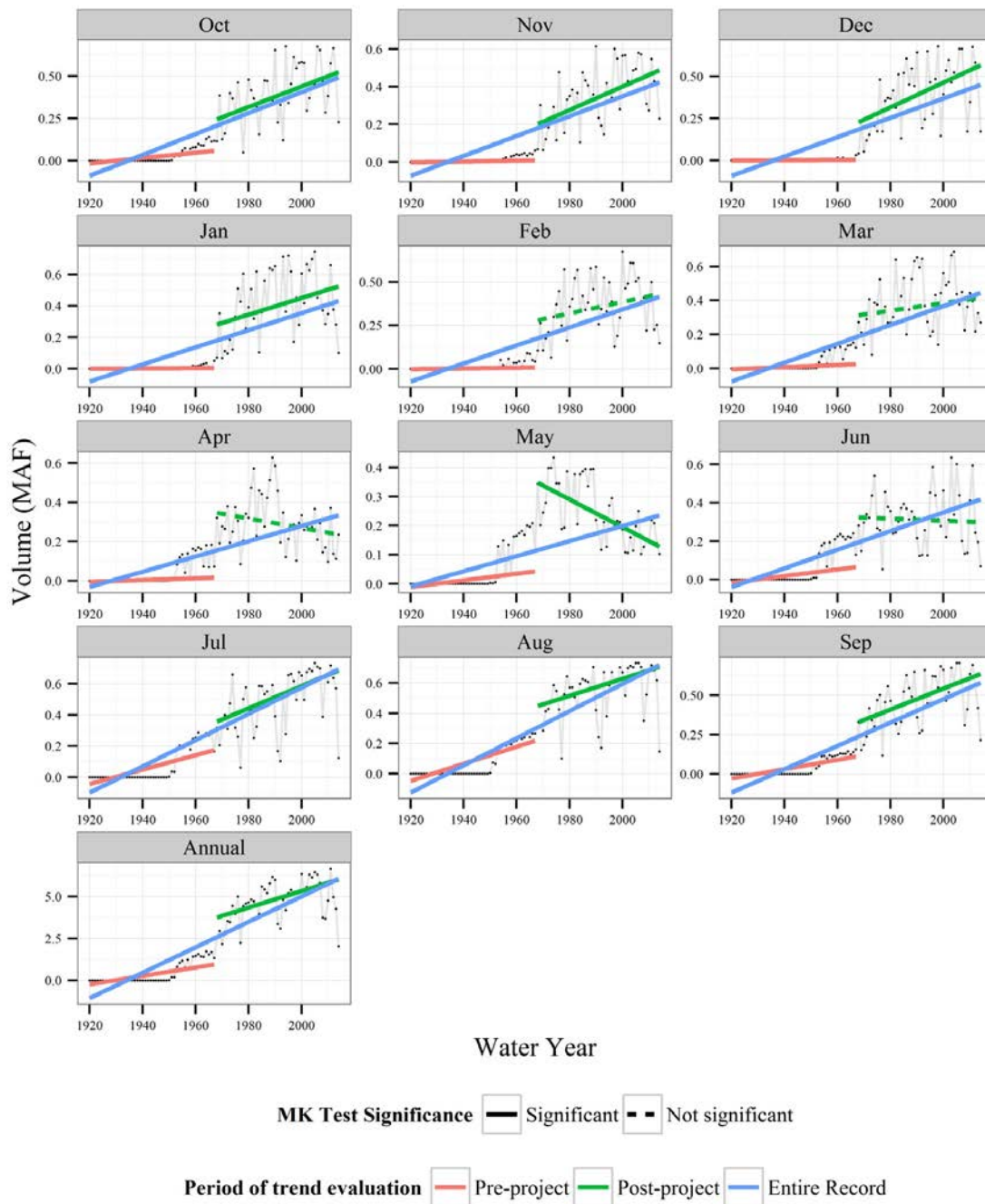


Figure 4-11 Mann-Kendall trend evaluation of Delta exports (CVP + SWP + NBAQ + CCWD).

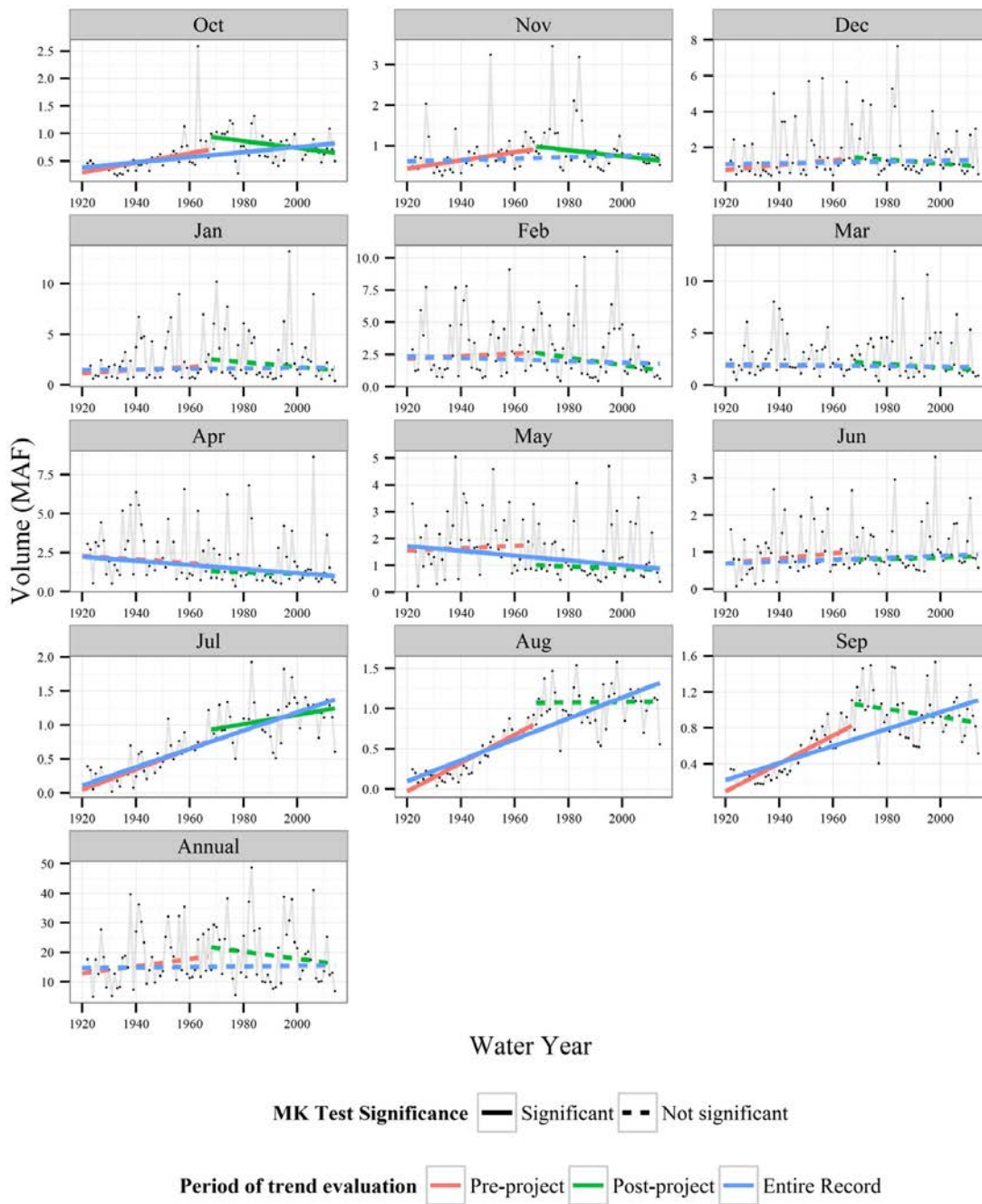


Figure 4-12 Mann-Kendall trend evaluation for Sacramento Valley inflow to Delta (SAC + YOLO)

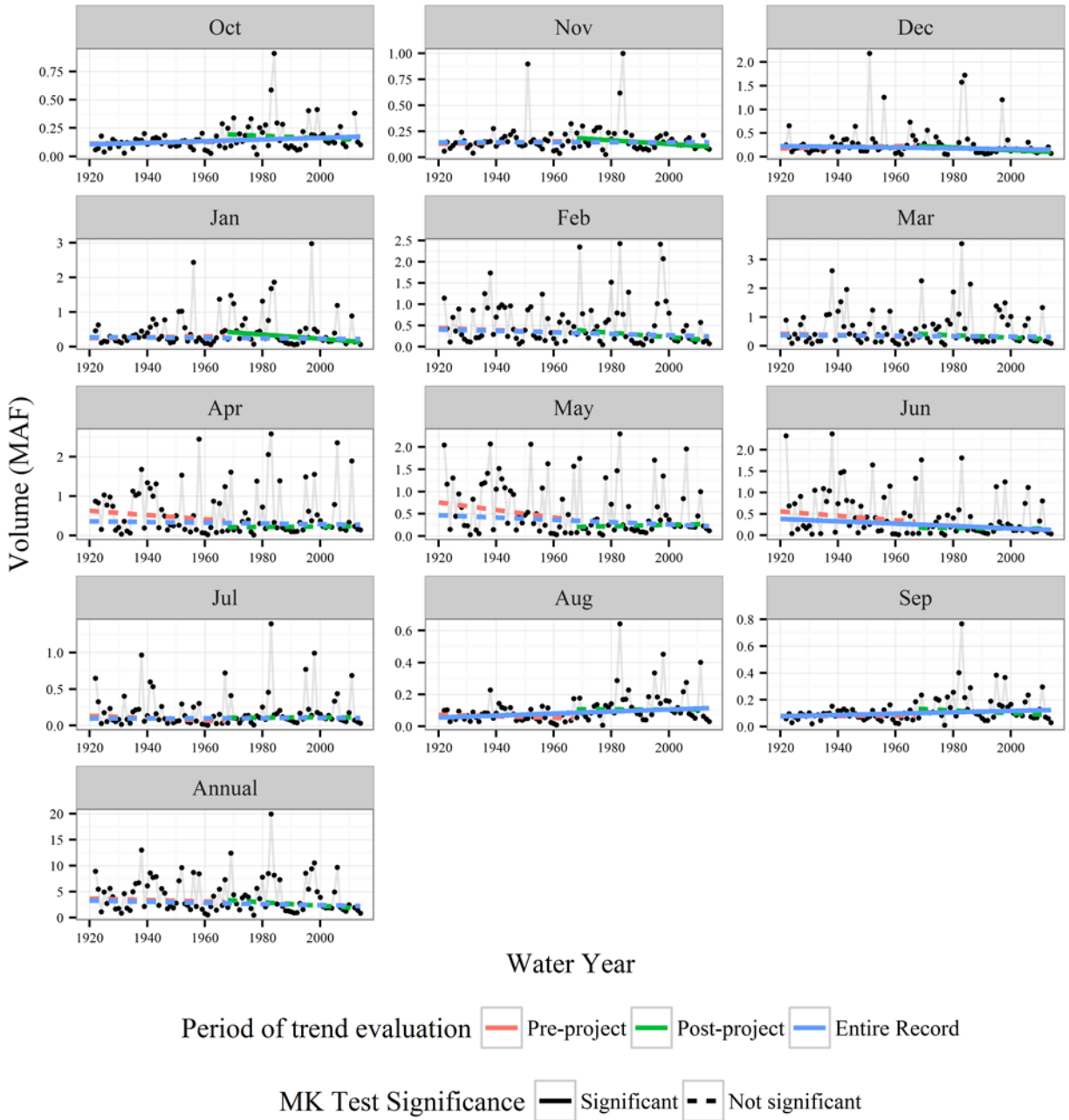


Figure 4-13 Mann-Kendall trend evaluation for Other Delta inflow (SJR + ESS)

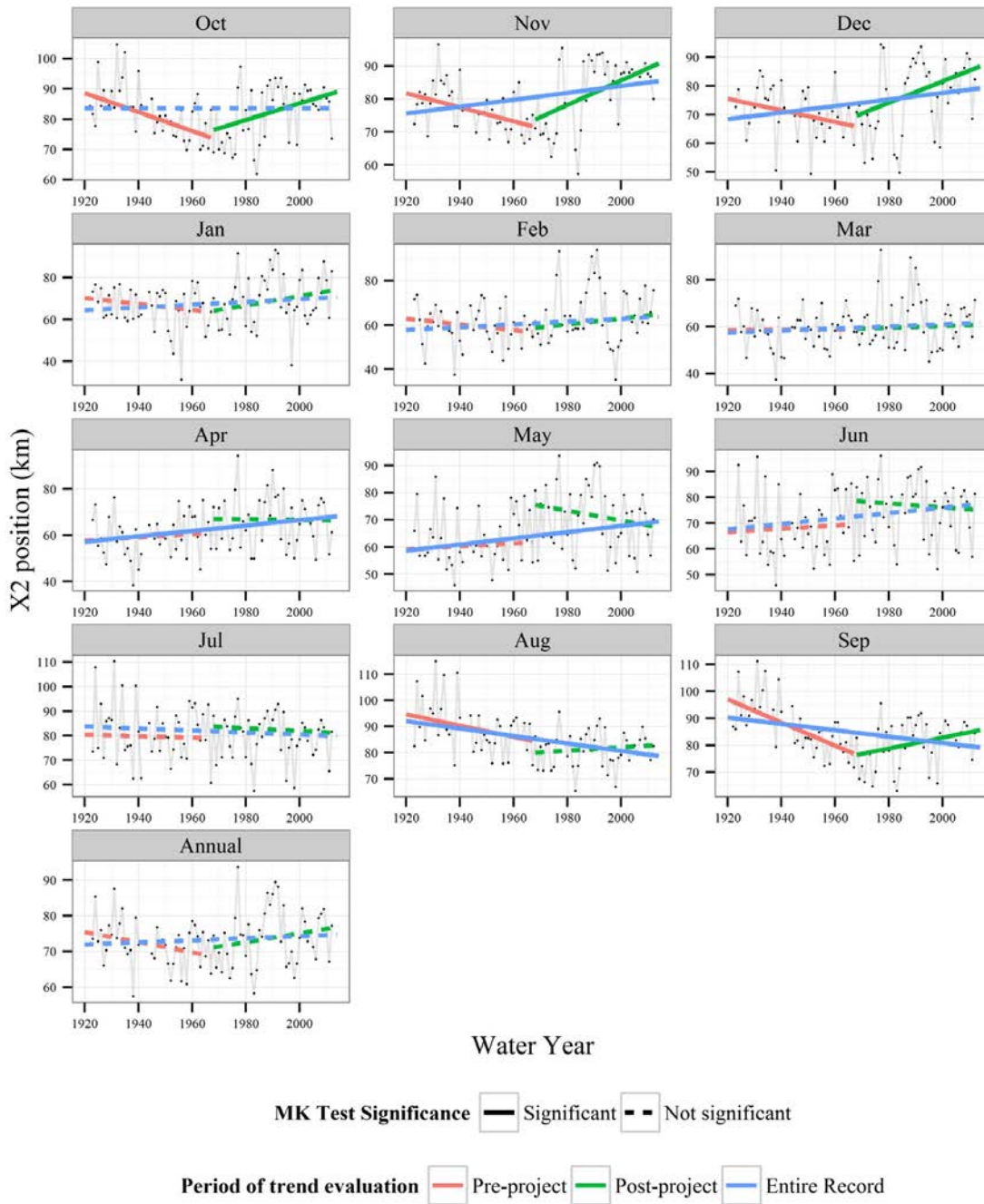


Figure 4-14 Mann-Kendall trend evaluation for X2

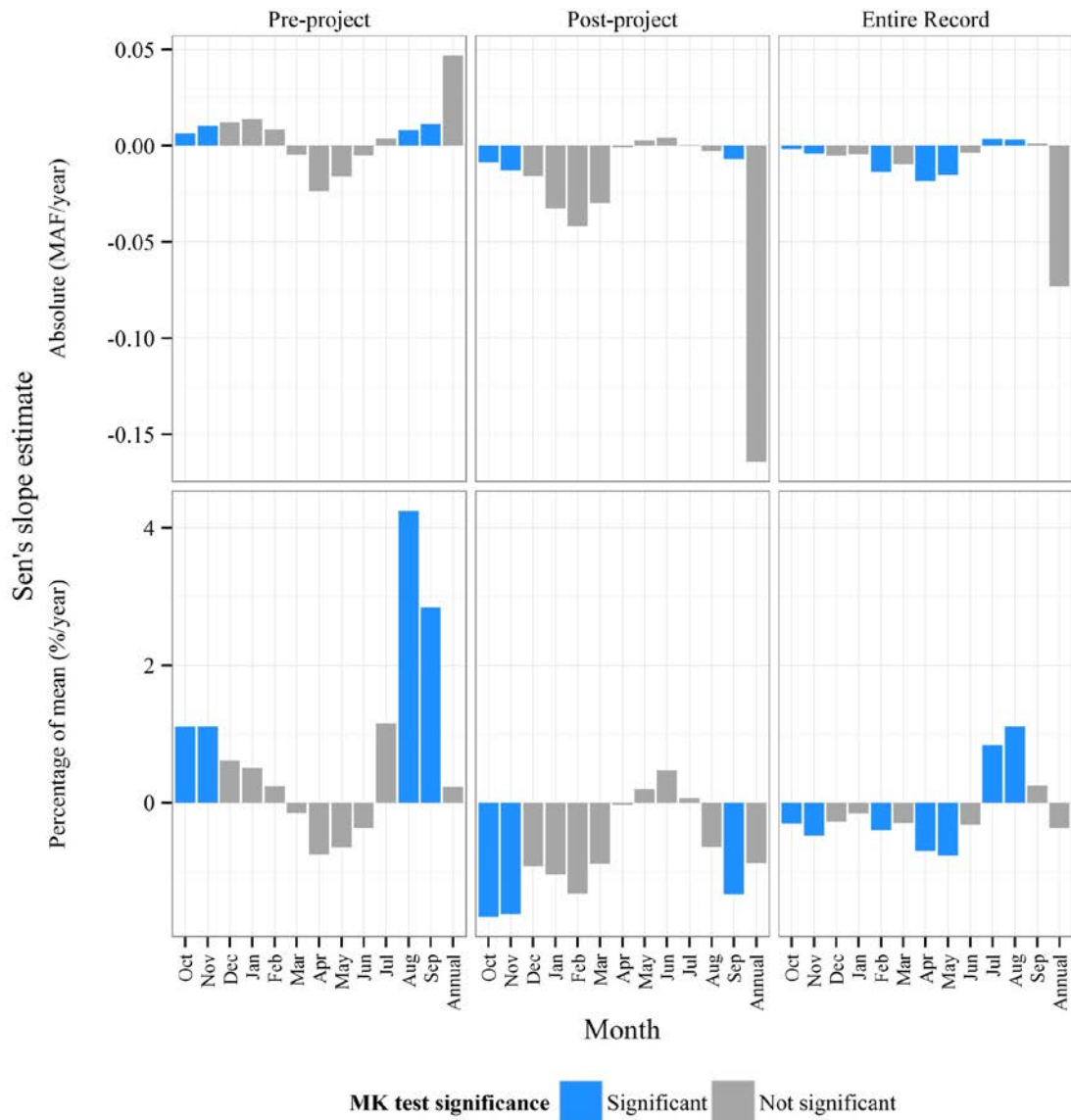


Figure 4-15 MK trend summary for net Delta outflow (DAYFLOW).

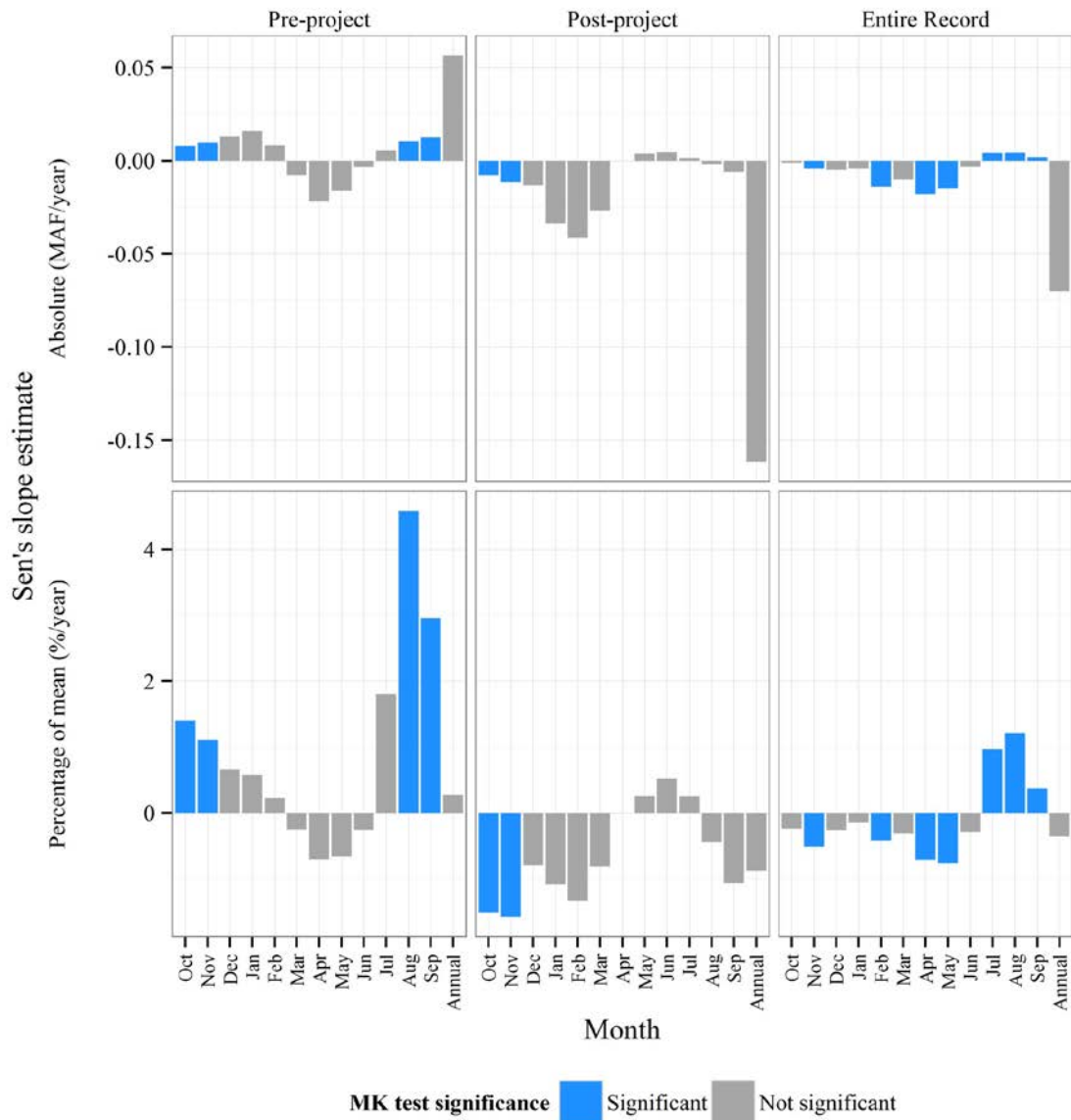


Figure 4-16 MK trend summary for net Delta outflow (DICU-model based estimate of net channel depletion).

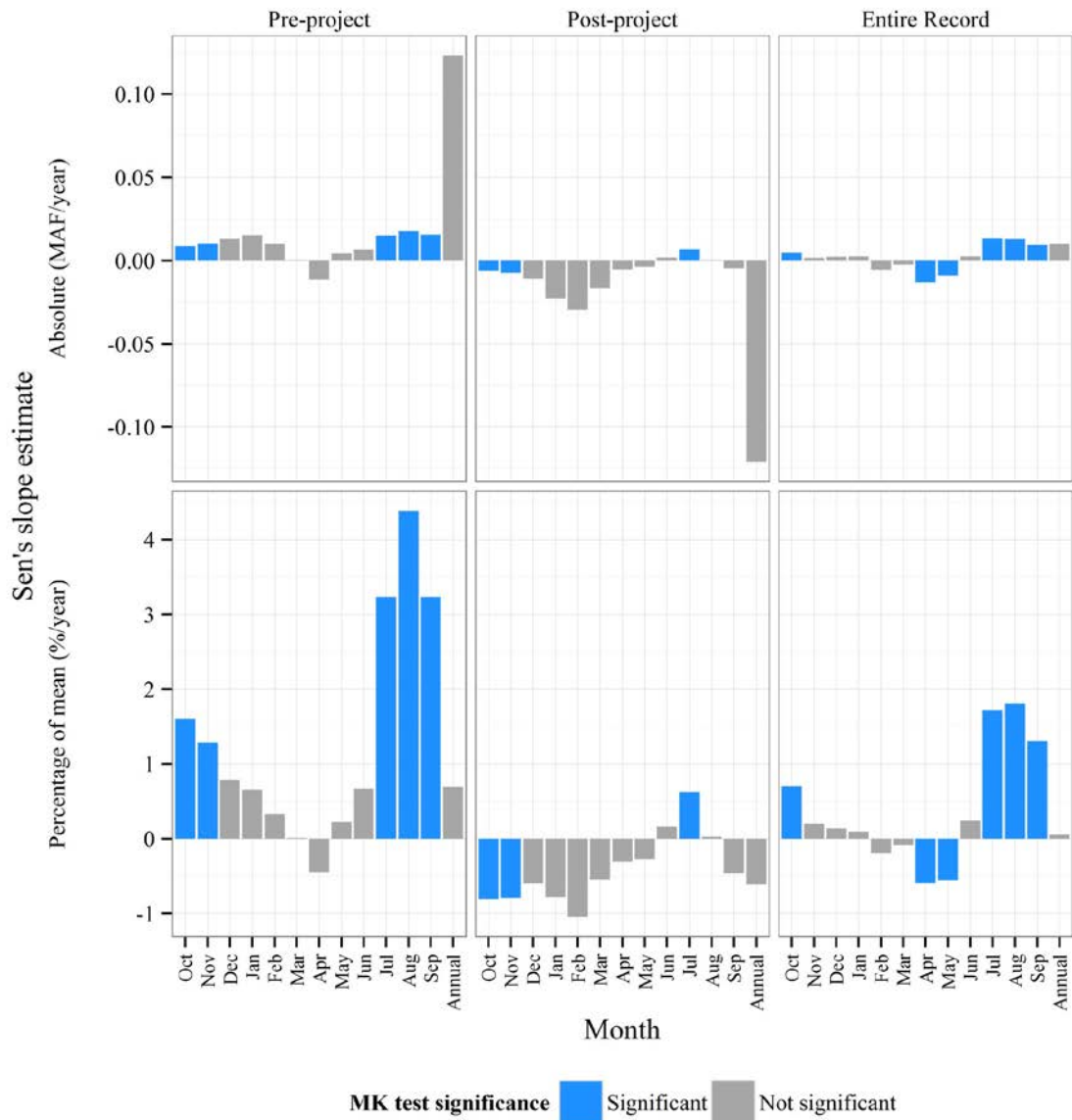


Figure 4-17 MK trend summary for Sacramento Valley inflow to Delta (SAC + YOLO).

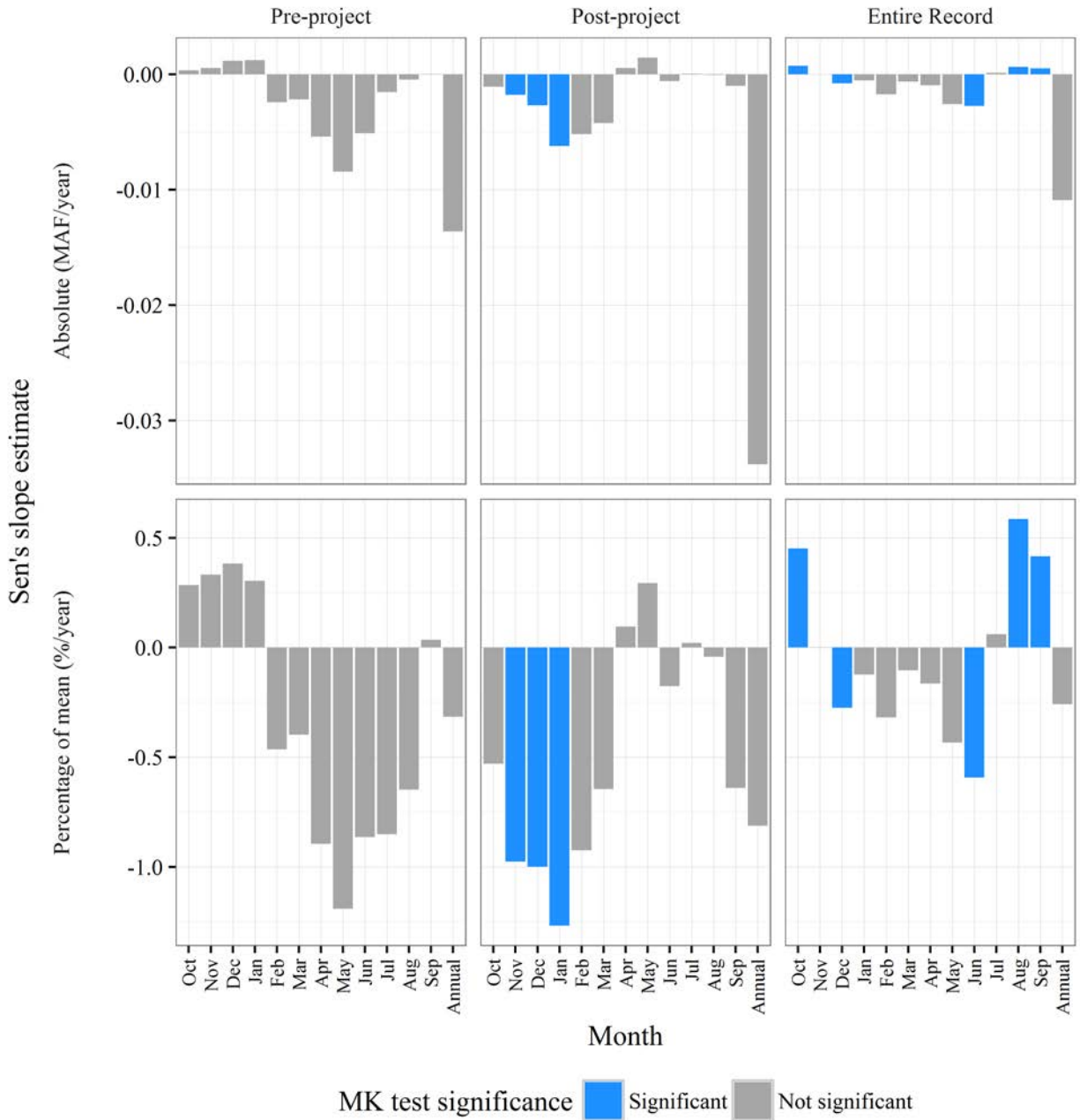


Figure 4-18 MK trend summary for Other Delta inflow (SJR + ESS).

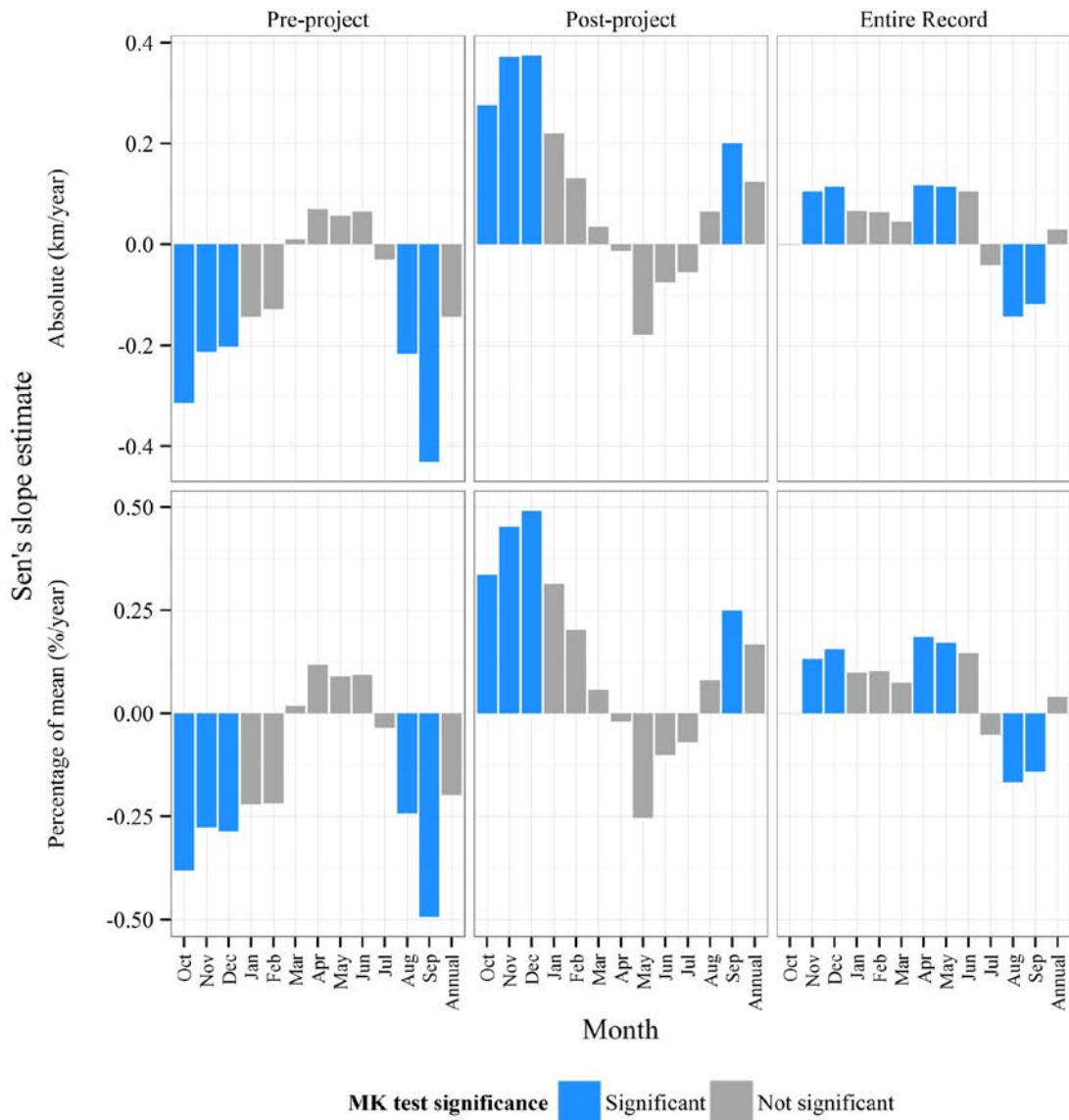


Figure 4-19 MK test results for X2

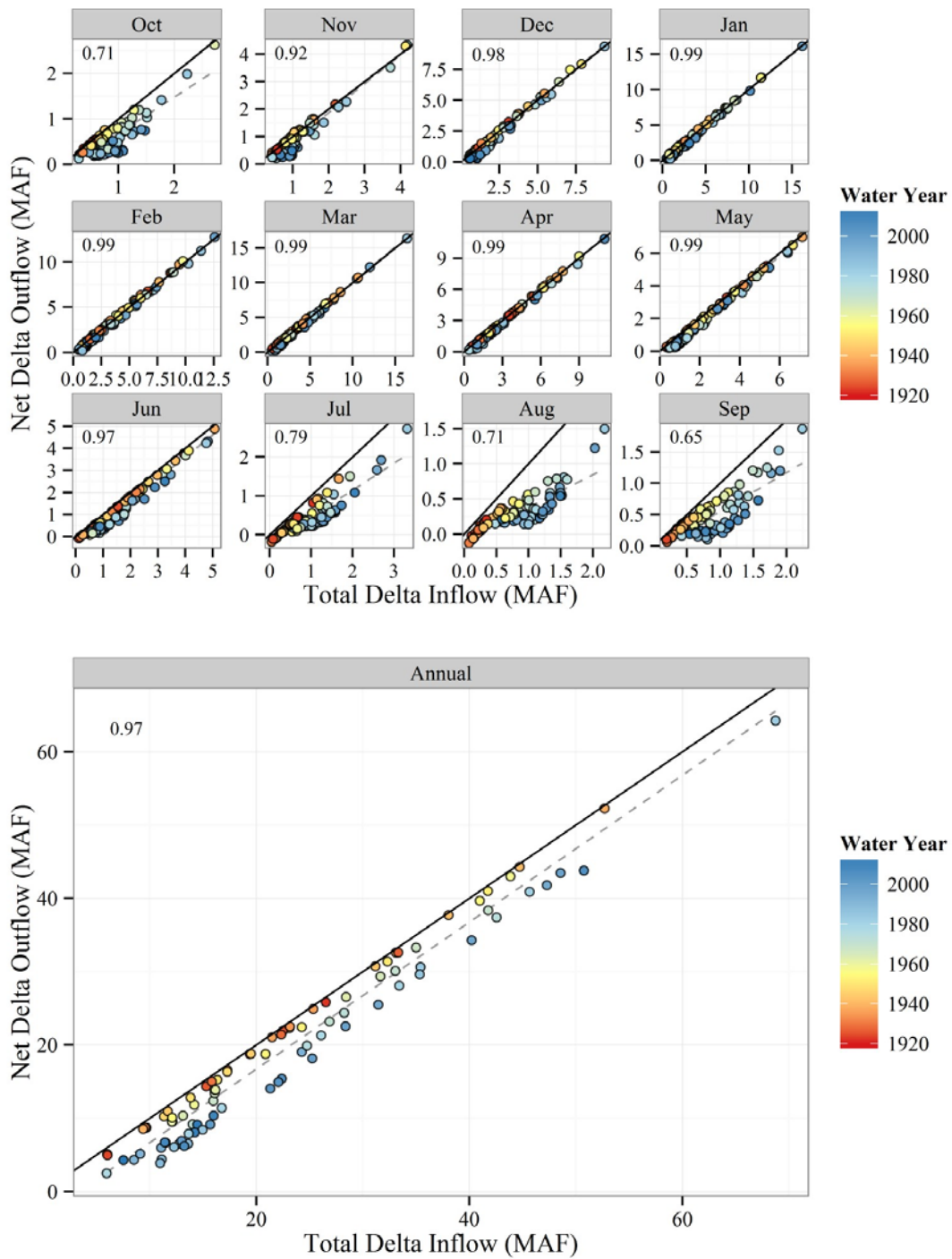


Figure 4-20 Delta water balance accounting only for total inflow. Solid black line is the 1:1 line. Dashed gray line is linear best fit, with  $r^2$  value shown on upper left.

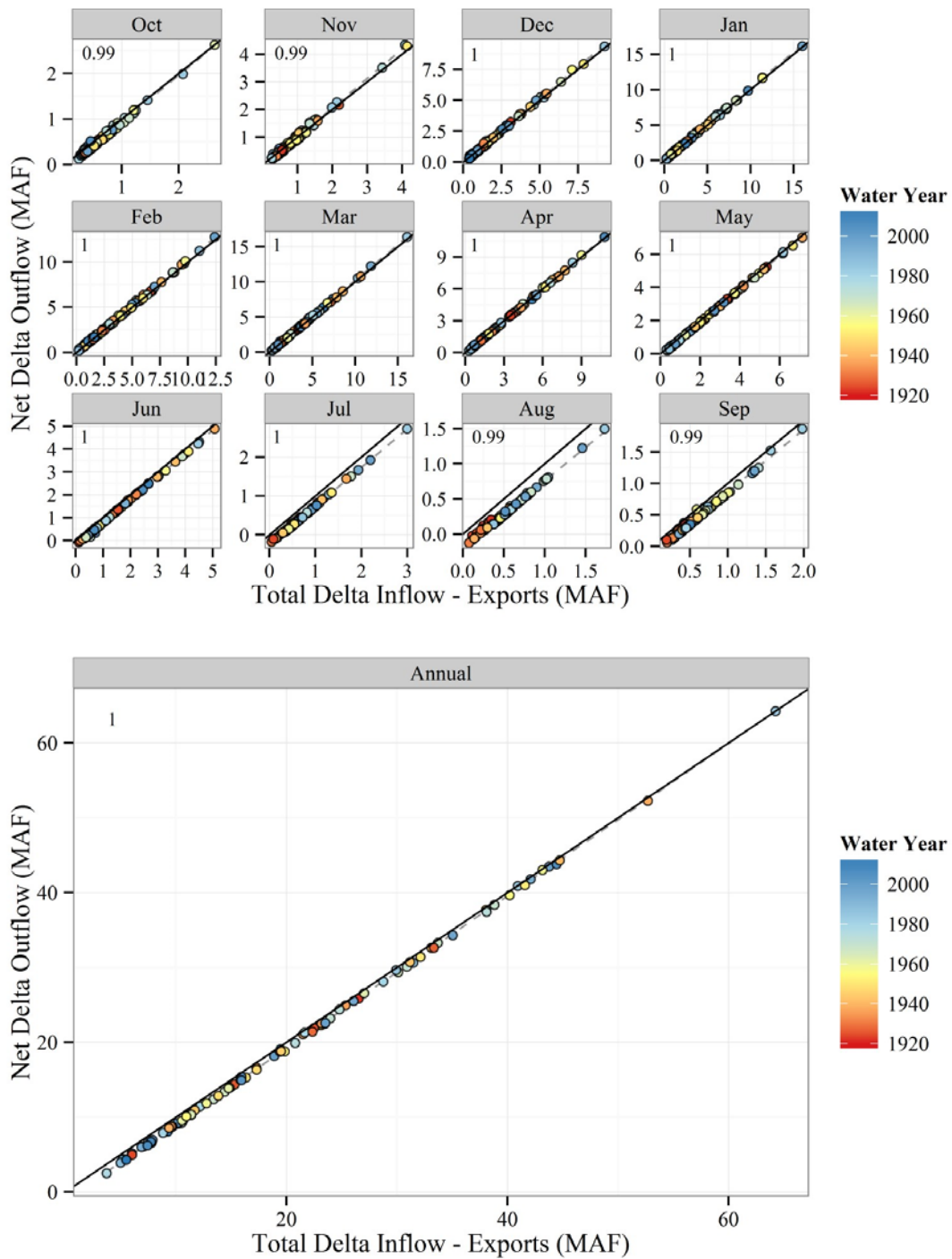


Figure 4-21 Delta water balance accounting only for total inflow and major exports. Solid black line is the 1:1 line. Dashed gray line is linear best fit, with  $r^2$  value shown on upper left.

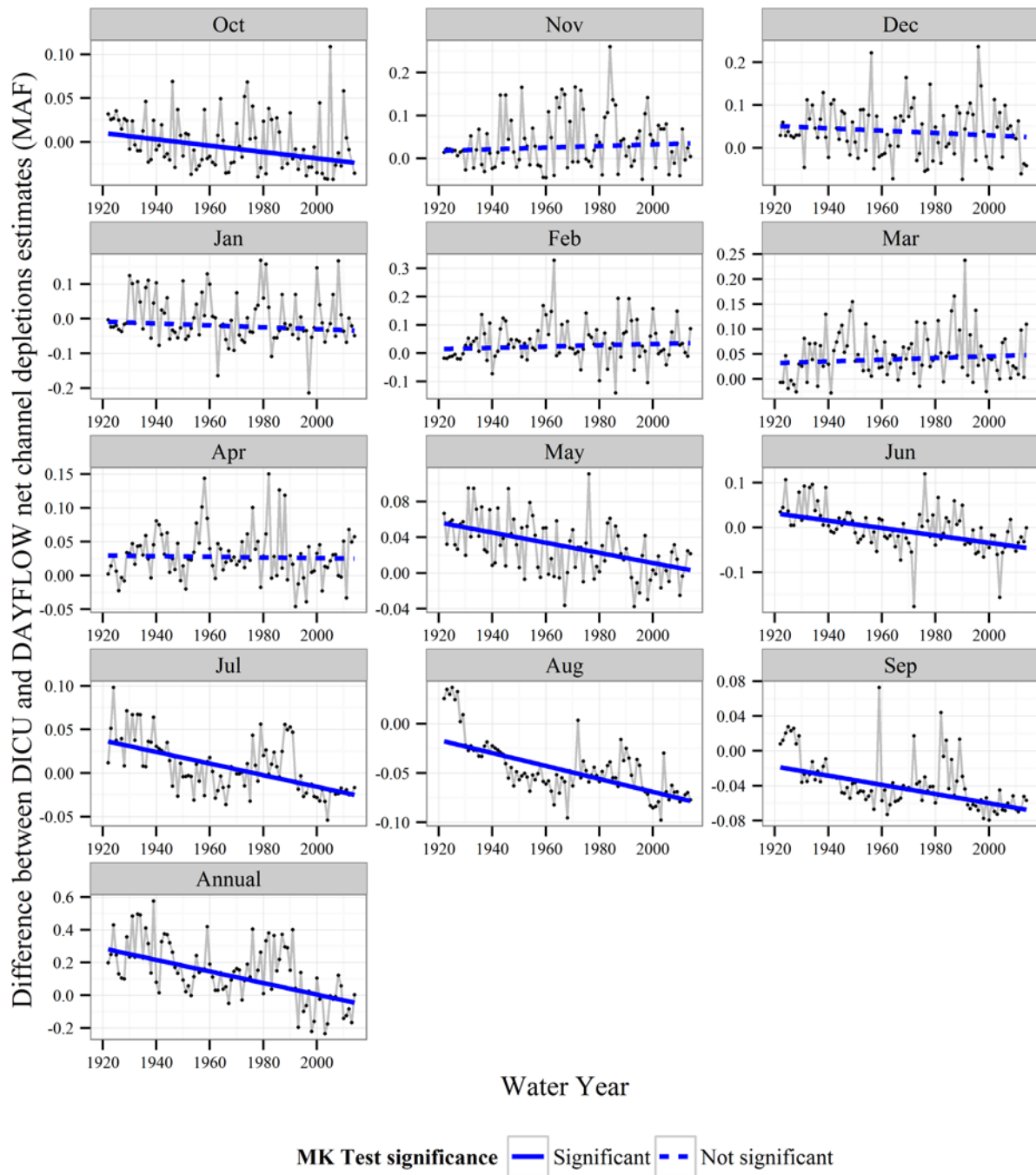


Figure 4-22 Difference between DICU model and DAYFLOW net channel depletion estimates over time, and estimates of trend.

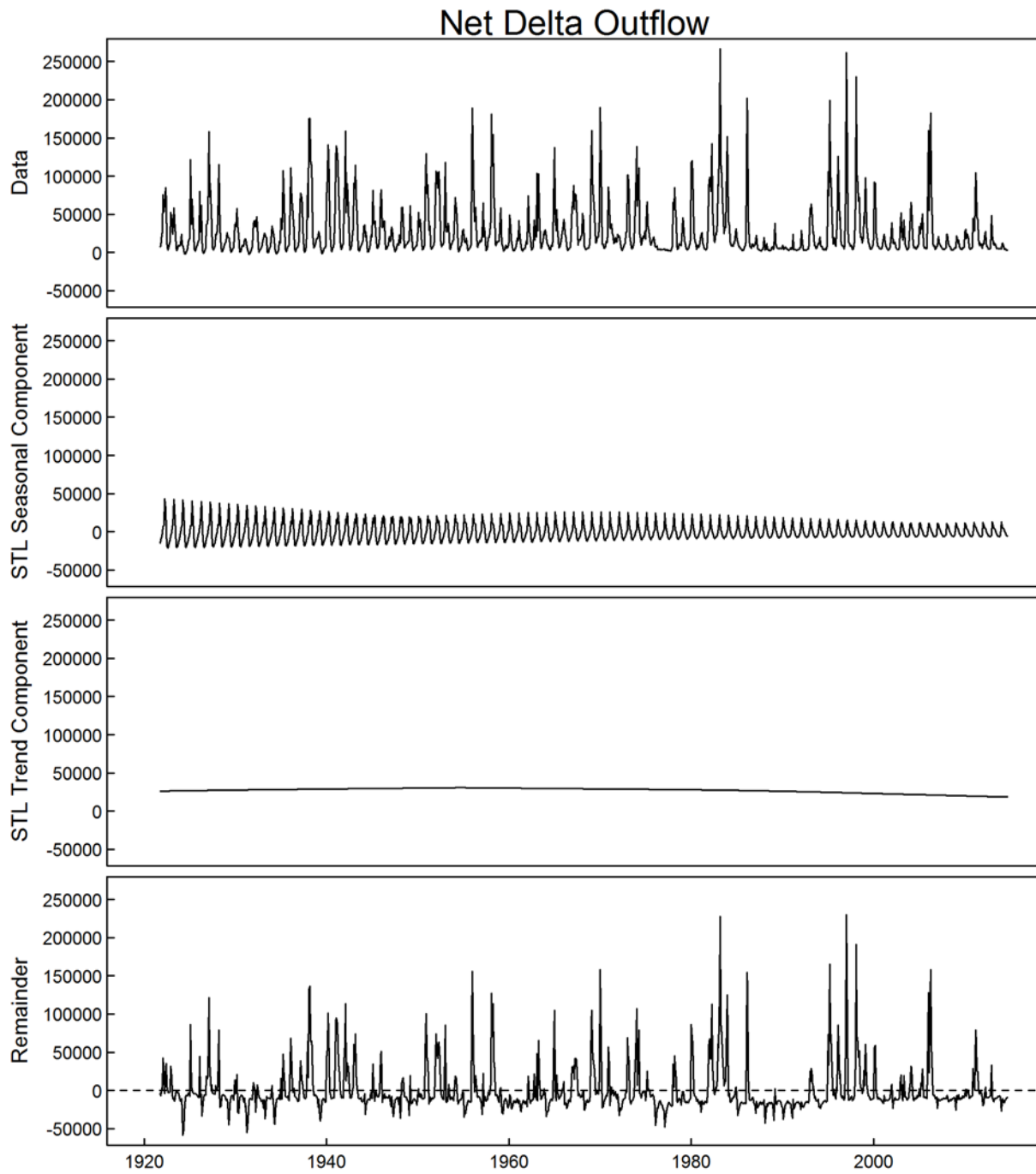


Figure 4-23 STL decomposition of net Delta outflow data (all units cfs), with a common y-axis for all components.

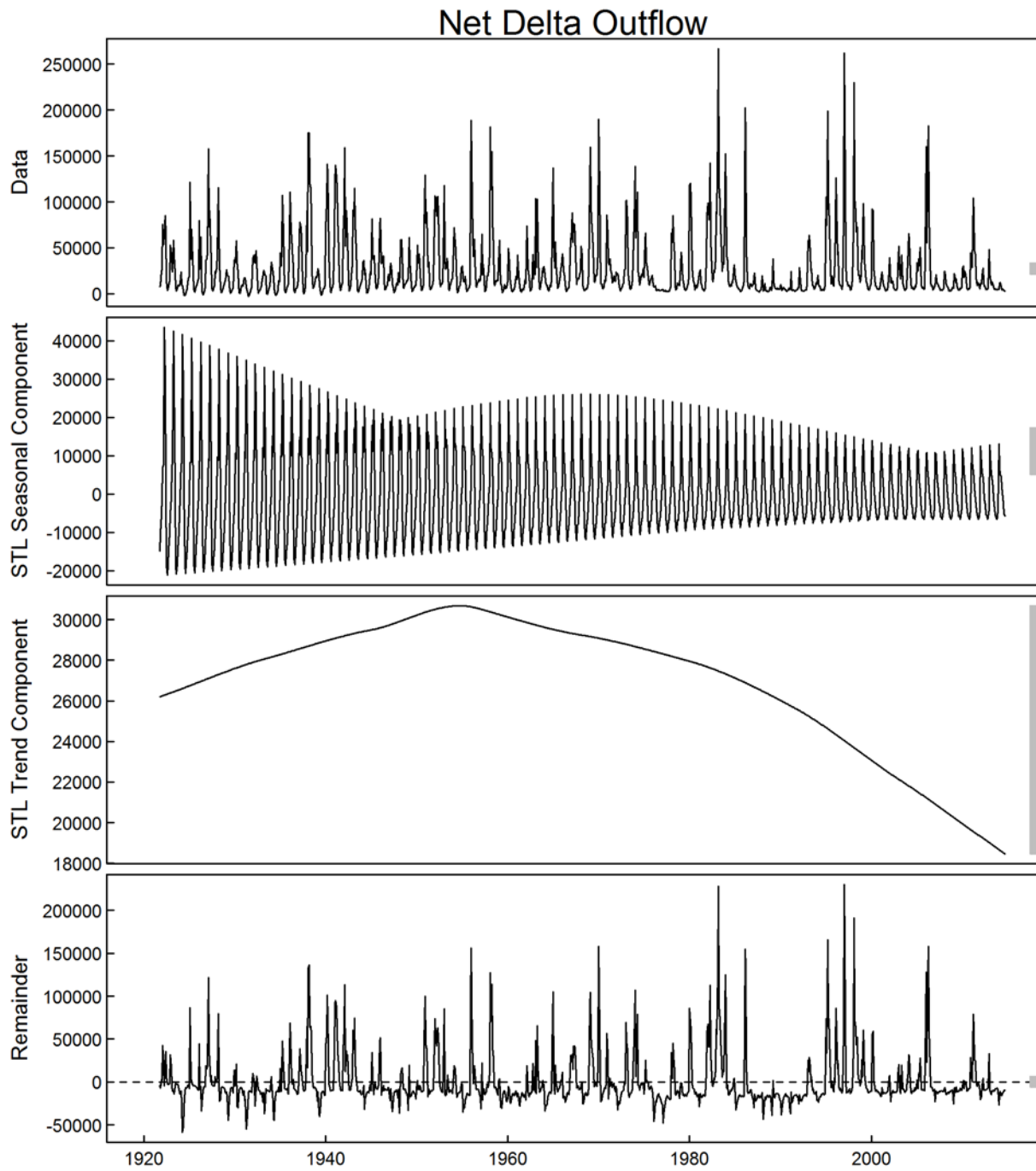


Figure 4-24 STL decomposition of net Delta outflow data (all units cfs). The gray bars on the right side of each panel are all the size of the smallest y-axis scale.

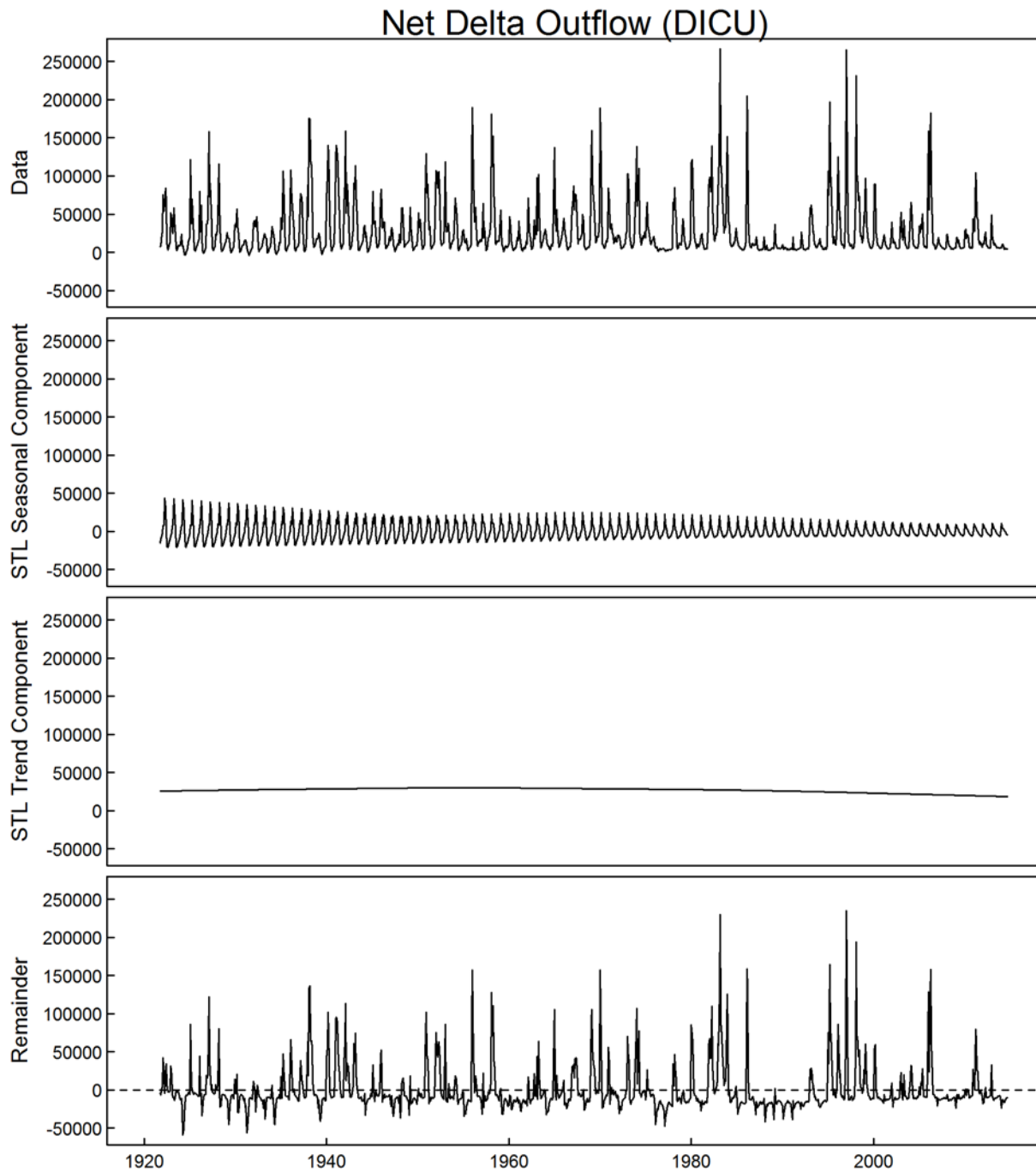


Figure 4-25 STL decomposition of net Delta outflow data (all units cfs) with a common y-axis for all components.

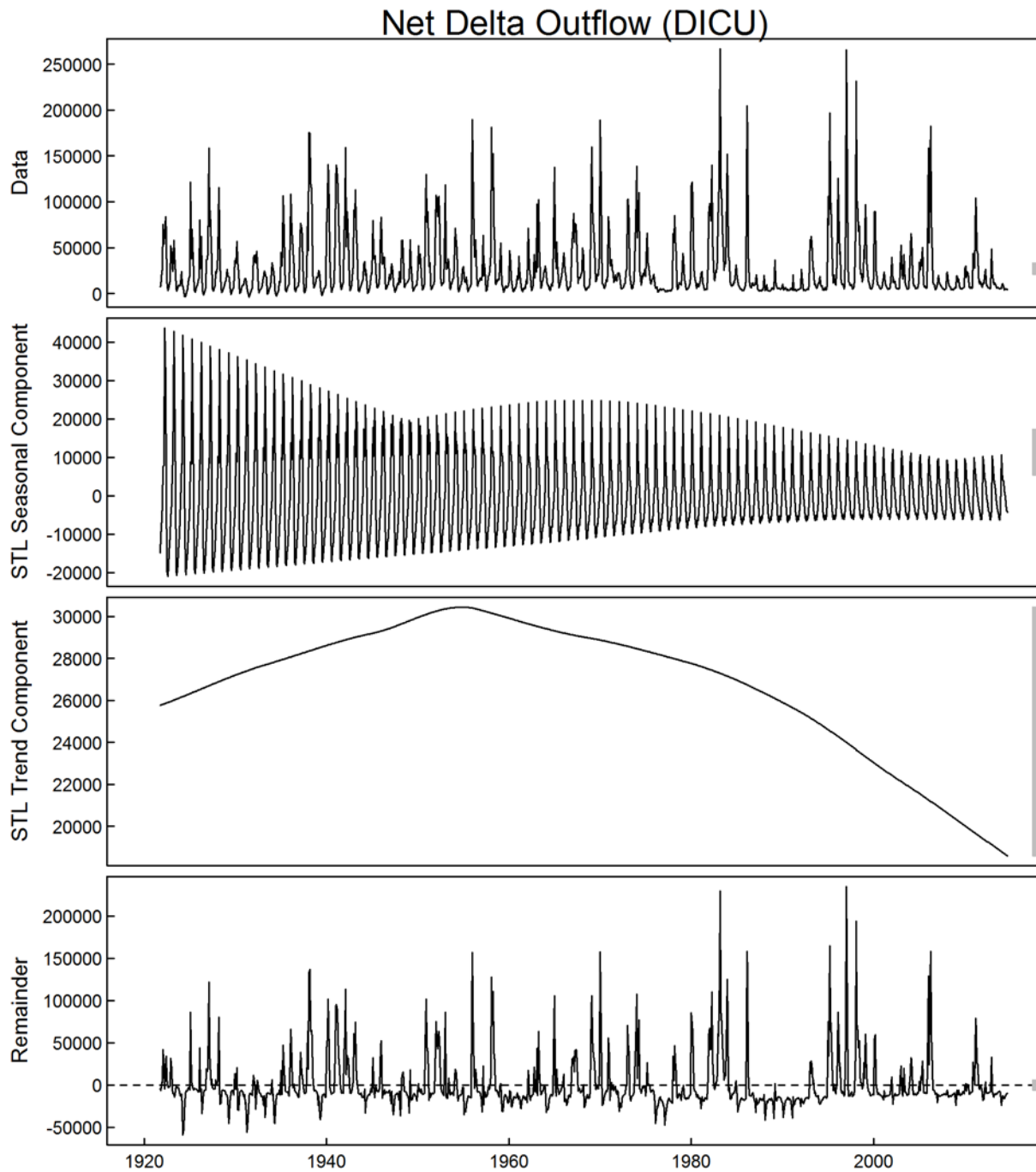
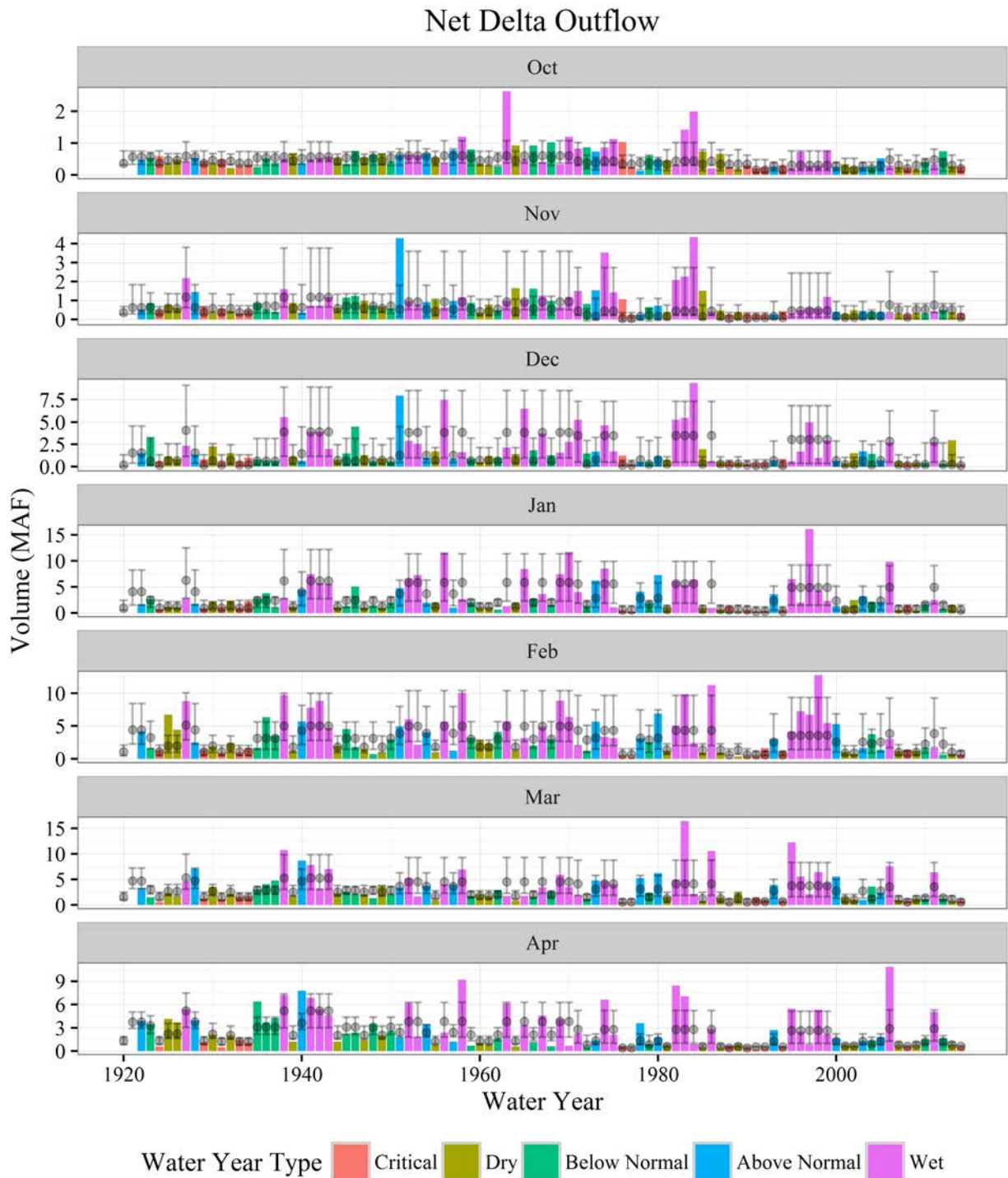


Figure 4-26 STL decomposition of net Delta outflow data using DICU model-based estimates (all units cfs). The gray bars on the right side of each panel are all the size of the smallest y-axis scale.



*Figure 4-27 Comparison of historical and LOD scenario Net Delta Outflow. Colored bars indicate historical value and water year type. The median and 10th-90th percentiles of values from the corresponding month and water year type from the chronologically closest LOD scenario are indicated by points and error-bars.*

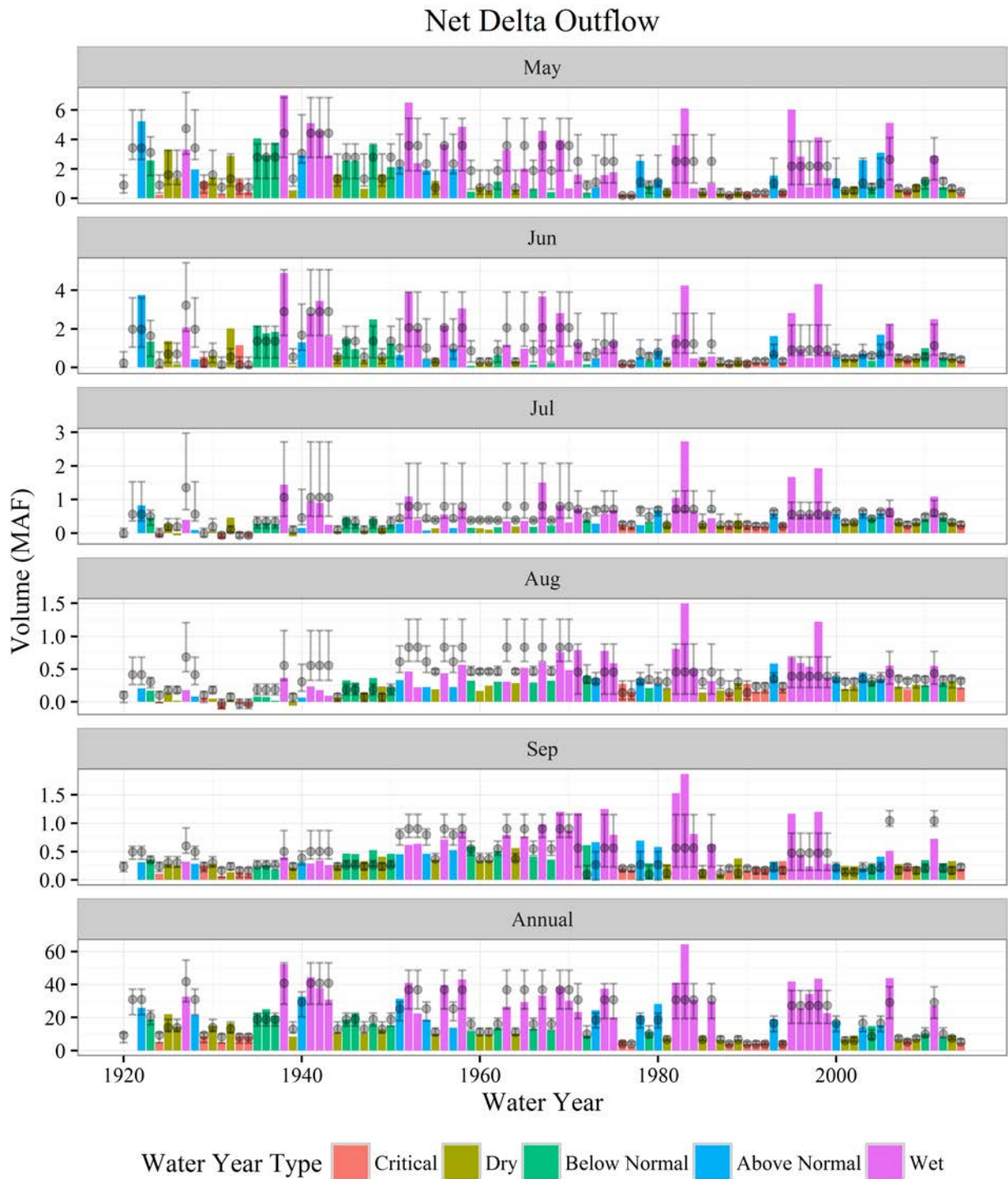
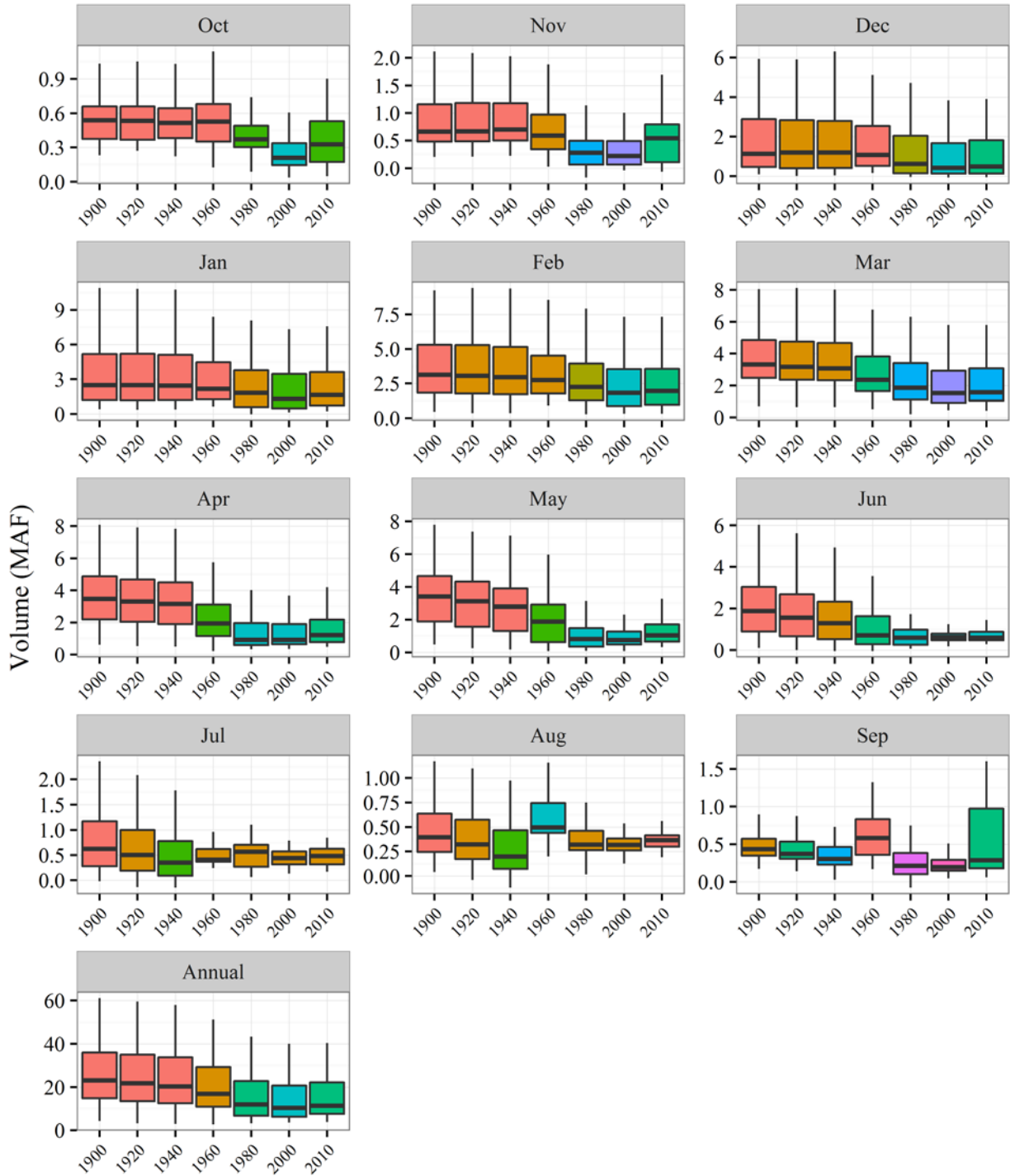


Figure 4-28 Comparison of historical and LOD scenario Net Delta Outflow (continued). Colored bars indicate historical value and water year type. The median and 10th-90th percentiles of values from the corresponding month and water year type from the chronologically closest LOD scenario are indicated by points and error-bars.



LOD

Figure 4-29 Multiple Kruskal-Wallis procedure for net Delta outflow. Boxplots filled with the same color indicate samples that were not found to differ significantly in a location by a multiple comparisons Kruskal-Wallis procedure.

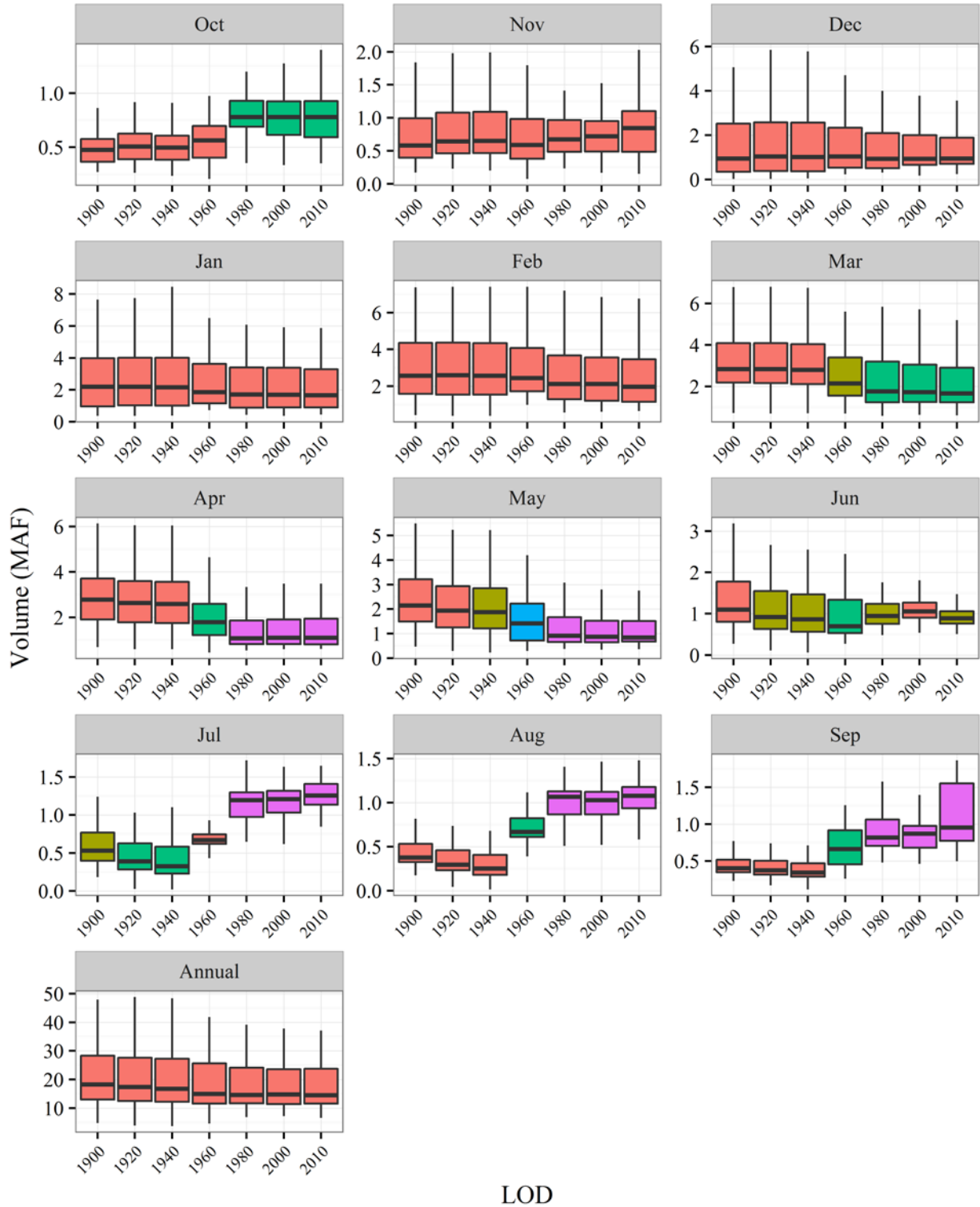
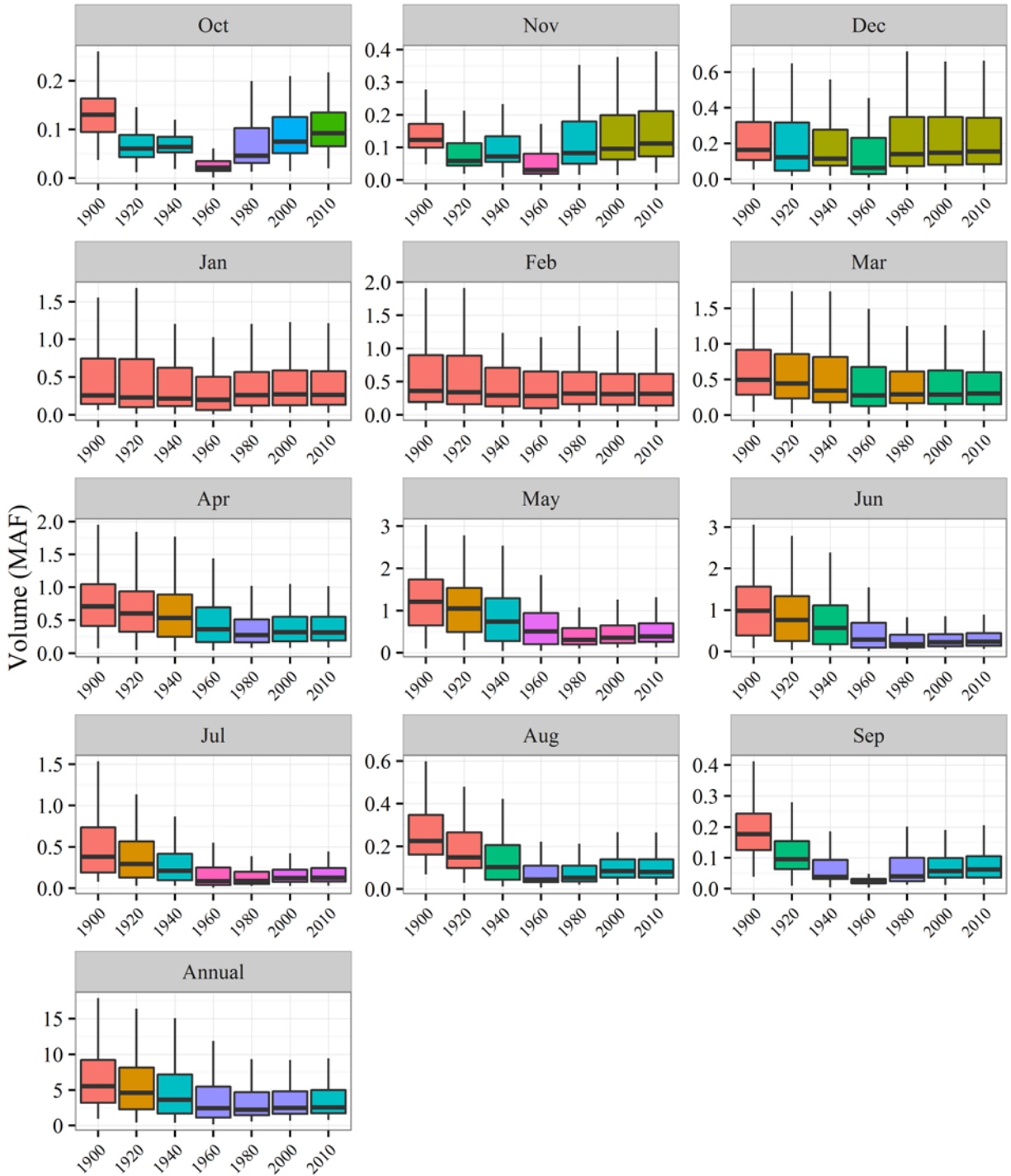


Figure 4-30 Multiple Kruskal-Wallis procedure for Sacramento Valley inflow to Delta (SAC + YOLO). Boxplots filled with the same color indicate samples that were not found to differ significantly in a location by a multiple comparisons Kruskal-Wallis procedure.



LOD

Figure 4-31 Multiple Kruskal-Wallis procedure for Other Delta inflow (SJR + ESS). Boxplots filled with the same color indicate samples that were not found to differ significantly in a location by a multiple comparisons Kruskal-Wallis procedure.

This page intentionally left blank.

# 5 EVALUATION OF SACRAMENTO VALLEY INFLOWS TO THE DELTA

---

## 5.1 HISTORICAL DATA

Time series plots of several important components of Sacramento Valley hydrology are shown in Figure 5-1 through Figure 5-8 and relate to streamflows, groundwater contributions to streamflow, surface water diversions, groundwater pumping, and precipitation. As in the previous chapter, each set of plots includes monthly data as well as annual data. Curves depicting the ten-year moving average of each time series are overlaid in red. Some changes in flows over time are immediately apparent in these plots. A visual interpretation of the plots follows.

The Four River inflow time series (Figure 5-1) shows a pattern similar to that in Sacramento Valley inflows to the Delta (Figure 4-6), with increasing July-October flows over the period of record, and variable annual flows without a clear visual trend. The Four River Index plots (Figure 5-2), which are based on unimpaired rim watershed conditions, do not show the same visual pattern in the summer/early fall months, indicating the contribution of stored water releases to actual inflows as reservoir storage came on line from the 1940s to the late 1960s. The eight station precipitation index shows a large month-to-month variation but no visual trends over time (Figure 5-3). Other inflows (Minor Rim flows) follow the general pattern associated with the Four River inflows, with increases in the summer/early fall months corresponding to reservoir releases (Figure 5-4). The groundwater contribution to Sacramento River flows (obtained from C2VSIM) is shown in Figure 5-5. Although the magnitude of this interaction is small compared to the Sacramento River flows (from -1 to +1 MAF), a visual trend is apparent in several months (June through September) and on an annual basis. The groundwater contribution declines in these months, possibly as a result of lower summer groundwater tables in the Sacramento Valley. Surface water diversions (primarily for agriculture) show a clear increase in the irrigation season spanning March through October. The increasing trend in surface diversions occurs primarily in the earlier part of the record from the 1920s to the 1960s (Figure 5-6). A similar pattern is seen for Sacramento groundwater pumping for agriculture (Figure 5-7). The surface water diversions are about twice as large as groundwater diversions. Sacramento Valley precipitation does not show any visual trends over time, similar to the eight-station index (Figure 5-8). These variables are used to develop a water balance for the Sacramento Valley.

A more formal evaluation of selected time trends is shown in Figure 5-9 and Figure 5-10. These plots show the trend line derived from Sen's slope estimator and the significance of the corresponding trend according to the Mann-Kendall test. Separate tests were performed for the pre-Project period (water years 1922–1967), post-Project period (water years 1968–2012), and the full period (1922–2012). The MK tests unanimously find a significant increase in summer and early fall inflows (Four River inflows, and Minor Rim inflows) over the pre-

Project period and the entire record. For spring inflows, the nominal directions of the trend lines are consistent with the decreases discussed above (negative values of Sen's slope), but the relative size of the changes are not always large enough to result in a significant MK test result.

The results of the trend tests are also shown as bar charts. Figure 5-11 shows the monthly and annual patterns in Four River inflows. As in the previous plots, these show the largest percentage increases occur in June through November for the pre-Project period and for the entire period, consistent with reservoir releases over these months. Post-project trends are much smaller, although there is a small negative trend in January and a positive trend in July. No significant trends exist on an annual basis.

The Four River inflows (Figure 5-11) and the unimpaired Four River Index (Figure 5-12) provide an interesting comparison for identifying the effects of reservoir development. The Four River inflow shows significant changes over the pre-Project and the entire period over much of the summer and fall (July through November). The Four River Index trends are smaller in magnitude, although there are significant positive trends in August through January (excluding December) of the pre-project period. Because the Four River Index explicitly removes reservoir effects, these trends are indicative of other alterations to the river system, such as channelization (which may be expected to increase flows) or changes in precipitation patterns, watershed characteristics, and runoff from the upper elevation catchments. Minor Rim inflows exhibit monthly trends similar to those for the Four River inflow (Figure 5-13).

To isolate the causes of these observed changes in Sacramento Valley inflows, we performed a water balance on the entire valley using available observed data and aggregated model output from C2VSIM on monthly and annual bases. The graphical approach employed is similar to the one discussed in the previous chapter. Plotting the major Four River inflows from the Sacramento, Feather, American, and Yuba rivers against Sacramento inflow to the Delta shows a mismatch in all but the driest conditions (Figure 5-14). This mismatch is defined as Sacramento Valley Accretions/Depletions in Table 2-1. The monthly mismatches identify depletions in the summer and accretions during the winter and spring, with a net annual accretion that can exceed 10 MAF in wetter years. By accounting for Minor Rim inflows and Trinity imports (Figure 5-15), much of the mismatch is accounted for in the wet months and in the annual balance. However, a sizable depletion term remains in July and August.

To further explain the accretion and depletion terms noted in Figure 5-15, we sought to account for the contribution of valley floor precipitation and return flows from surface water and groundwater use in the Sacramento Valley for both irrigation and municipal purposes. First, we tried estimating runoff flows from valley floor precipitation, applied irrigation water from groundwater pumping, and applied irrigation water from surface water diversions by using arbitrary but reasonably sized runoff factors (0.2, 0.2, and 0.1, respectively). These "constant" runoff factors, together with C2VSIM estimates of Sacramento River gain from groundwater, were used to account for much of the remaining accretion terms in July and August (Figure 5-16) at the cost of slightly noisier estimates on the annual scale. The remaining mismatches for the winter months suggested the need to account for a variable (also referred to as "optimized") runoff factor. We proceeded to statistically estimate runoff coefficients using a robust linear regression of the terms with unknown runoff factors against the net effect of all other available Sacramento Valley accretion/depletion terms. We allowed

only the precipitation runoff factor to vary by month, and all runoff factors were constrained to fall between 0 and 1 in the fitting. The estimated runoff coefficients and associated uncertainties are shown in Figure 5-17. While the minimal rainfall amounts in the summer months result in (essentially) undetermined runoff factors, the pattern of runoff factors in other months makes intuitive sense and is consistent with the published literature. In early wet season months such as November and December, the ground is unsaturated and the runoff factors are lower, compared to January through March, when the ground is saturated and more of the precipitation appears as runoff.

When the variable or “optimized” factors were used, the graphical deviations were significantly reduced for the wettest years (Figure 5-18).

The contribution of the runoff terms by year for the two different approaches used are shown in Figure 5-19 and Figure 5-20. These plots show the relative magnitudes of the different terms, and their levels across different months. Thus, surface water diversion and resulting runoff dominates in the summer months, and precipitation runoff dominates in the winter months.

The coloring of points by water year in Figure 5-18 suggests there is a change in the remaining unexplained accretion term over time. Indeed, MK tests of trend reveal significant positive trends in most months and in the annual series (Figure 5-21). Potential causes of these trends include changes in land use (increasing impermeable surface area), greater channelization and reduced loss of water to the floodplain, and the time-independent manner in which we have incorporated runoff terms in the water balance, i.e., the runoff factors may be changing with time but are assumed constant in this work.

Another potentially important change to the system’s hydrology is the timing of runoff within the season. As average temperatures continue to rise under global climate change, we expect to see earlier arrival of runoff from snowmelt in the mountainous parts of the watershed. However, reservoir operations can serve to mask this signal in the observed flows downstream of the reservoirs. Examining the cumulative proportion of unimpaired flow at the end of each month within the season (Oct–Sep) is one way to quantify this effect using the available data. Figure 5-22 shows how this quantity has changed over the period of record within each month; the nominal direction of the trend is positive (i.e., more of the season’s flow is arriving earlier) in Jan–May, although only March is significant according to the MK test. Other methods may be more informative on this type of data; we therefore fit this cumulative time series as a smooth function of month and water year with auto-correlated residuals (order 1) within each water year using a GAMM (Wood, 2006).

Figure 5-23a compares the cumulative unimpaired flow curves for the beginning and end of the record as predicted by the GAMM model. The results are consistent with the nominal direction of the trends in Jan–May in Figure 5-22, but the added intra-seasonal structure of the GAMM results in small standard errors and good confidence that earlier arrival of winter runoff is consistent with the data.

By associating the end of each month with the number of days since the beginning of the water year and interpolating cumulative proportions between months, this model can also be used to visualize trends in the time of arrival of 50% of the season’s unimpaired flow. This quantity has been used to characterize changes in flow arrival timing in other studies (Hidalgo et al., 2009). Figure 5-23b shows the day of 50% of unimpaired flow is about 10 days

earlier in the later part of the record than it was in the beginning of the record. Changes in the timing of arrival of snowmelt runoff can have important consequences for water supply in managed watersheds due to flood control rules for reservoir operations.

In contrast, a similar calculation using the reservoir-impacted Four River inflows shows much stronger evidence of changes, and the signs of the change in the spring and winter are the opposite of those using the unimpaired index flows (Figure 5-24). This serves to highlight how the management operations implicit in many of the observed flow series can serve to mask the underlying climate signal.

## 5.2 LOD SCENARIO DATA

LOD scenario calculations for the Sacramento Valley inflow to the Delta are compared to the observed flows in Figure 5-25 and Figure 5-26. These plots follow the style used in Chapter 4 for the Delta outflows (Figure 4-28). The bars represent the observed value for a given month and year, colored by water year, and the LOD-computed range for the nearest LOD year for the same water year type is shown as a circular symbols with error bars representing the 10<sup>th</sup> to 90<sup>th</sup> percentile range. The observed and modeled values are in the same range over the period of record spanning a wide range of LODs and water year types. Additional evaluation of the model results is presented below.

The three major contributors to Sacramento Valley inflows to the Delta (the Four River inflow, Sacramento Valley Accretions/Depletions, and Trinity Imports) are shown as a function of LOD and by month and year in Figure 5-27. Each bar in these plots represents average values over the entire period of record. On an annual basis, there is a slight decrease in the total flows, largely resulting from a decrease in the Four River inflows. On a monthly basis, one can see the seasonal change in the Four River flows, with increases in the summer months, and decreases in the winter and spring months. Although the average of the LOD results across different water years shows a decrease in the annual Sacramento Valley inflows to the Delta, the observed data do not show this trend (Figure 4-12 and Figure 4-17). On a monthly basis, these plots show an increase in the flows in the July through November period in the observed data that is not seen in the modeled values.

The LOD data can also be evaluated using the KW test instead of the averages, as done for the Delta inflows and outflows and shown in Figure 4-29 through Figure 4-31. This analysis is shown for the Four River inflow in Figure 5-28. On an annual basis, this shows no statistically significant trend over the LODs. This is consistent with the trends in the observed data (Figure 5-11). However, the model shows minimal increase in the July-October flows in the pre-Project LOD years (1900, 1920, and 1940), with the exception of the 1960 LOD. In comparison the observed data show a statistically significant increase in these flows over the pre-Project period. Post-Project LOD changes in Four River inflow are generally not significant for most months, largely consistent with the observed data patterns.

Although it is difficult to exactly compare continuous time trend estimates as given by the MK test with the discrete changes across LOD datasets using the multiple KW procedure, the two sources provide some agreement, although there are key differences when looked at specific time periods. For example, the two data sources agree that June–October flows are higher than they used to be, although they disagree on when the change occurred. Both datasets show decreases in the winter and spring, although the LOD dataset is more confident of a decrease in January–March. This is generally consistent with the Sacramento Valley inflows to the Delta (Sacramento River and Yolo Bypass), which suggest higher flows in July through

October with the later LOD scenarios. Based on the above examination, the LOD data provide valuable insight into the broader causes of the observed flow changes over the time period of the study, but are not adequate to parse out changes in specific periods.

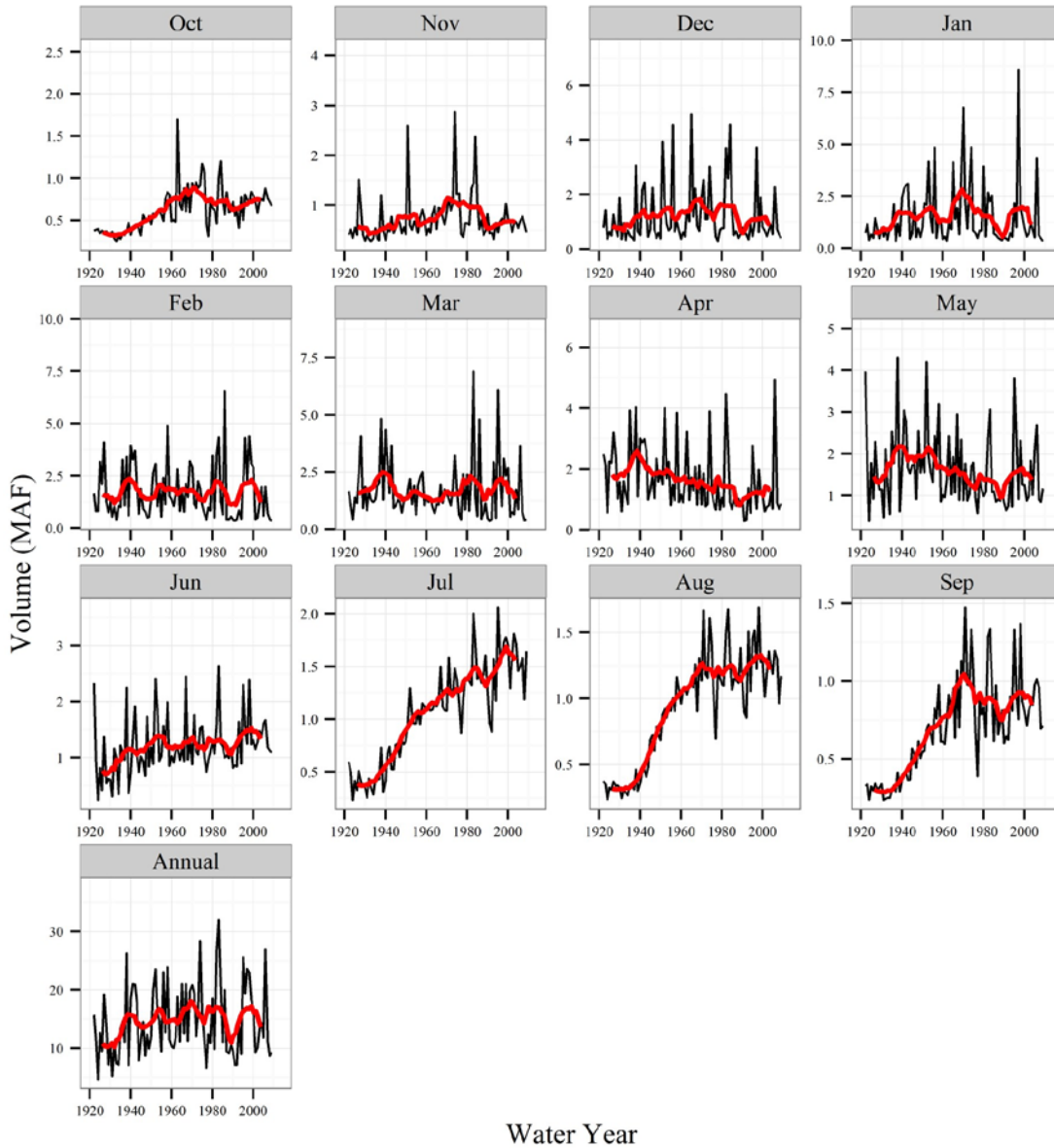


Figure 5-1 Four River inflow time series plots with 10 year moving average (red)

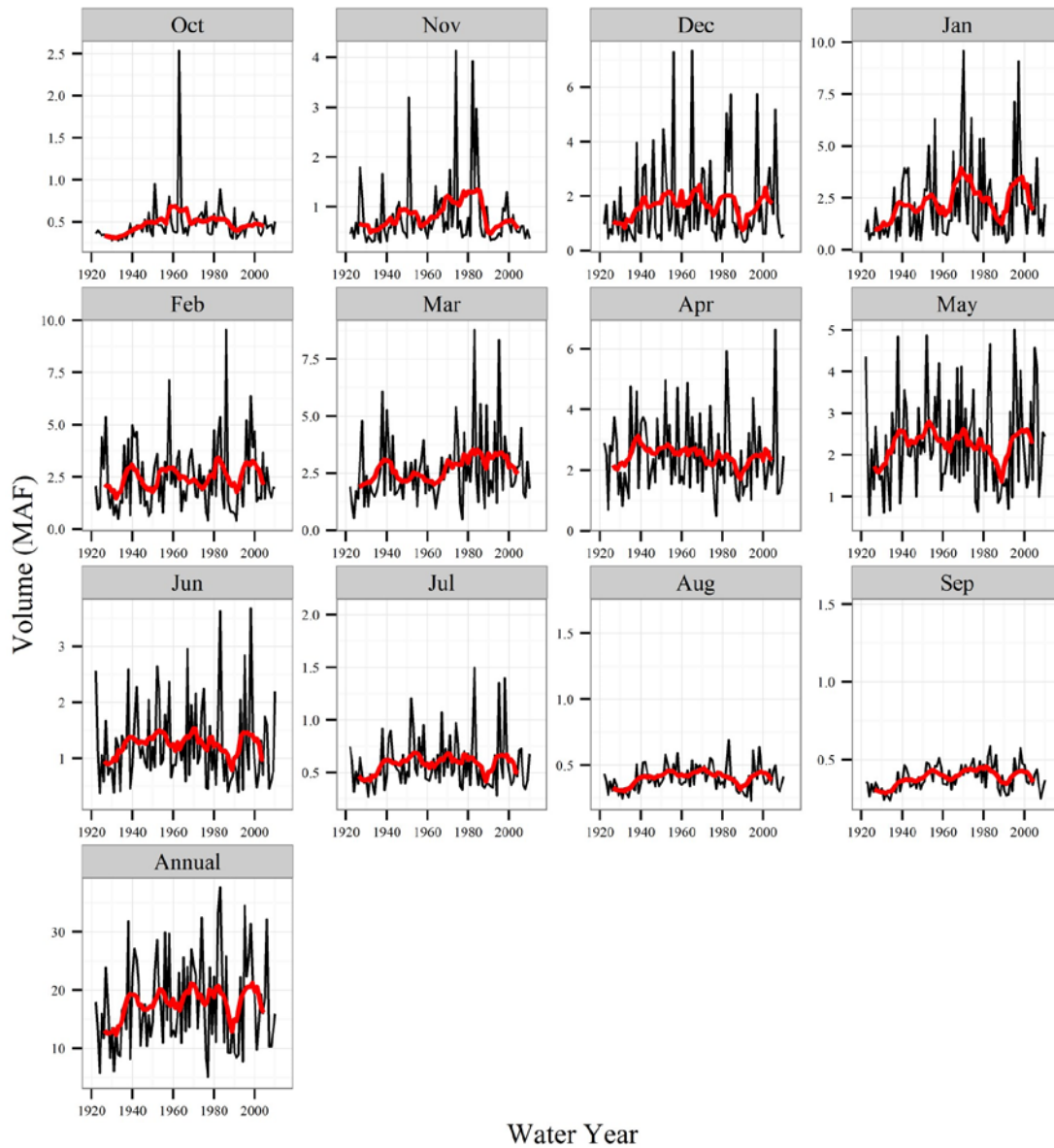


Figure 5-2 Four River Index time series plots with 10 year moving average (red)

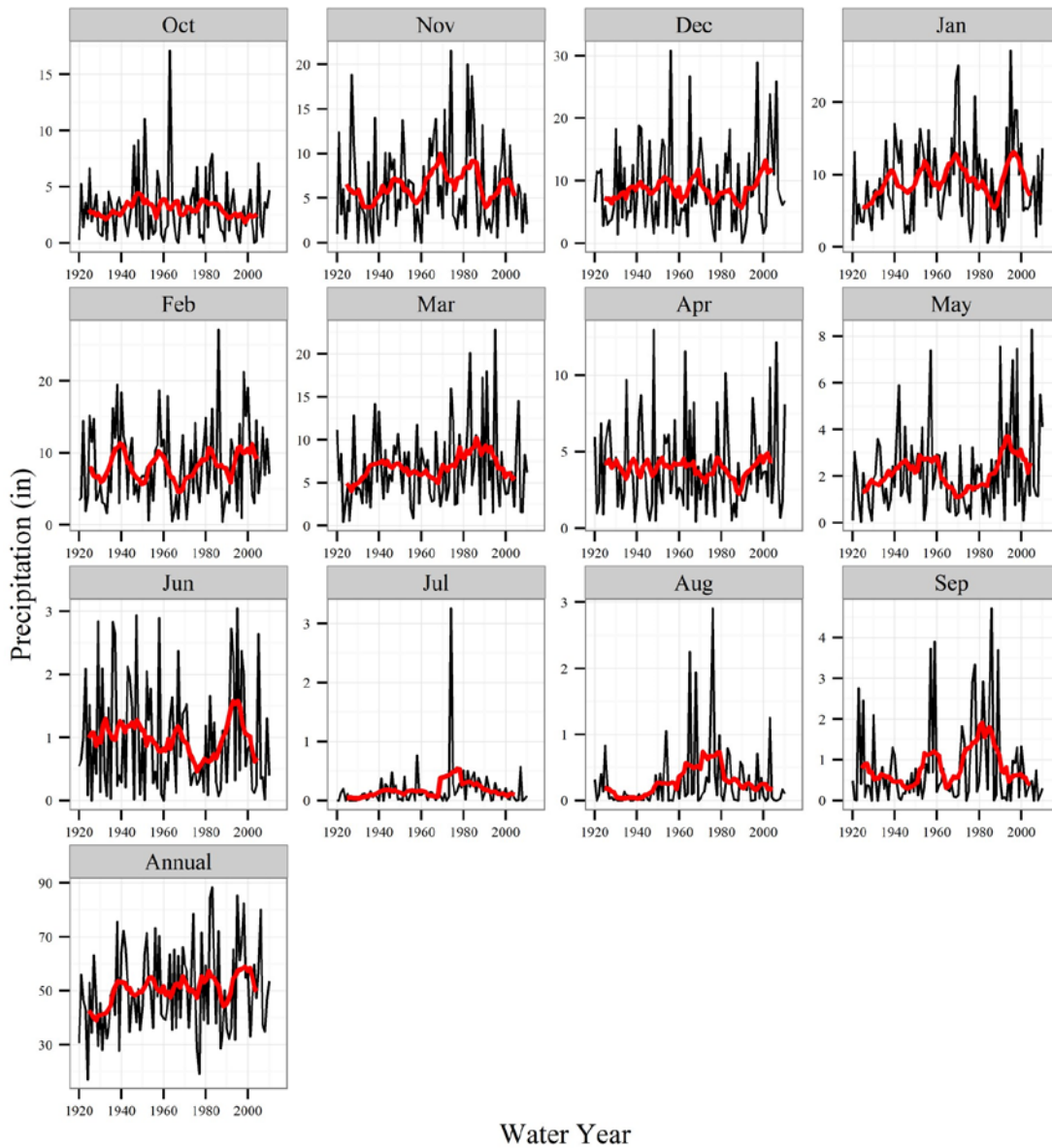


Figure 5-3 Eight station precipitation index time series plots with 10 year moving average (red)

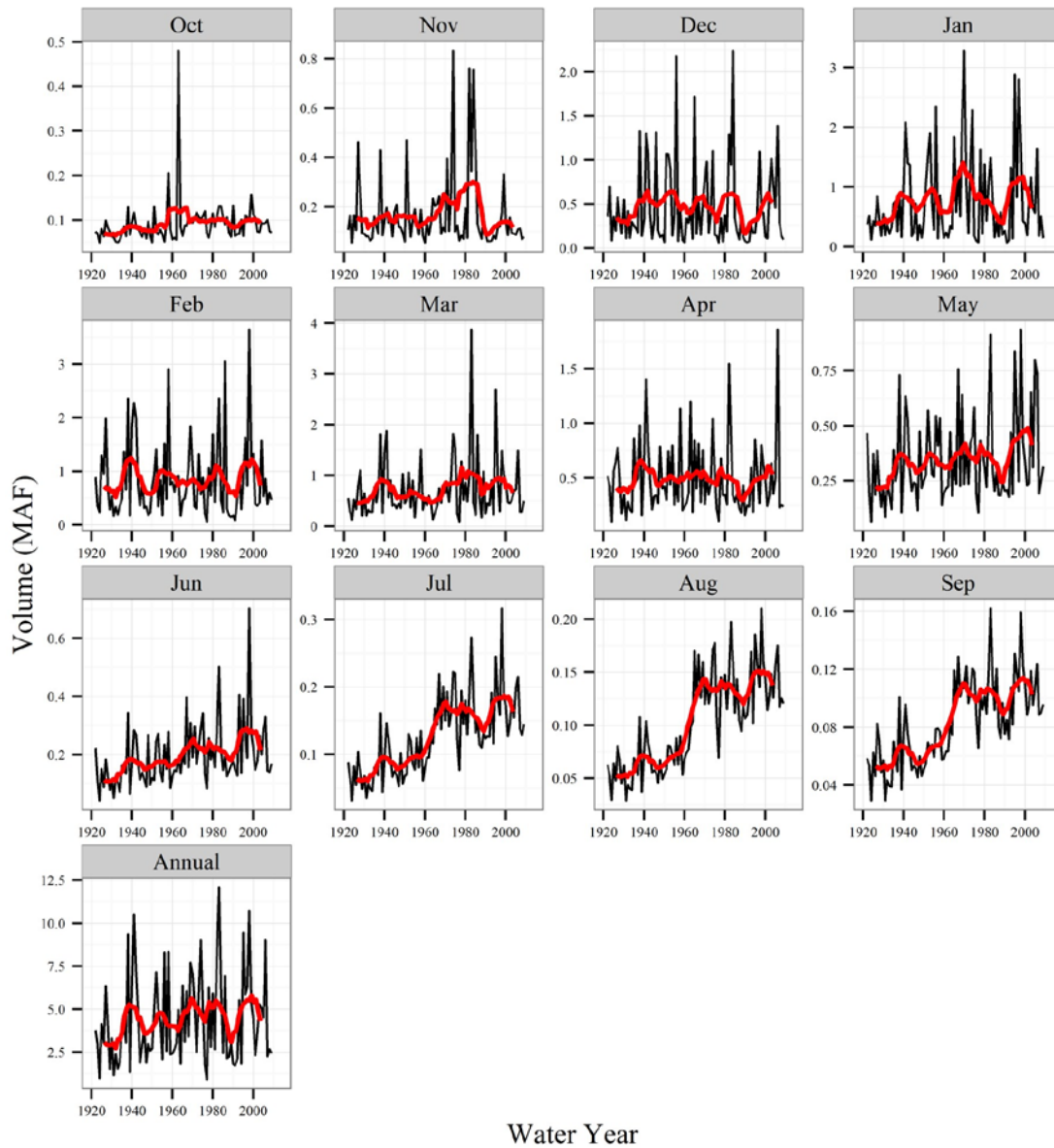


Figure 5-4 Minor Rim inflows time series plots with 10 year moving average (red)

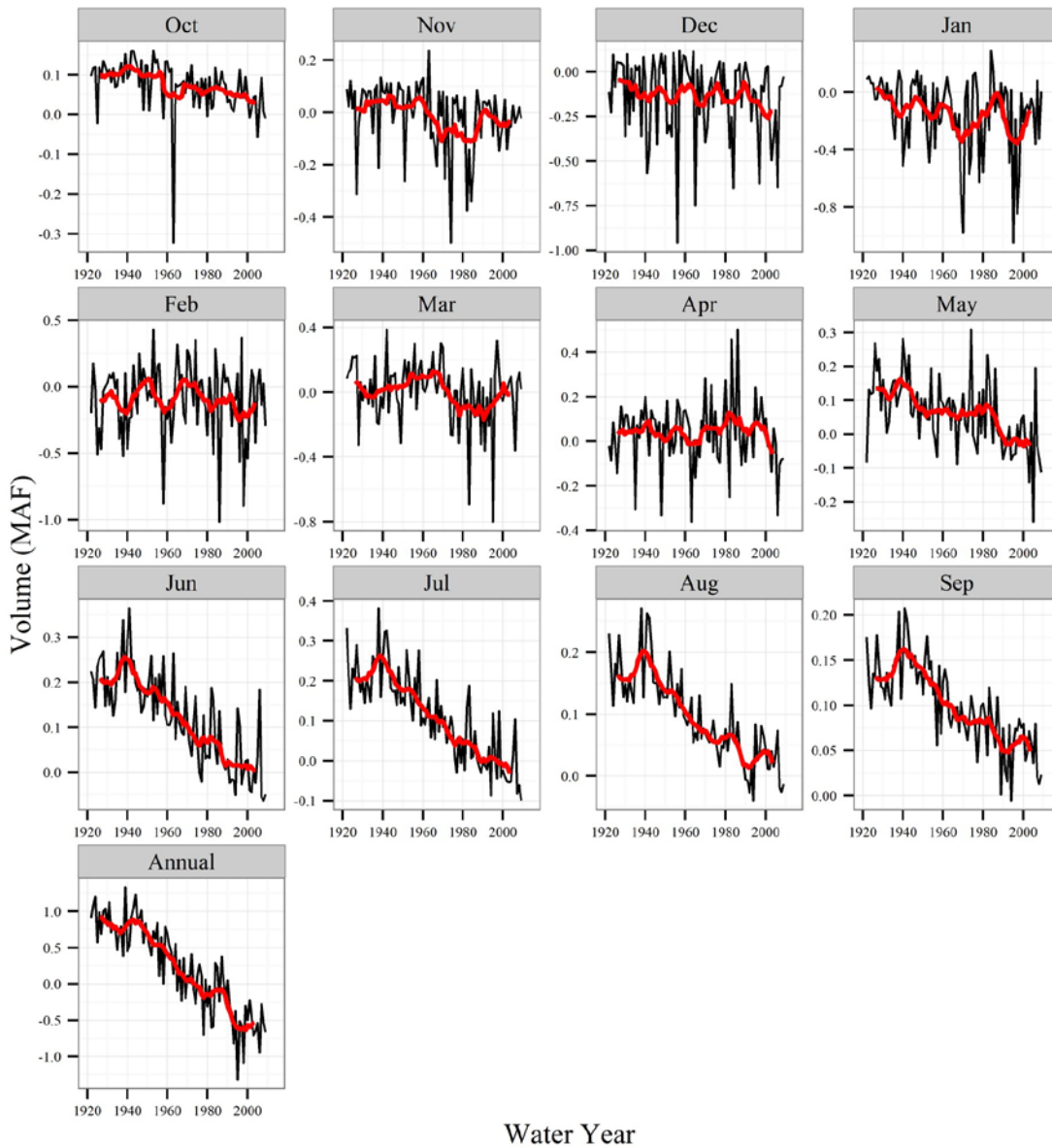


Figure 5-5 Sacramento River gain from groundwater time series plots with 10 year moving average (red)

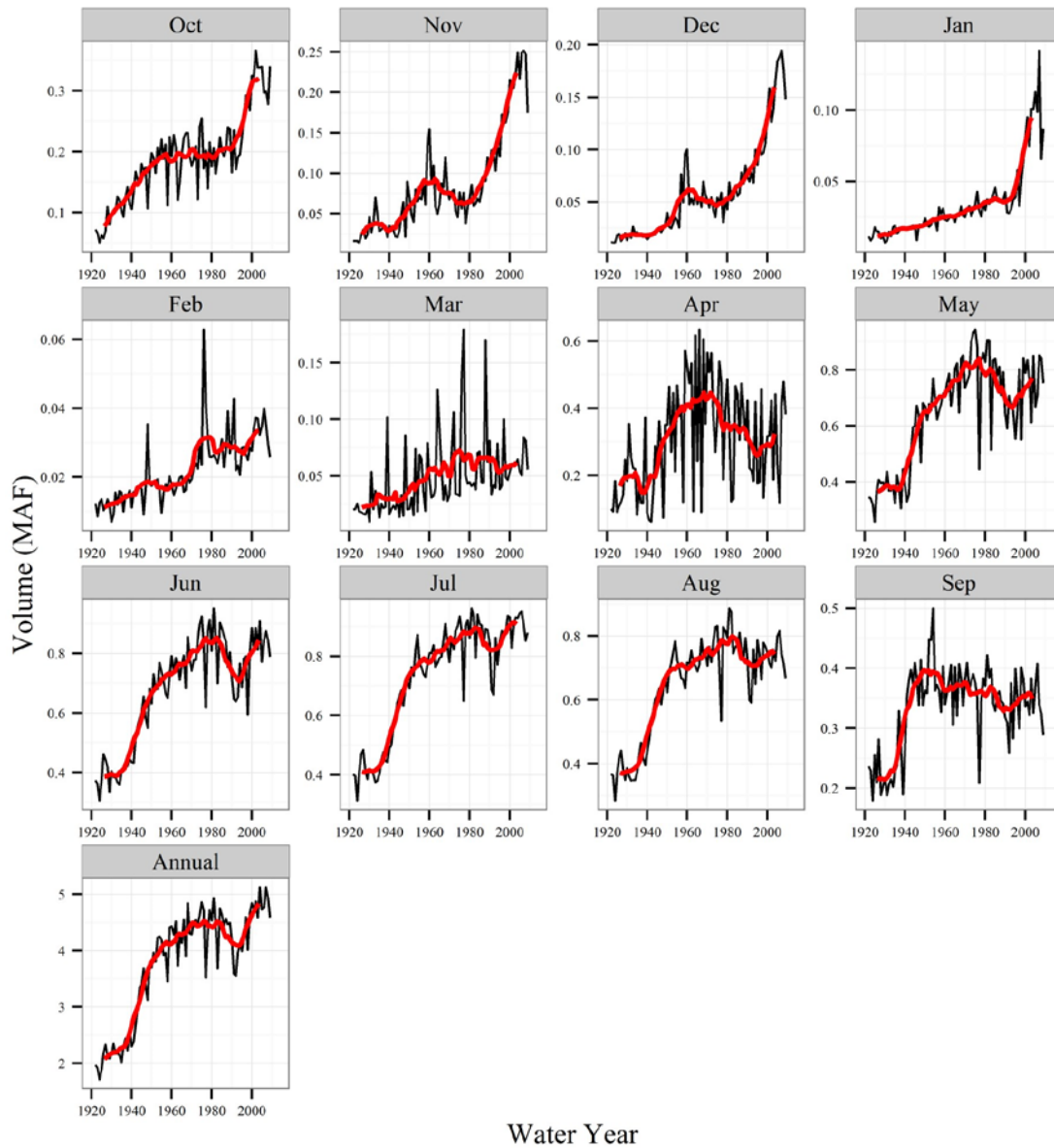


Figure 5-6 Sacramento Valley surface water diversions time series plots with 10 year moving average (red)

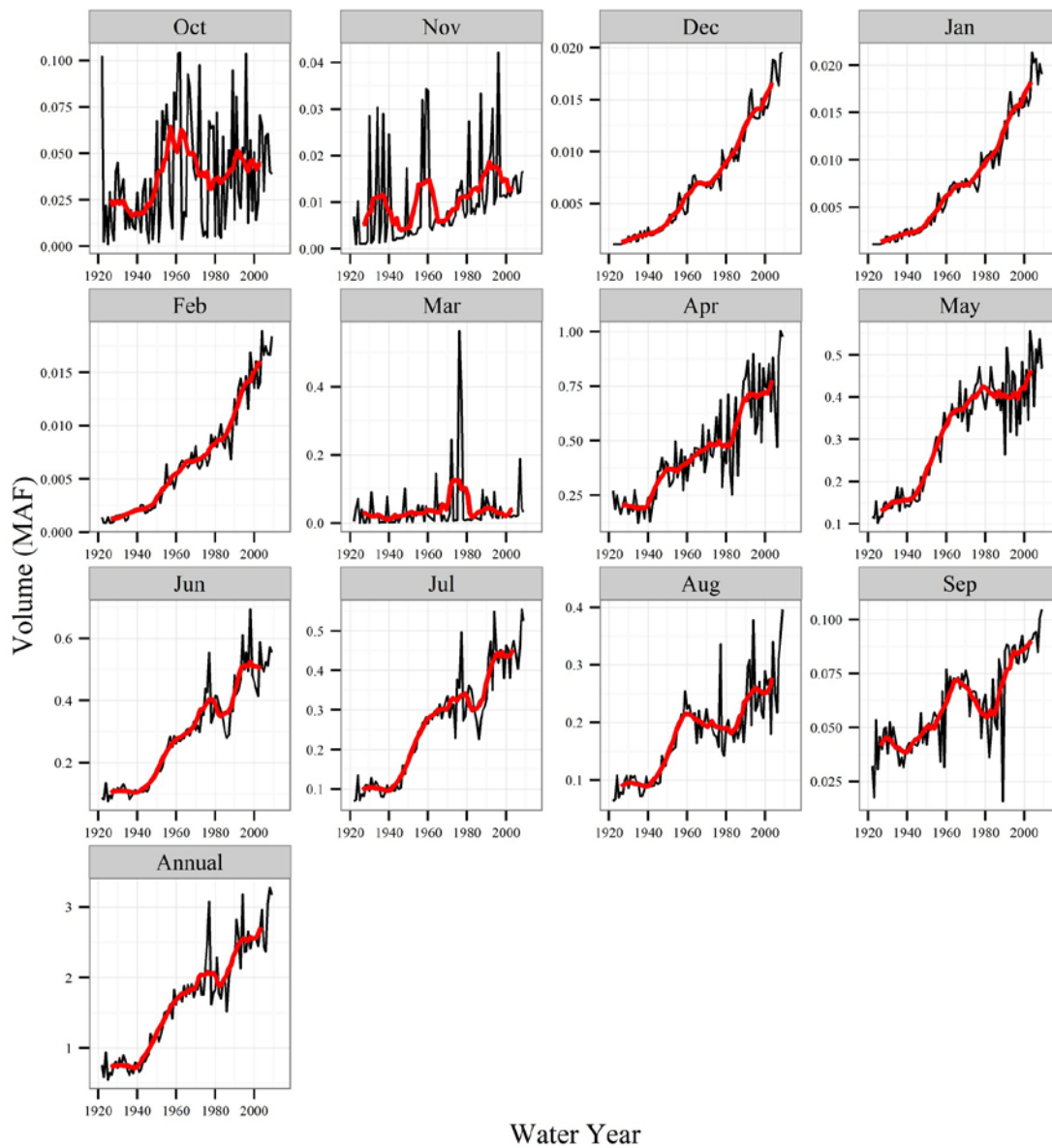


Figure 5-7 Sacramento Valley groundwater pumping time series plots with 10 year moving average (red)

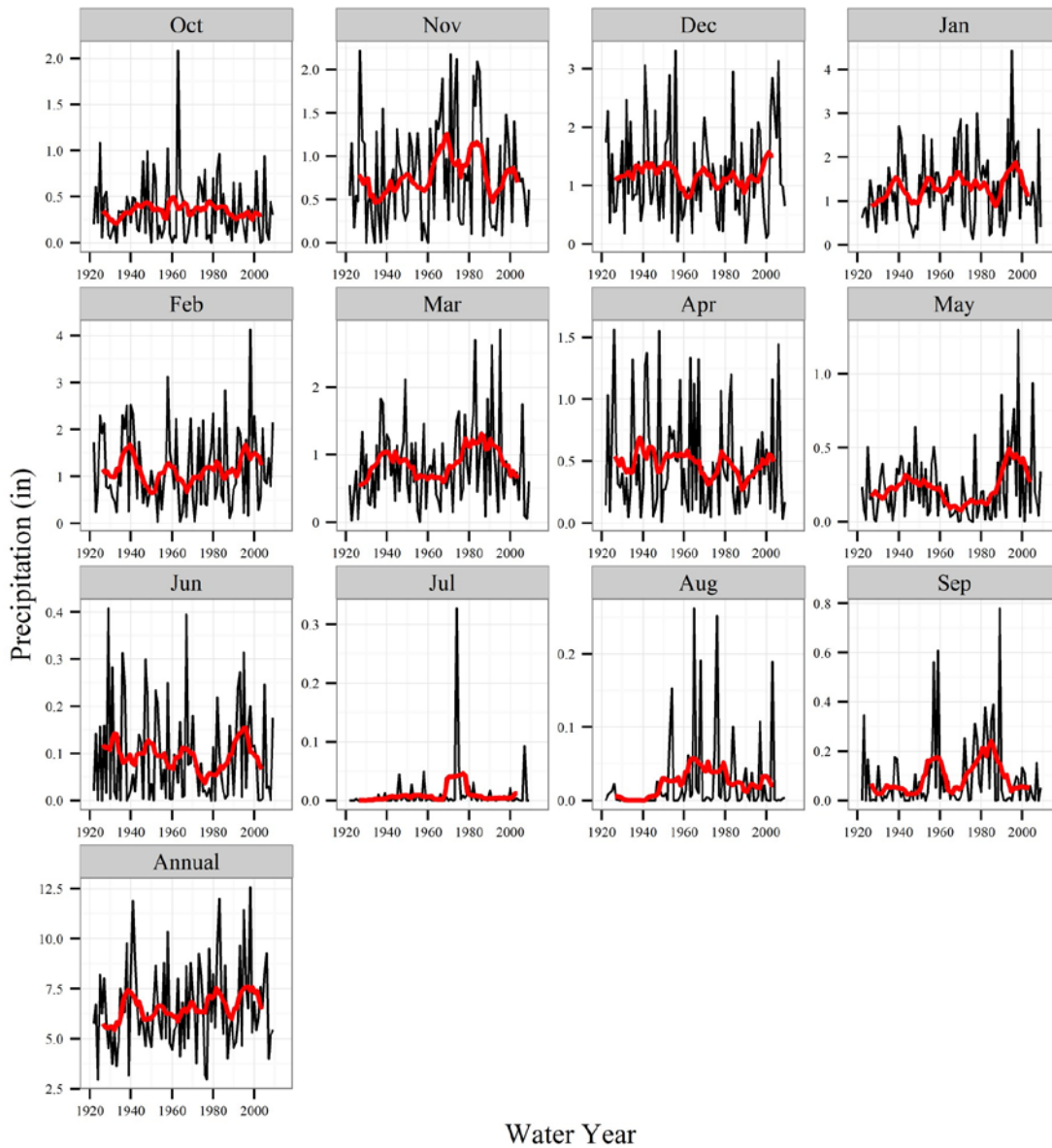


Figure 5-8 Sacramento Valley floor precipitation time series plots with 10 year moving average (red)

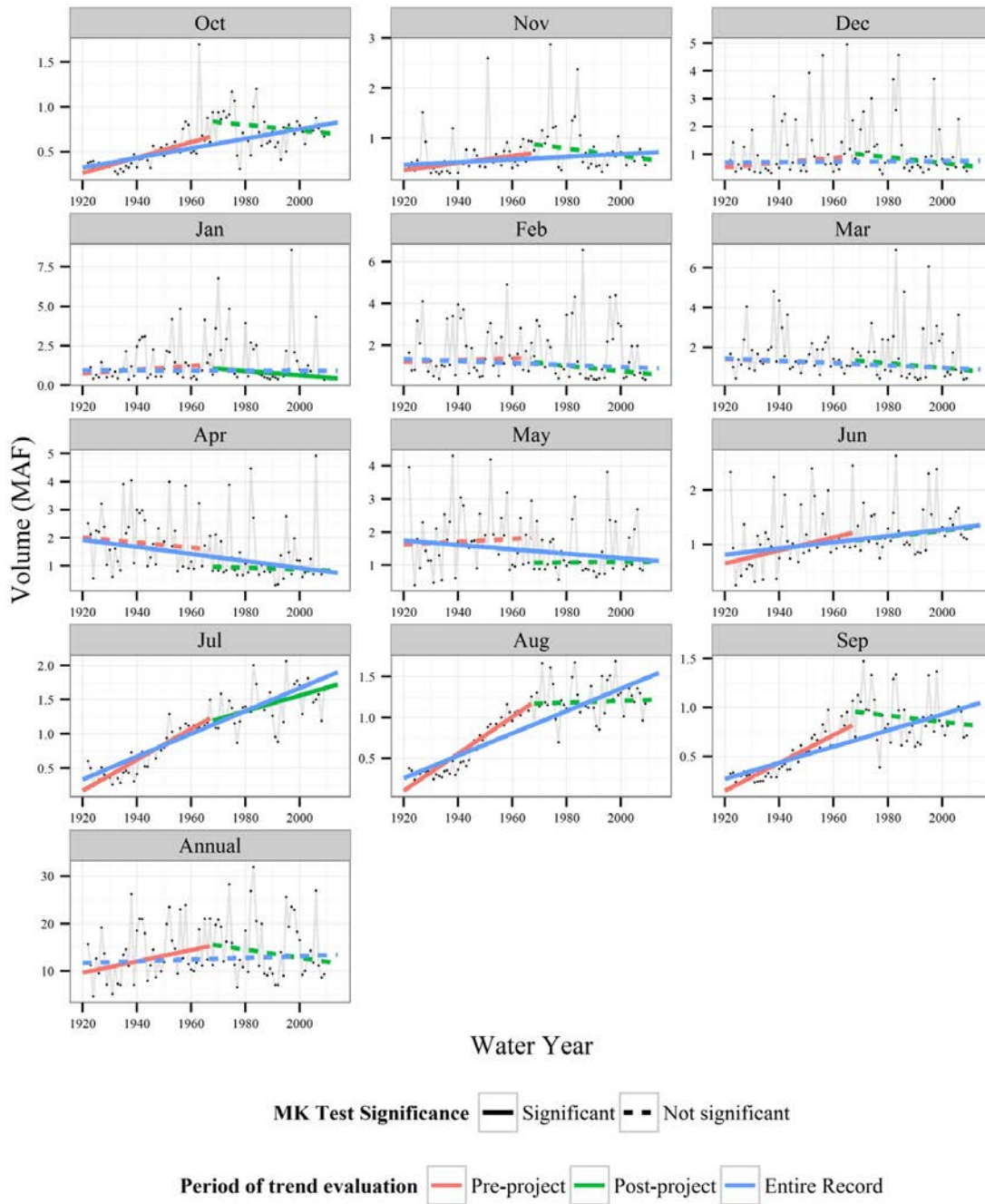


Figure 5-9 Mann-Kendall trend evaluation for Four River Inflow

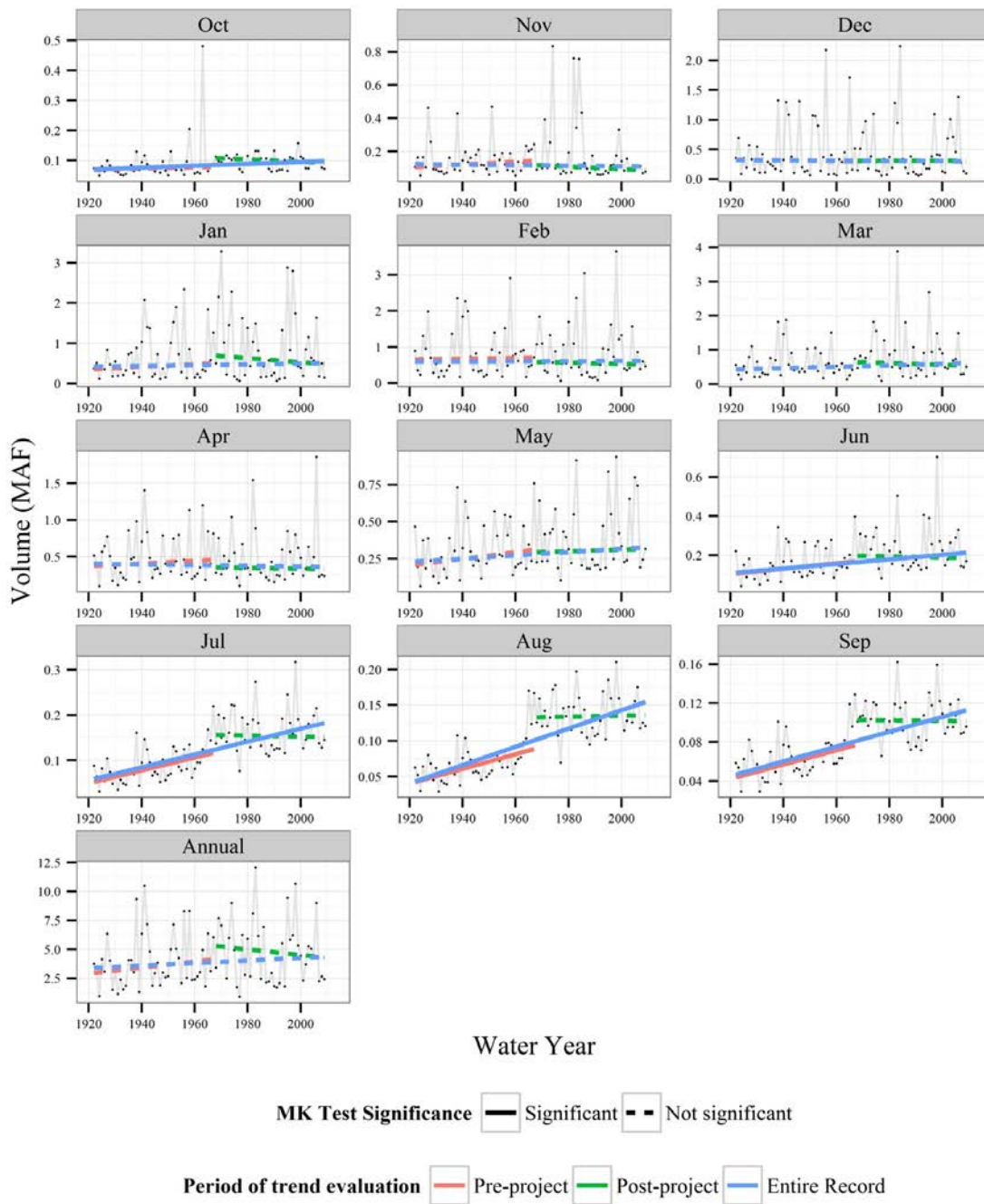


Figure 5-10 Mann-Kendall trend evaluation for Minor Rim inflows

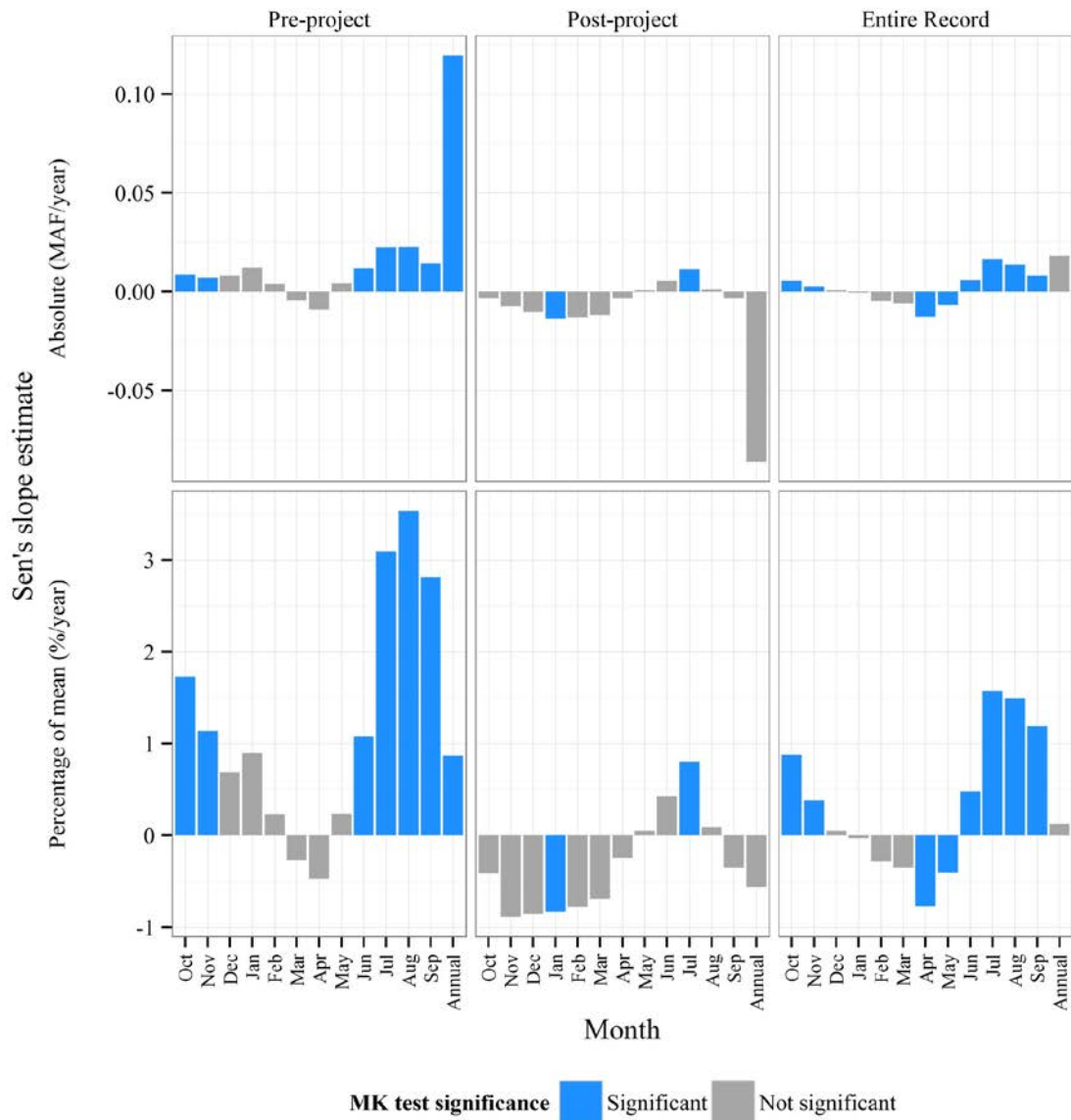


Figure 5-11 MK test results for Four River inflow.

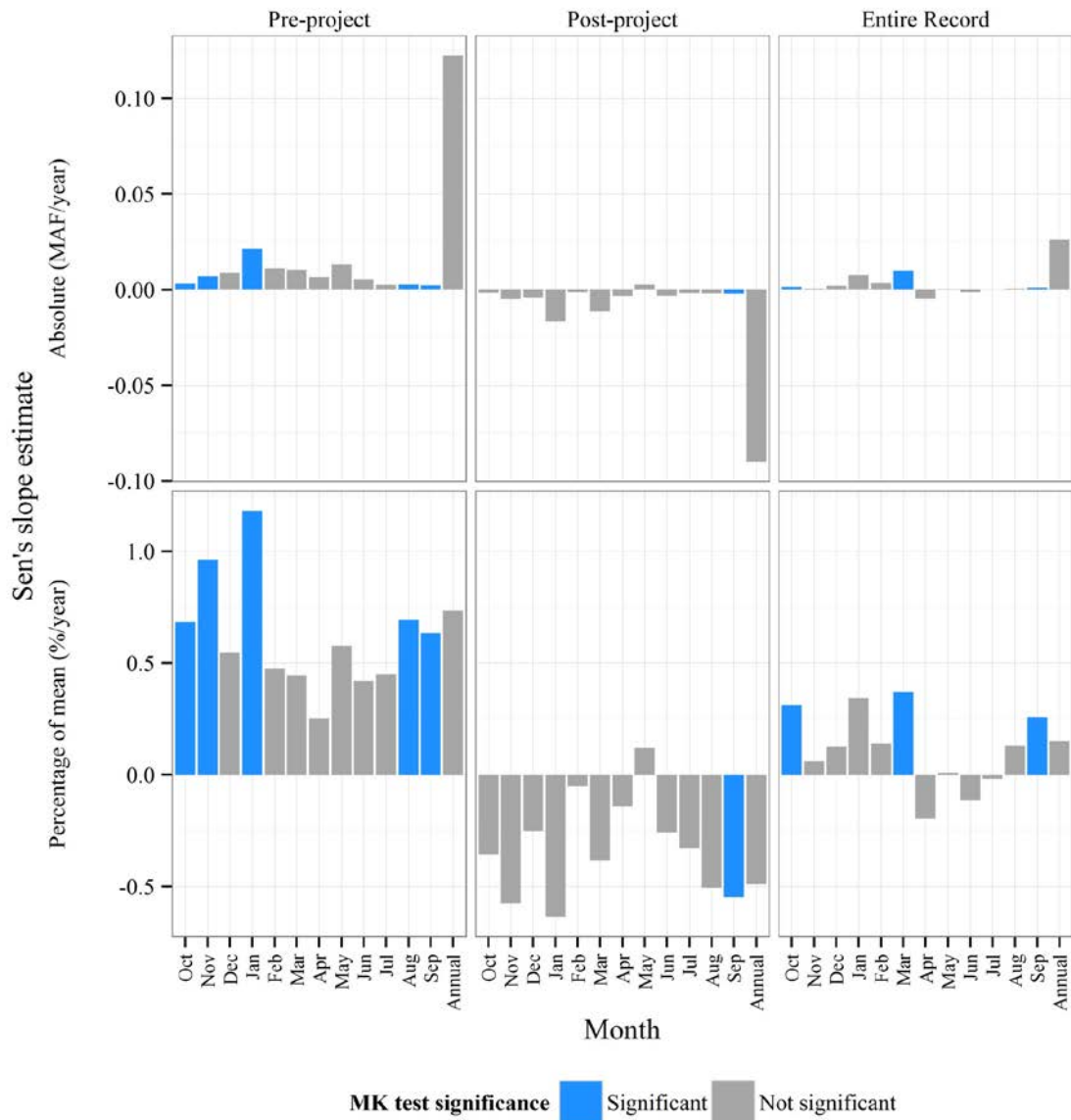


Figure 5-12 MK test results for Four River Index.

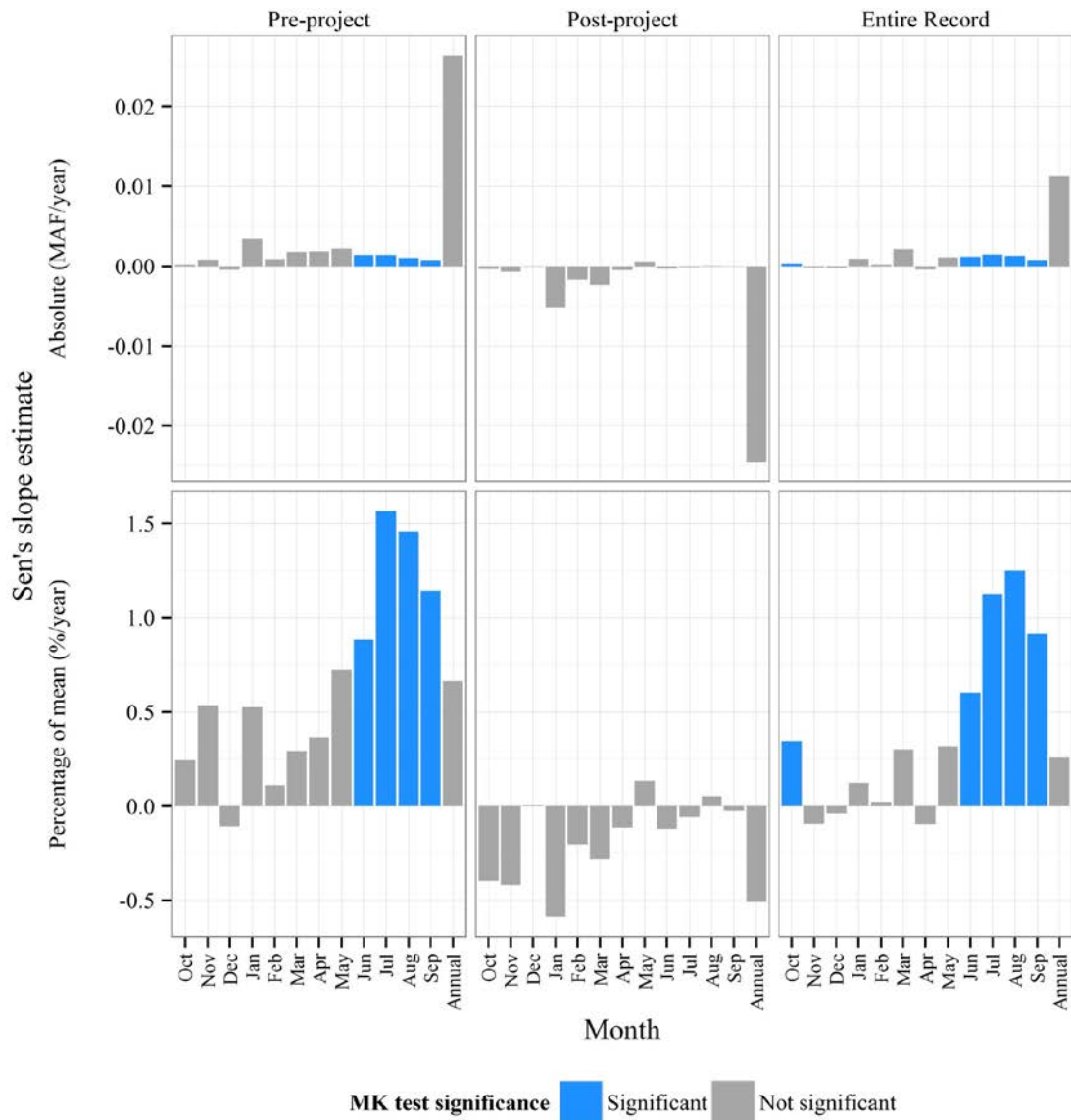


Figure 5-13 MK test results for Minor Rim inflows.

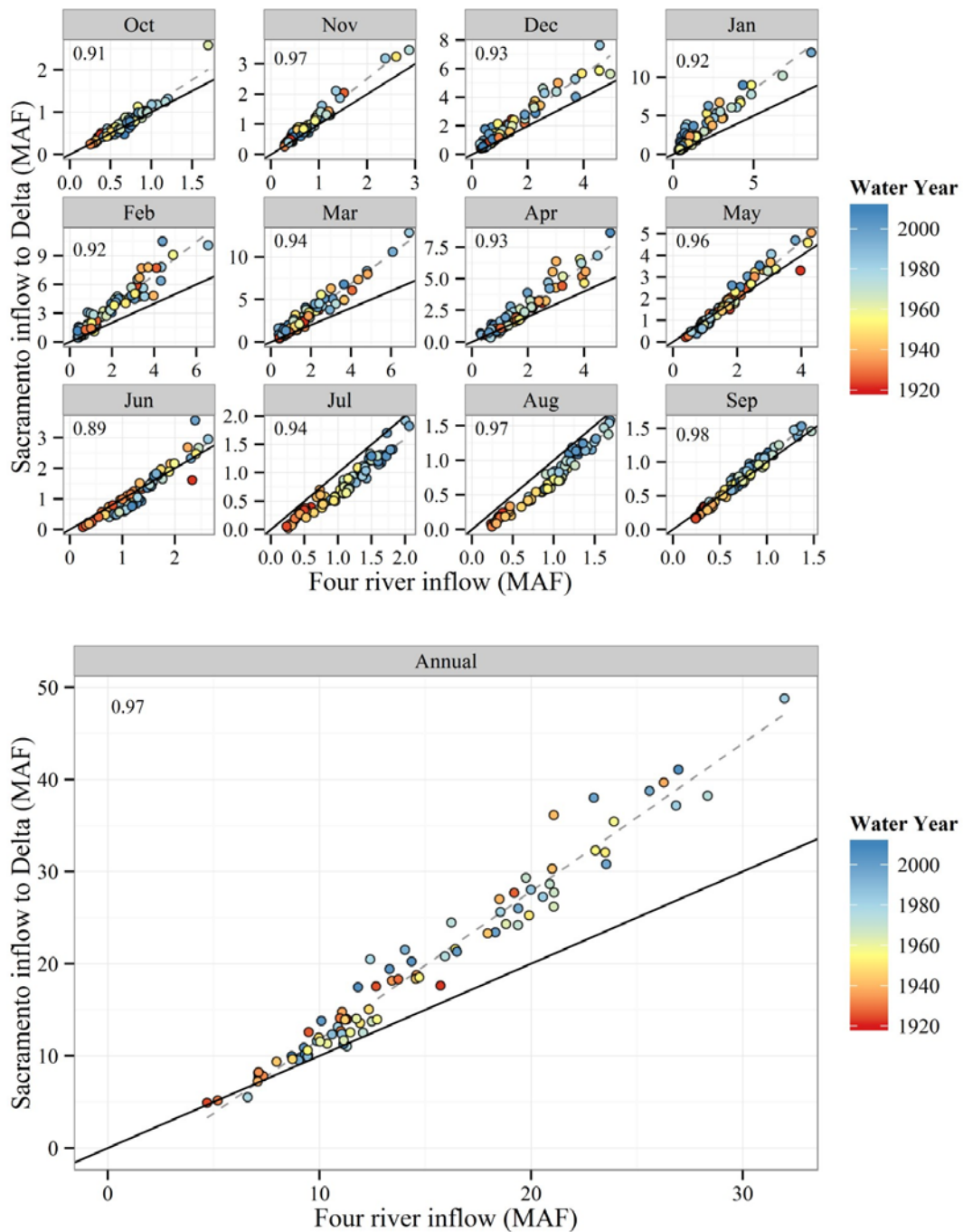


Figure 5-14 Changes in unexplained Sacramento Valley accretions/depletions considering only Four River inflow. Solid black line is the 1:1 line. Dashed gray line is linear best fit, with  $r^2$  value shown on upper left.

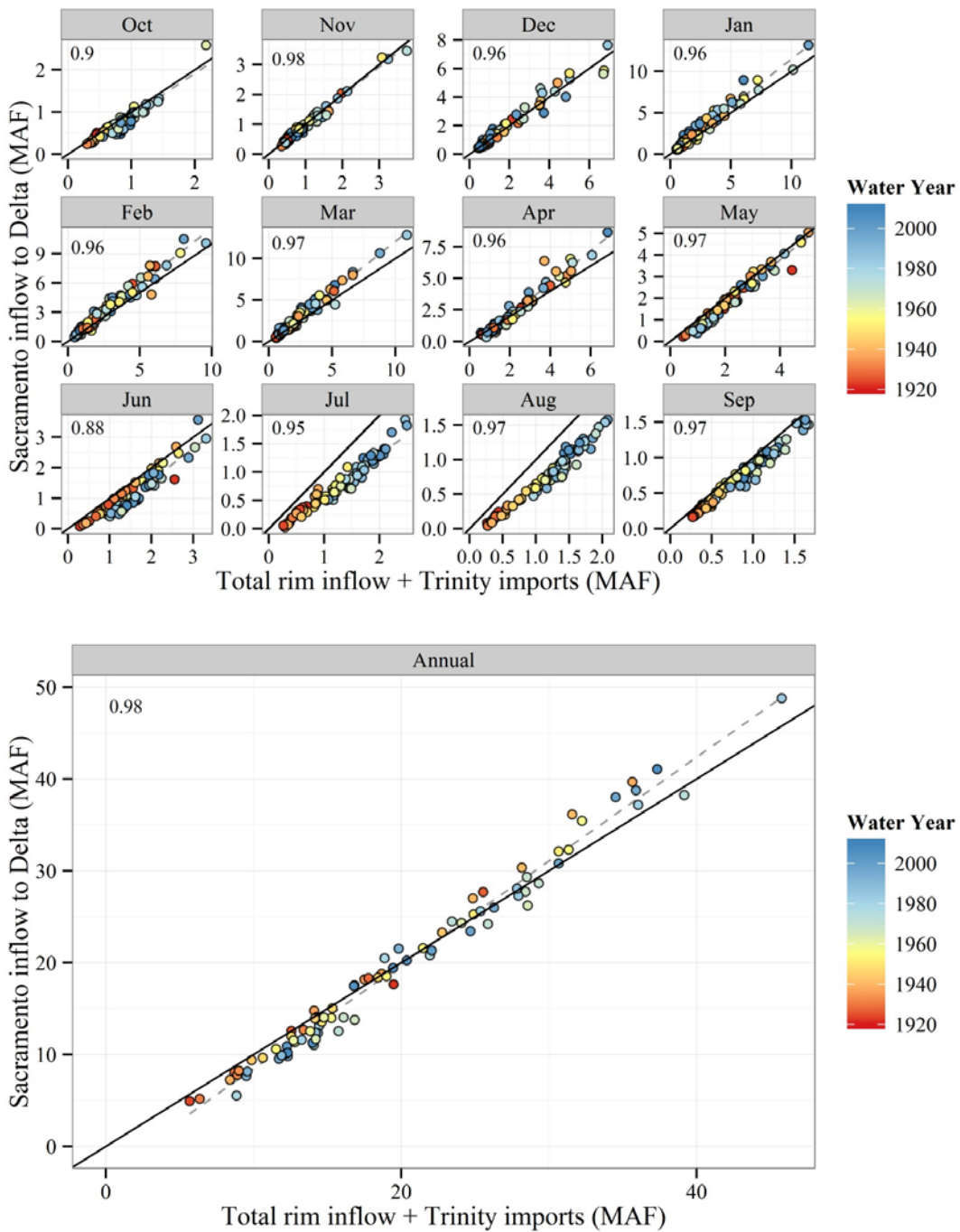


Figure 5-15 Changes in unexplained Sacramento Valley accretions/depletions considering Four River inflows, Minor Rim inflows, and Trinity imports. Solid black line is the 1:1 line. Dashed gray line is linear best fit, with  $r^2$  value shown on upper left.

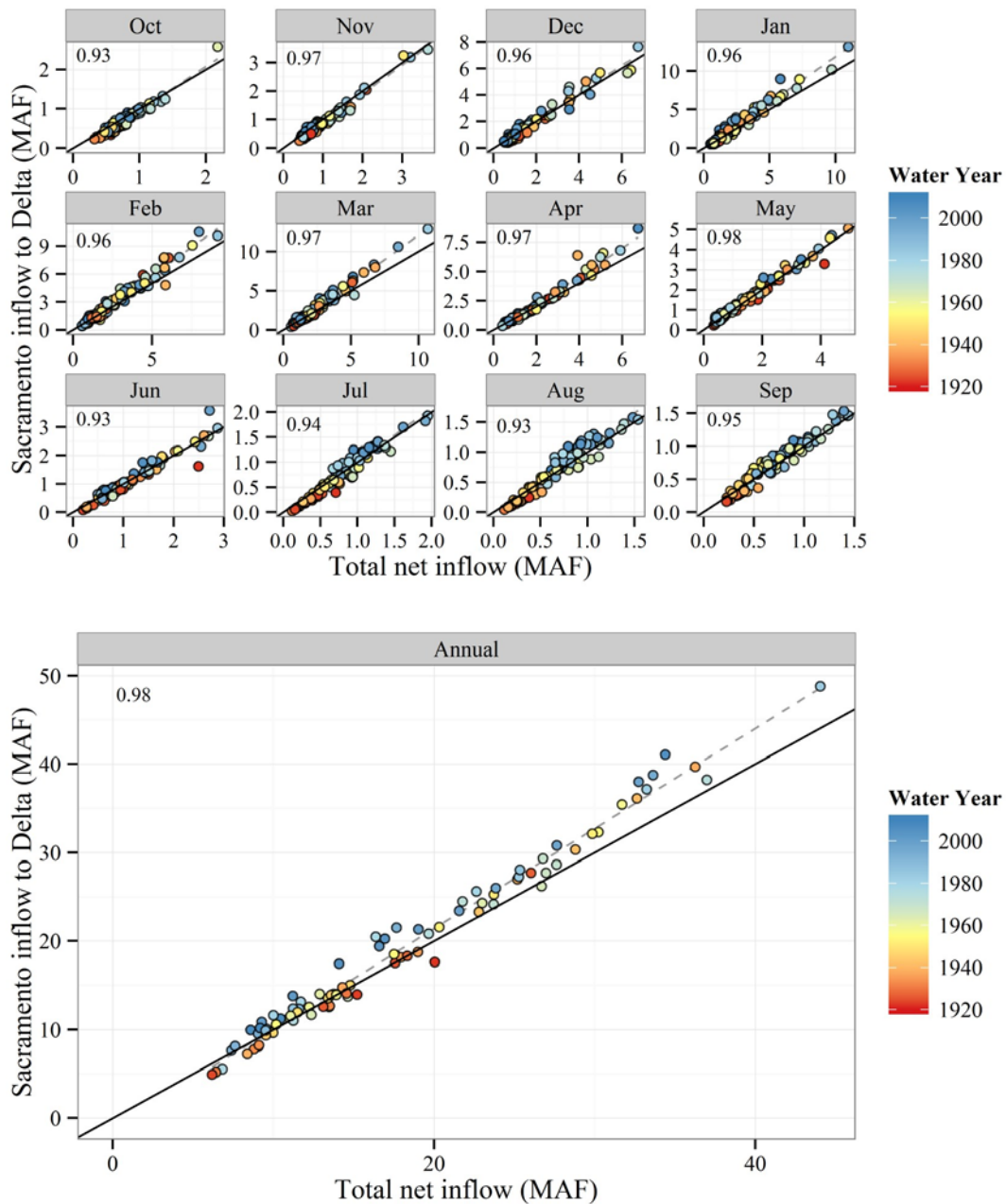


Figure 5-16 Changes in unexplained Sacramento Valley accretions/depletions considering Four River inflows; Minor Rim inflows; valley floor precipitation runoff (C2VSIM input, runoff factor 0.20); gain from groundwater (C2VSIM output); runoff from groundwater pumping (C2VSIM output, runoff factor 0.10); and diversions and related runoff (C2VSIM output, runoff factor 0.20). Solid black line is the 1:1 line. Dashed gray line is linear best fit, with  $r^2$  value shown on upper left.

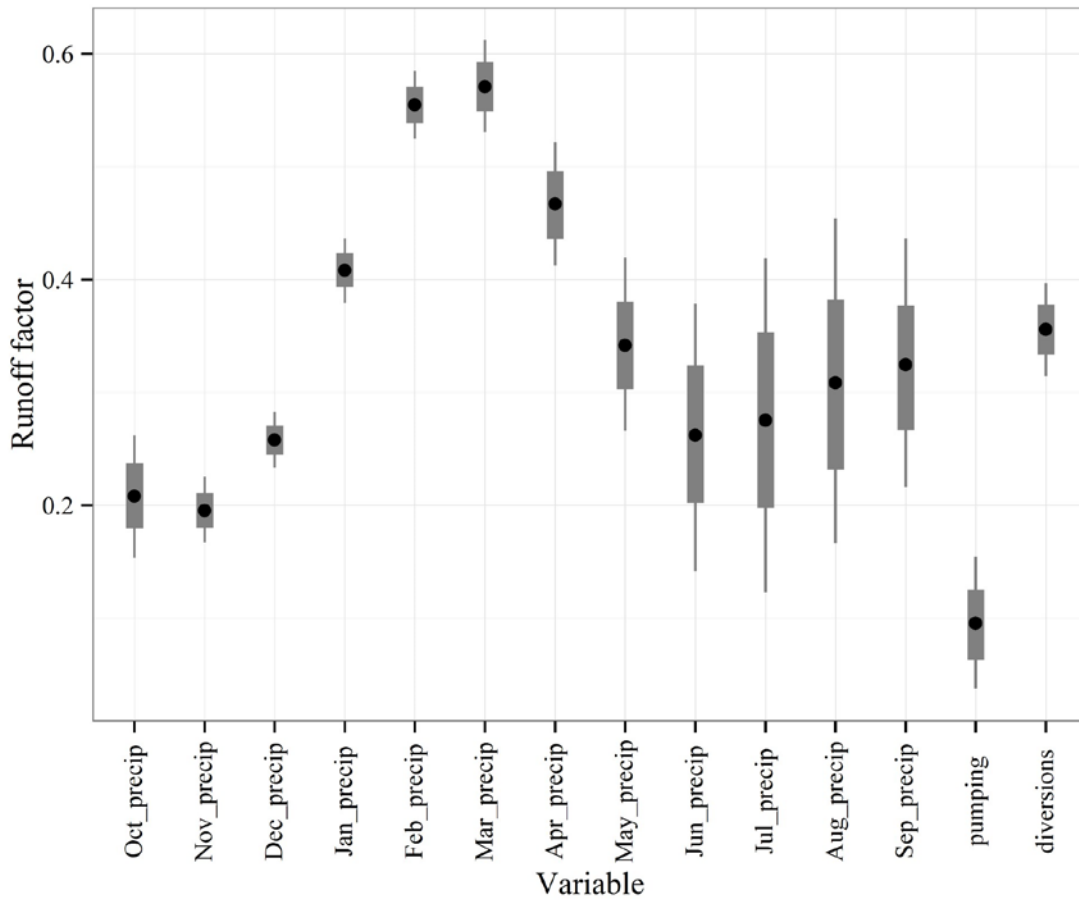


Figure 5-17 Optimized runoff factors in Sacramento Valley accretion/depletion calculations. Points, thick gray lines, and thin gray lines represent posterior means, 25–75% intervals, and 10–90% intervals, respectively.

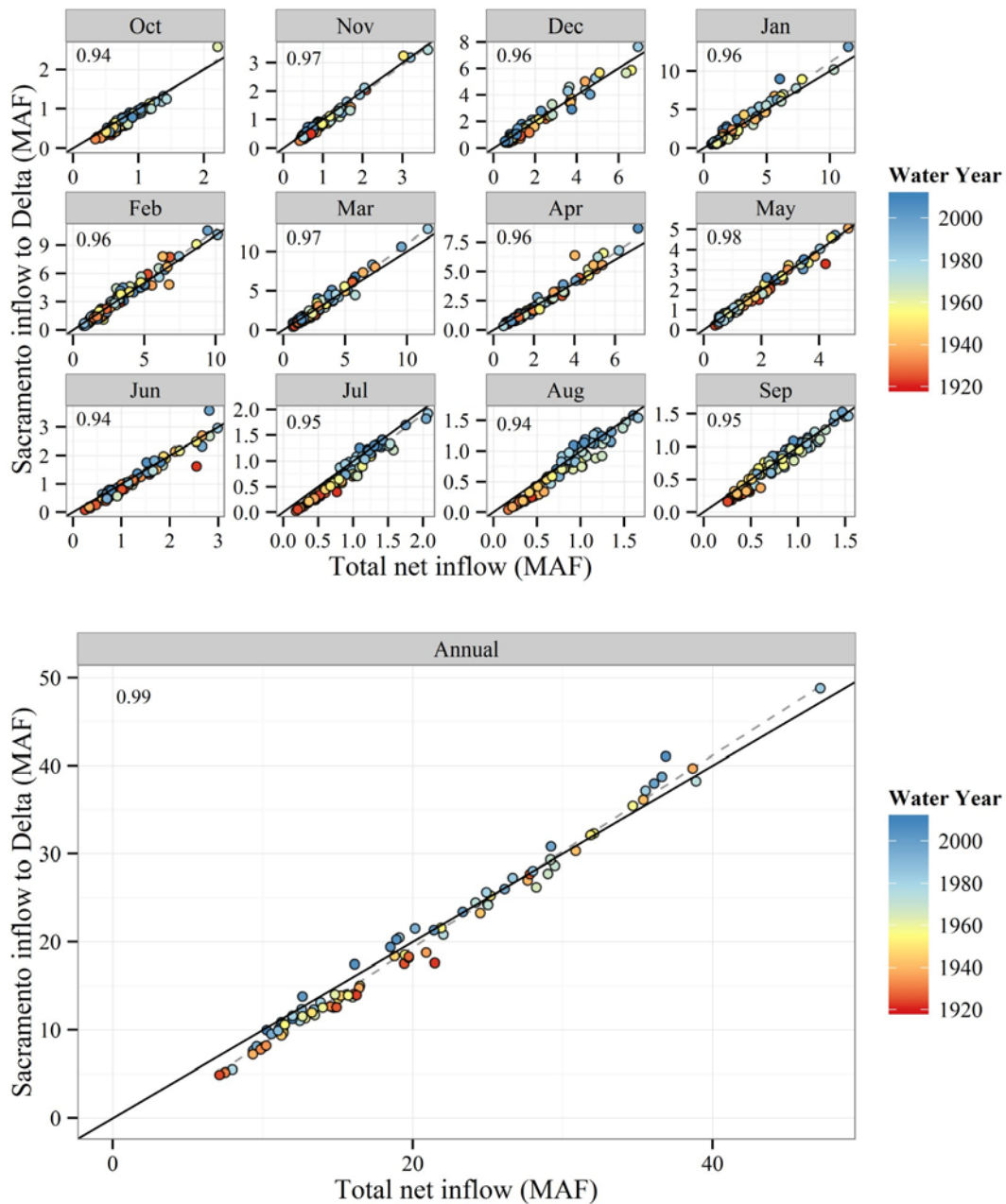


Figure 5-18 Changes in unexplained Sacramento Valley accretions/depletions considering Four River inflows; Minor Rim inflows; valley floor precipitation runoff (C2VSIM input, average runoff factor 0.35); gain from groundwater (C2VSIM output); runoff from groundwater pumping (C2VSIM output, runoff factor 0.10); and diversions and related runoff (C2VSIM output, runoff factor 0.36). Solid black line is the 1:1 line. Dashed gray line is linear best fit, with  $r^2$  value shown on upper left.

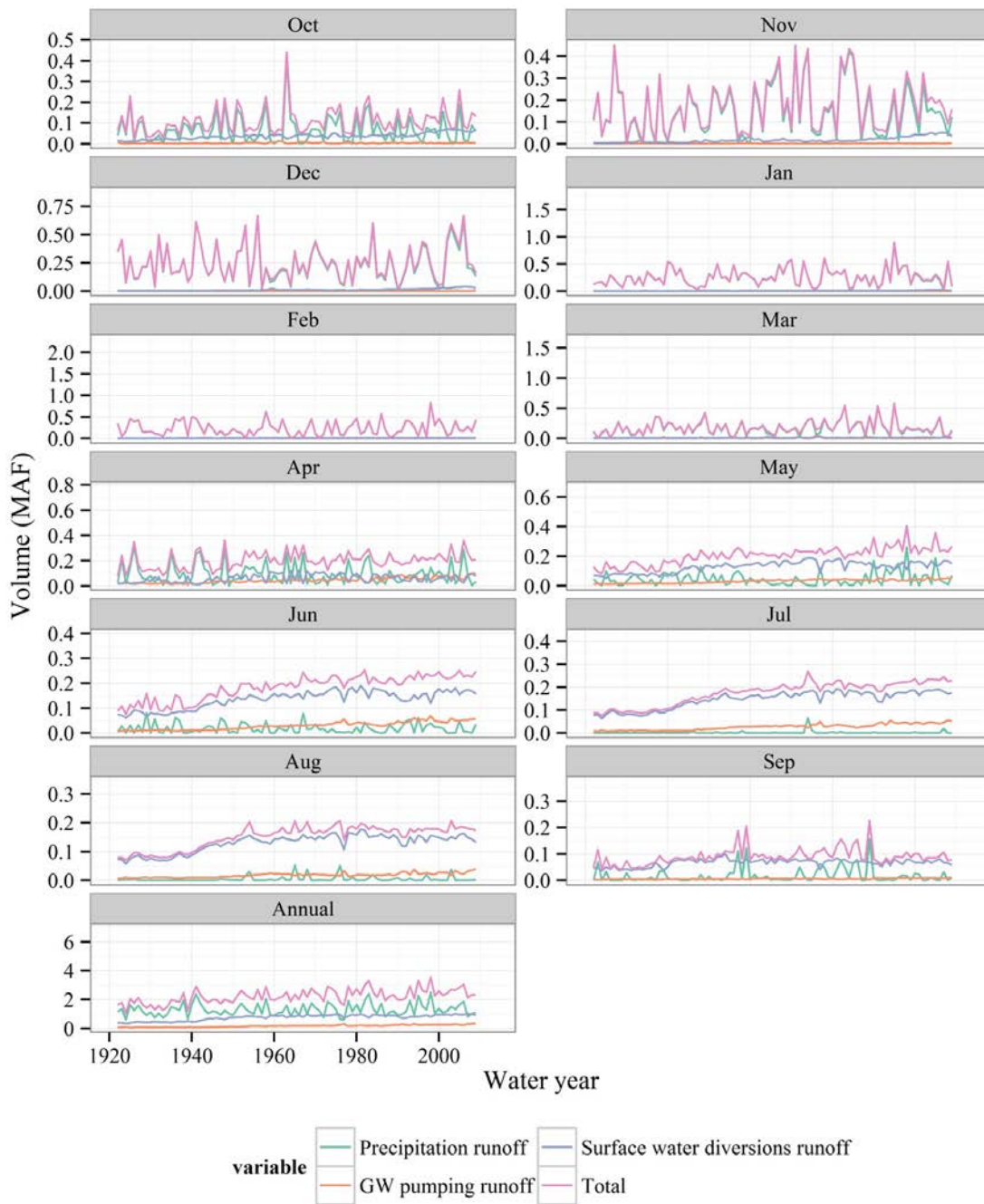


Figure 5-19 Runoff flow volumes (constant factors)

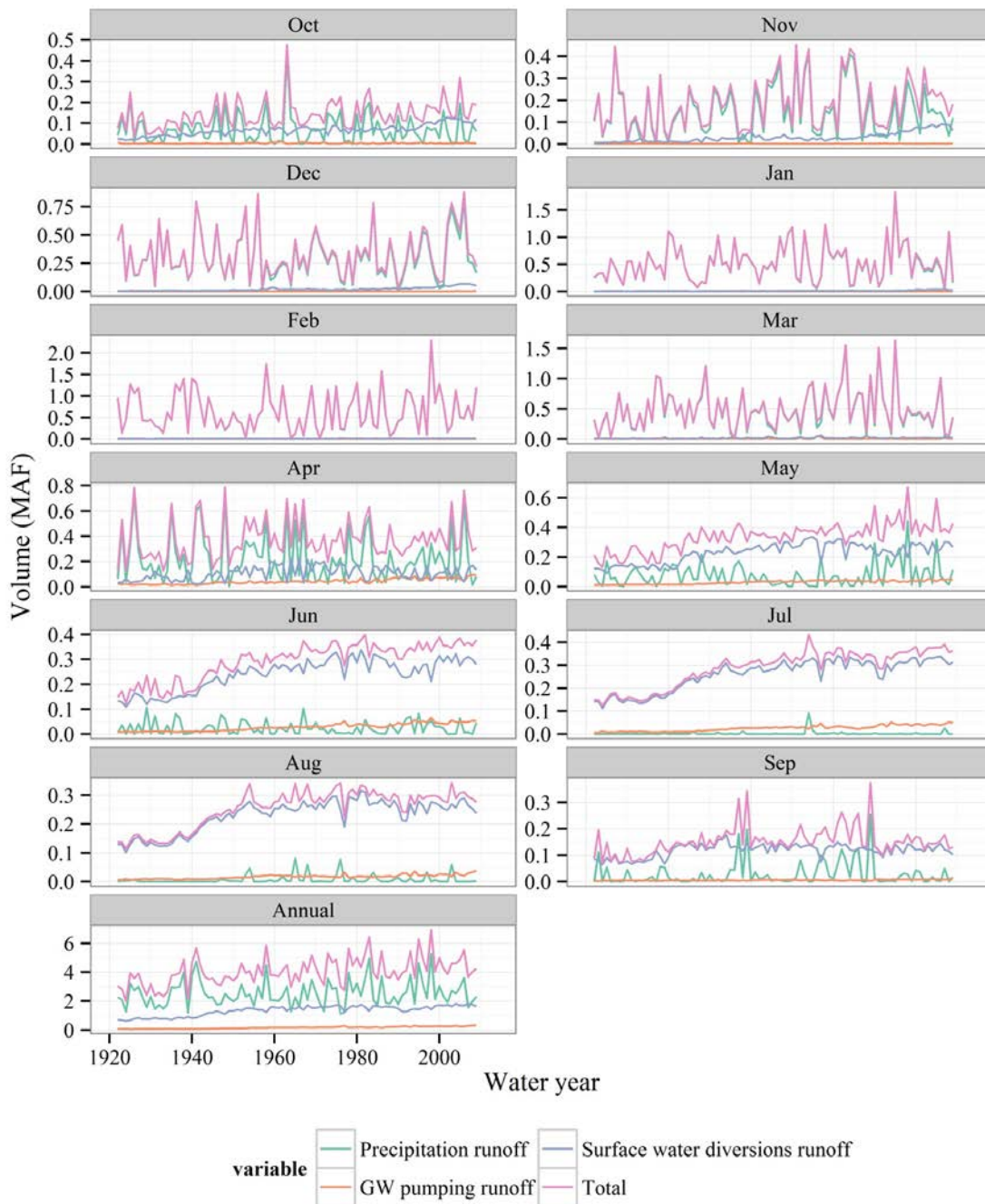


Figure 5-20 Runoff flow volumes (optimized factors, precipitation factor varies by month)

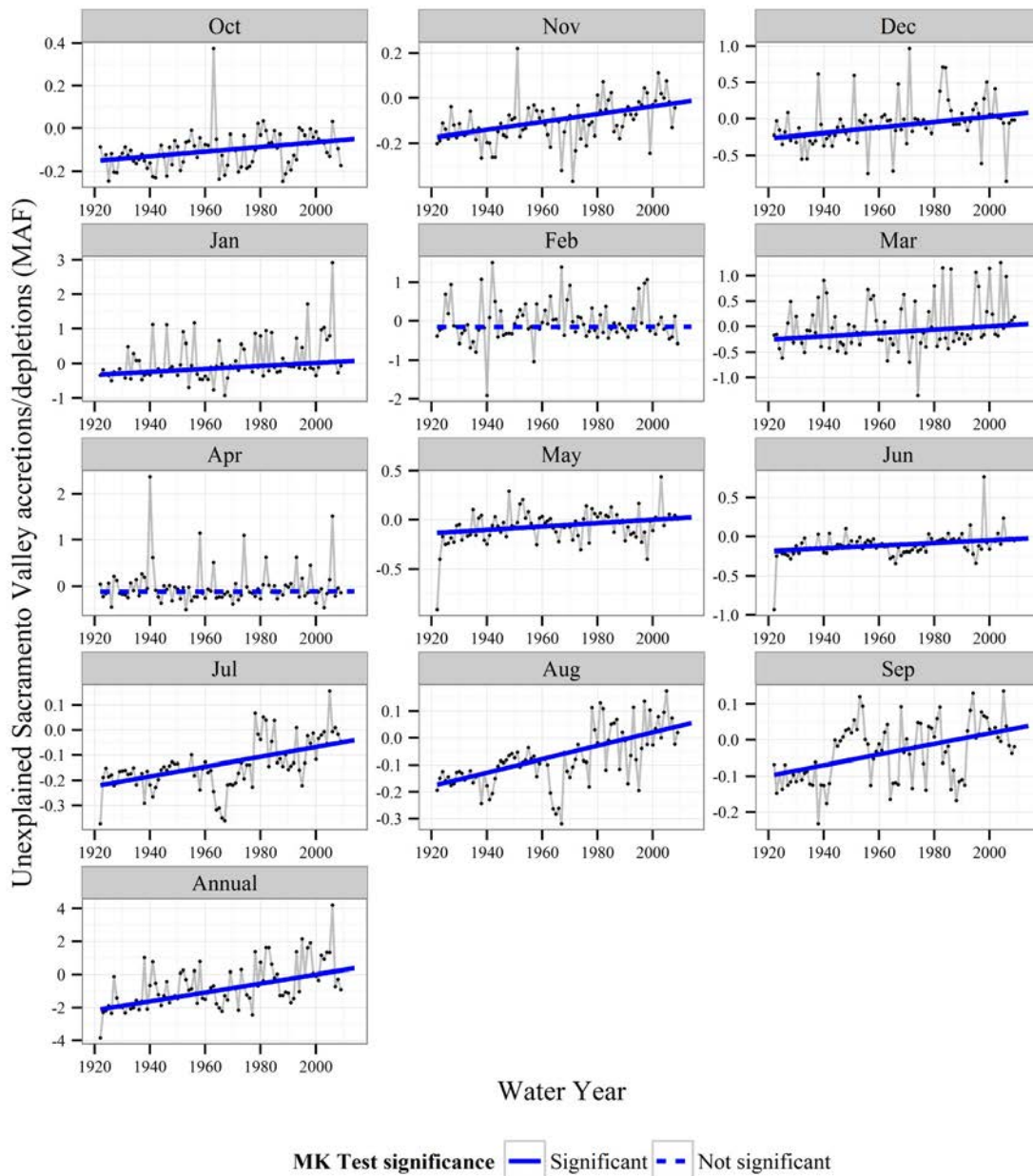


Figure 5-21 Time series plot of unexplained Sacramento Valley accretions/depletions considering Four River inflows; Minor Rim inflows; Trinity imports; valley floor precipitation runoff (C2VSIM input, runoff factor 0.35); gain from groundwater (C2VSIM output); runoff from groundwater pumping (C2VSIM output, runoff factor 0.10); and diversions and related runoff (C2VSIM output, runoff factor 0.36). The blue line illustrates a MK test of trend of the underlying data.

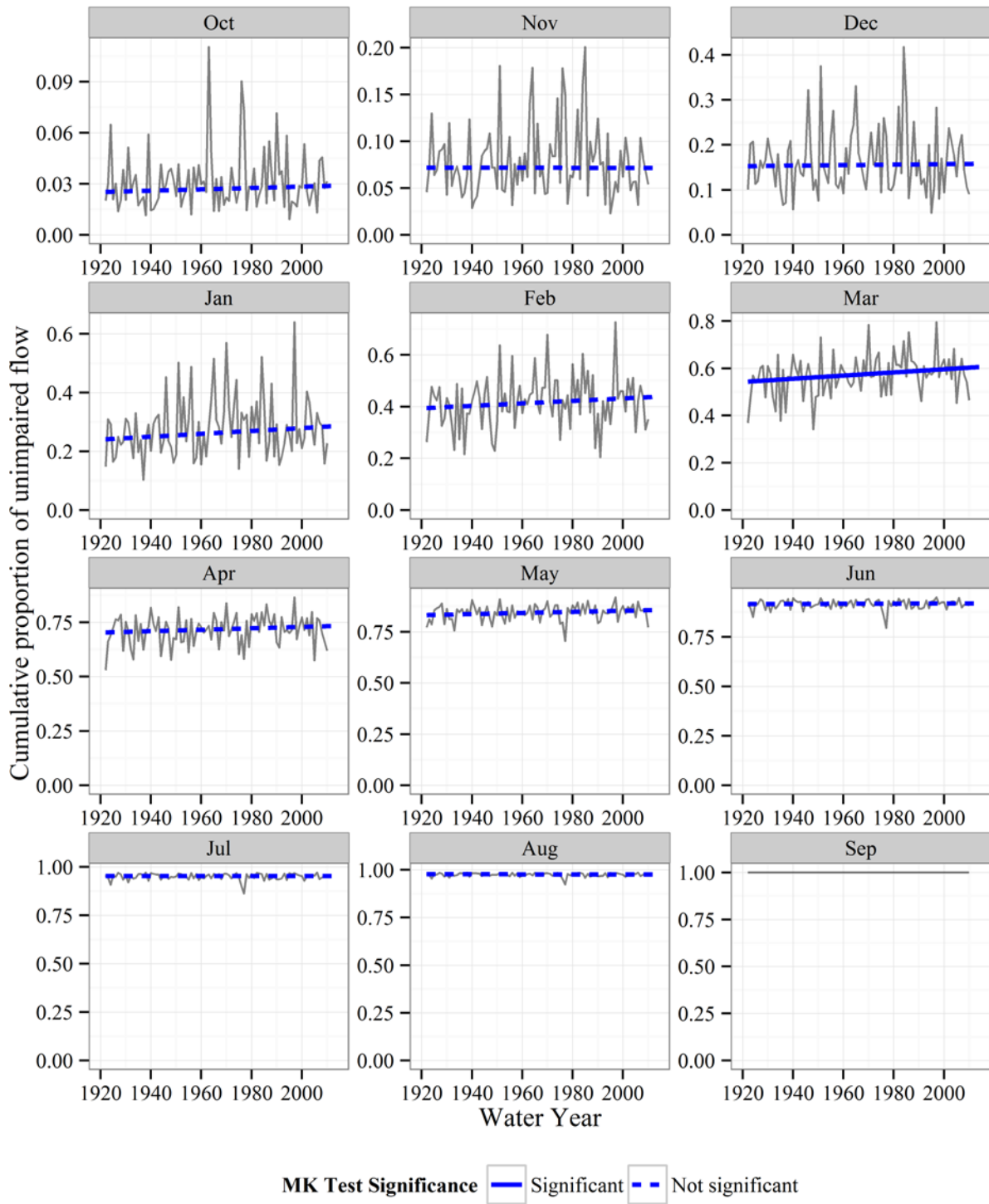
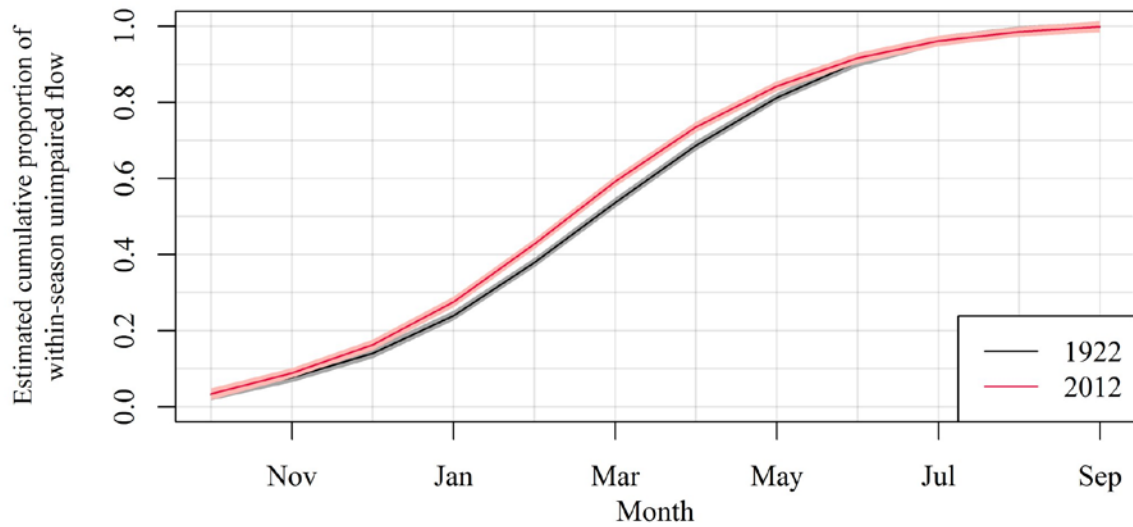
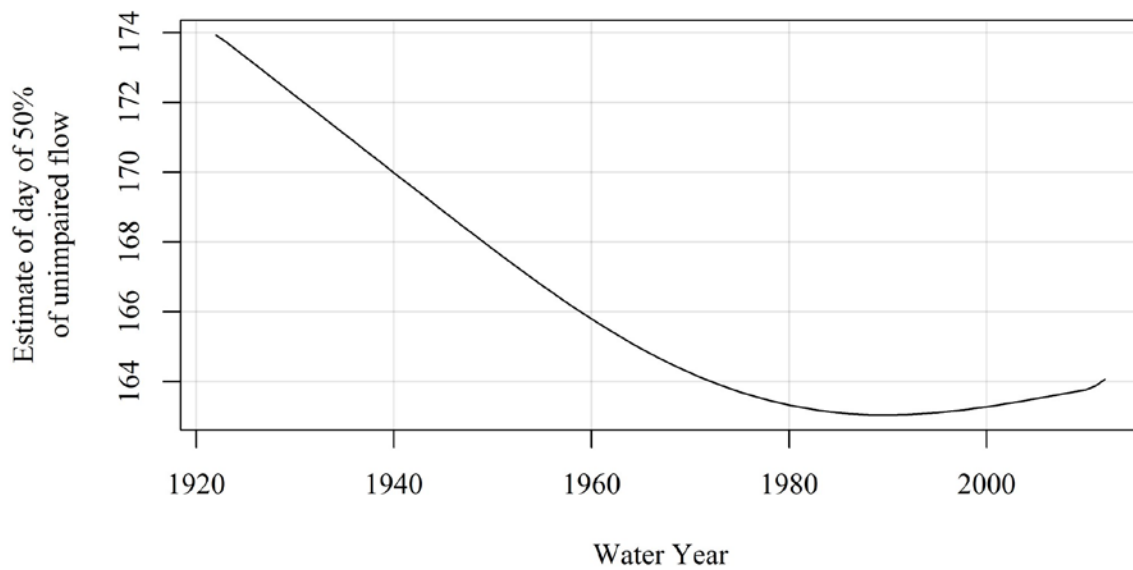


Figure 5-22 Trends in timing of cumulative wet season runoff (based on four-river index).



(a) Predictions for beginning and end of record unimpaired flow timings. Solid lines show point predictions, with shaded regions extending to  $\pm 1$  standard errors.



(b) Changes in timing of arrival of 50% of unimpaired flow.

Figure 5-23 Nonparametric GAMM model of unimpaired flow arrival times.

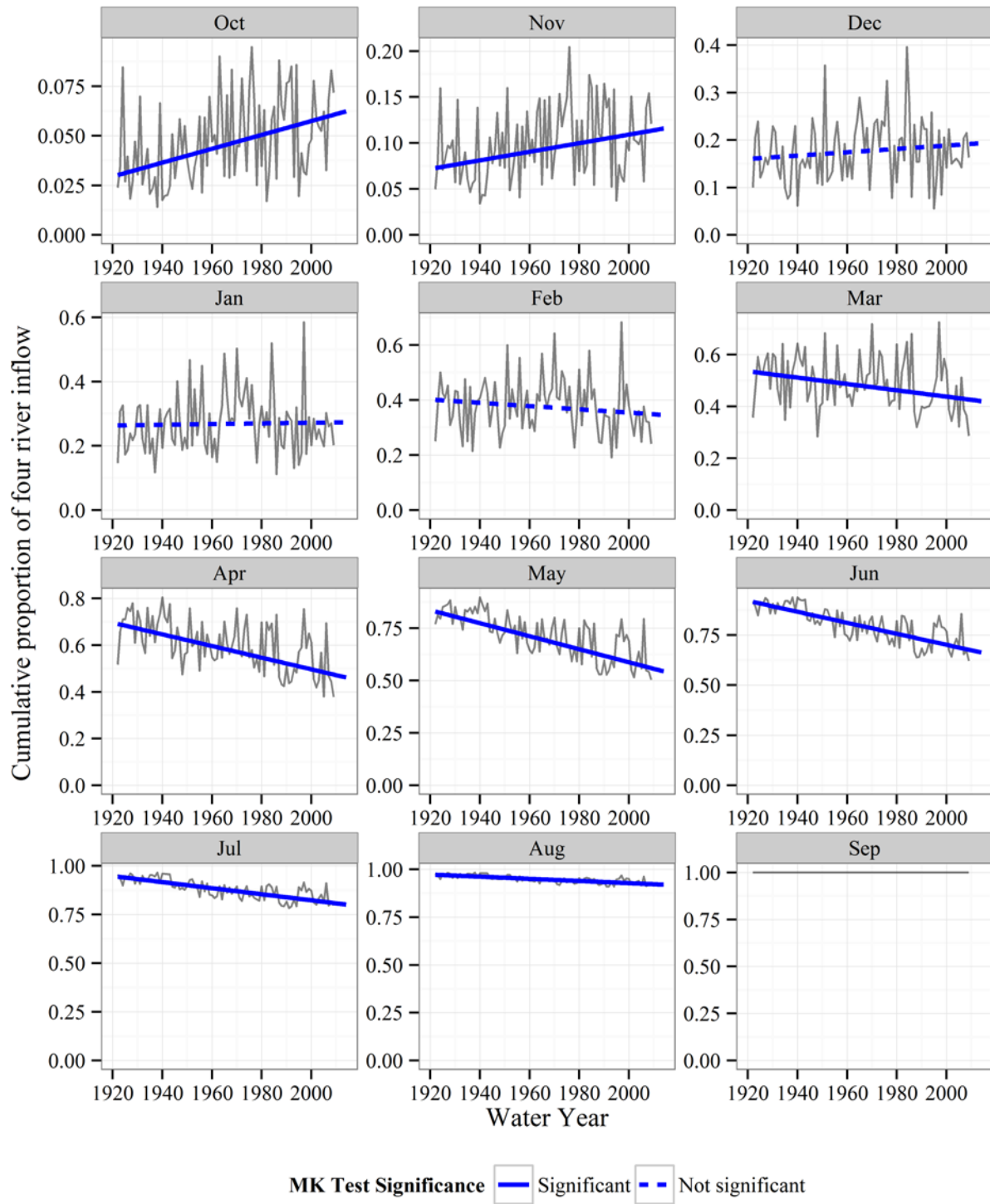


Figure 5-24 Trends in timing of Four River inflow

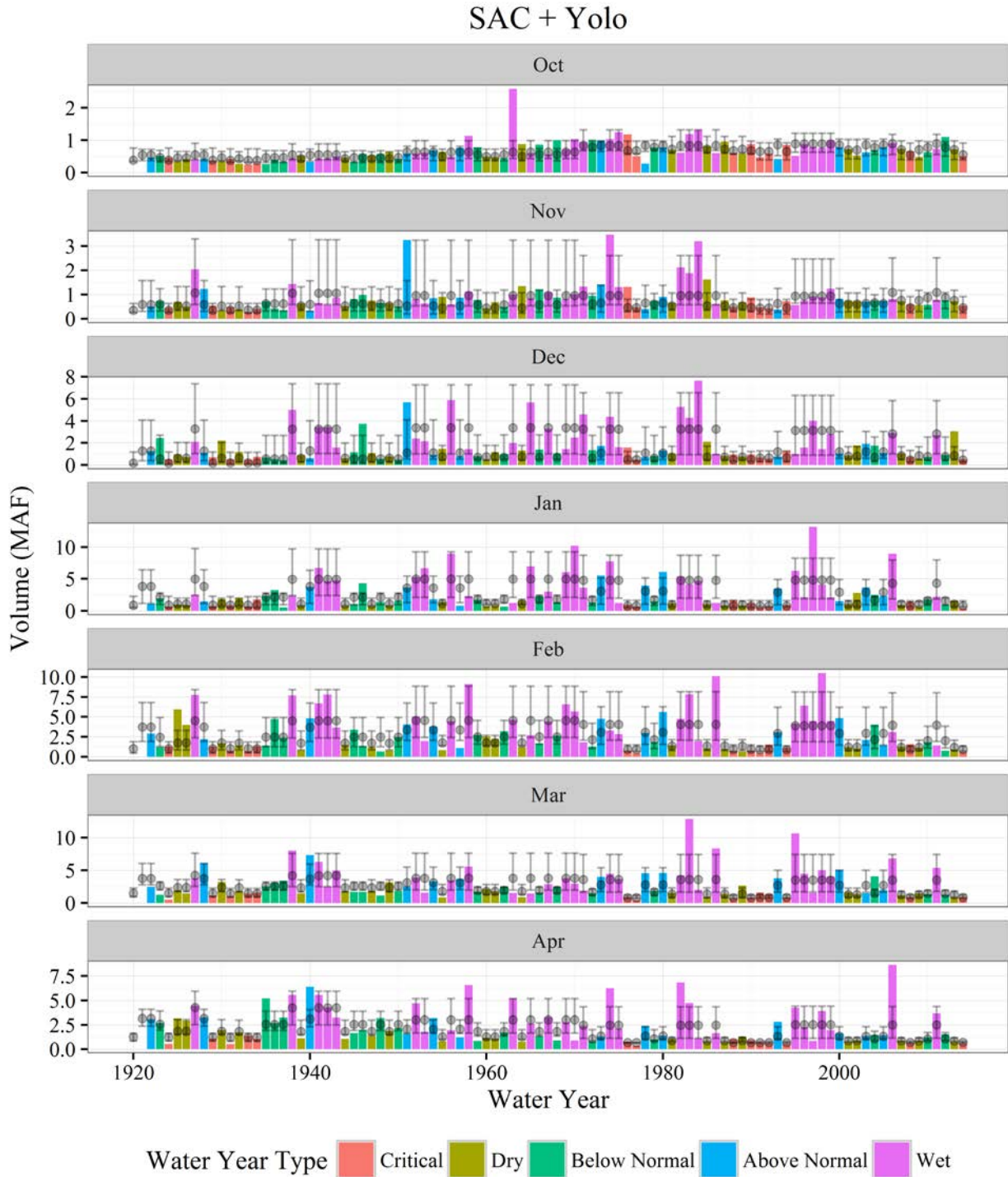


Figure 5-25 Comparison of historical and LOD scenario Sacramento Valley inflow to Delta. Colored bars indicate historical value and water year type. The median and 10th-90th percentiles of values from the corresponding month and water year type from the chronologically closest LOD scenario are indicated by points and error-bars.

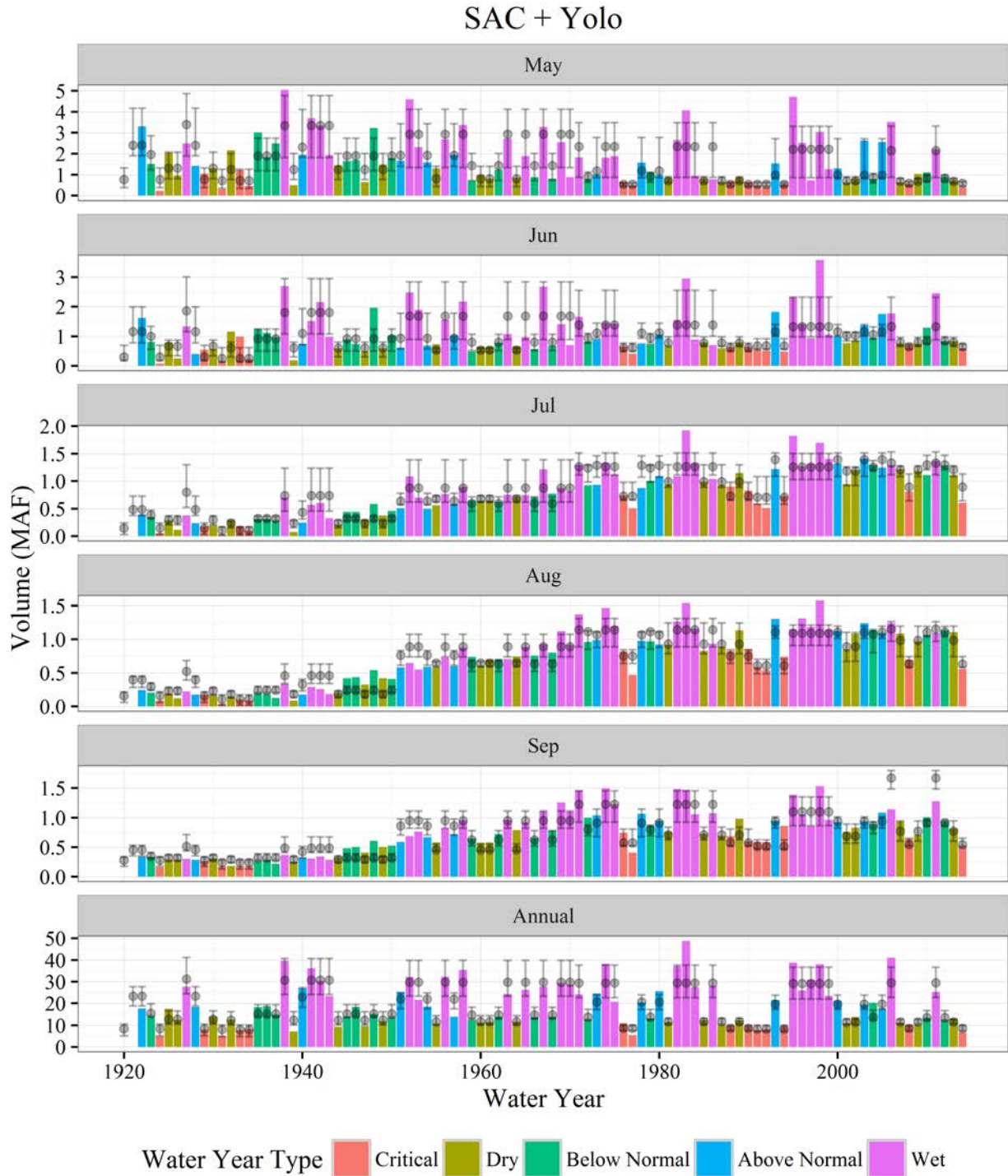


Figure 5-26 Comparison of historical and LOD scenario Sacramento Valley inflow to Delta (continued). Colored bars indicate historical value and water year type. The median and 10th-90th percentiles of values from the corresponding month and water year type from the chronologically closest LOD scenario are indicated by points and error-bars.

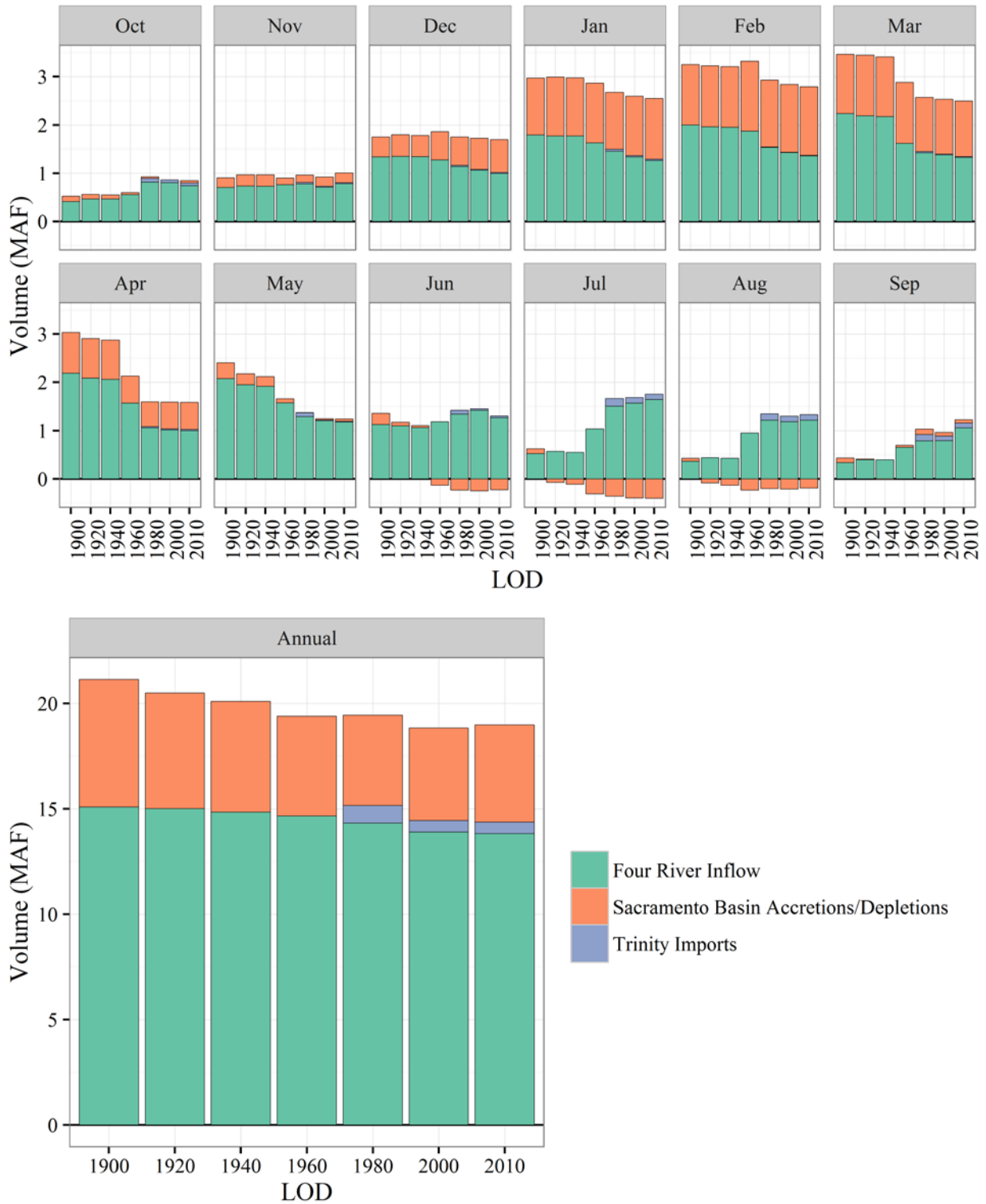


Figure 5-27 Sac Valley LOD flows by month and annually.

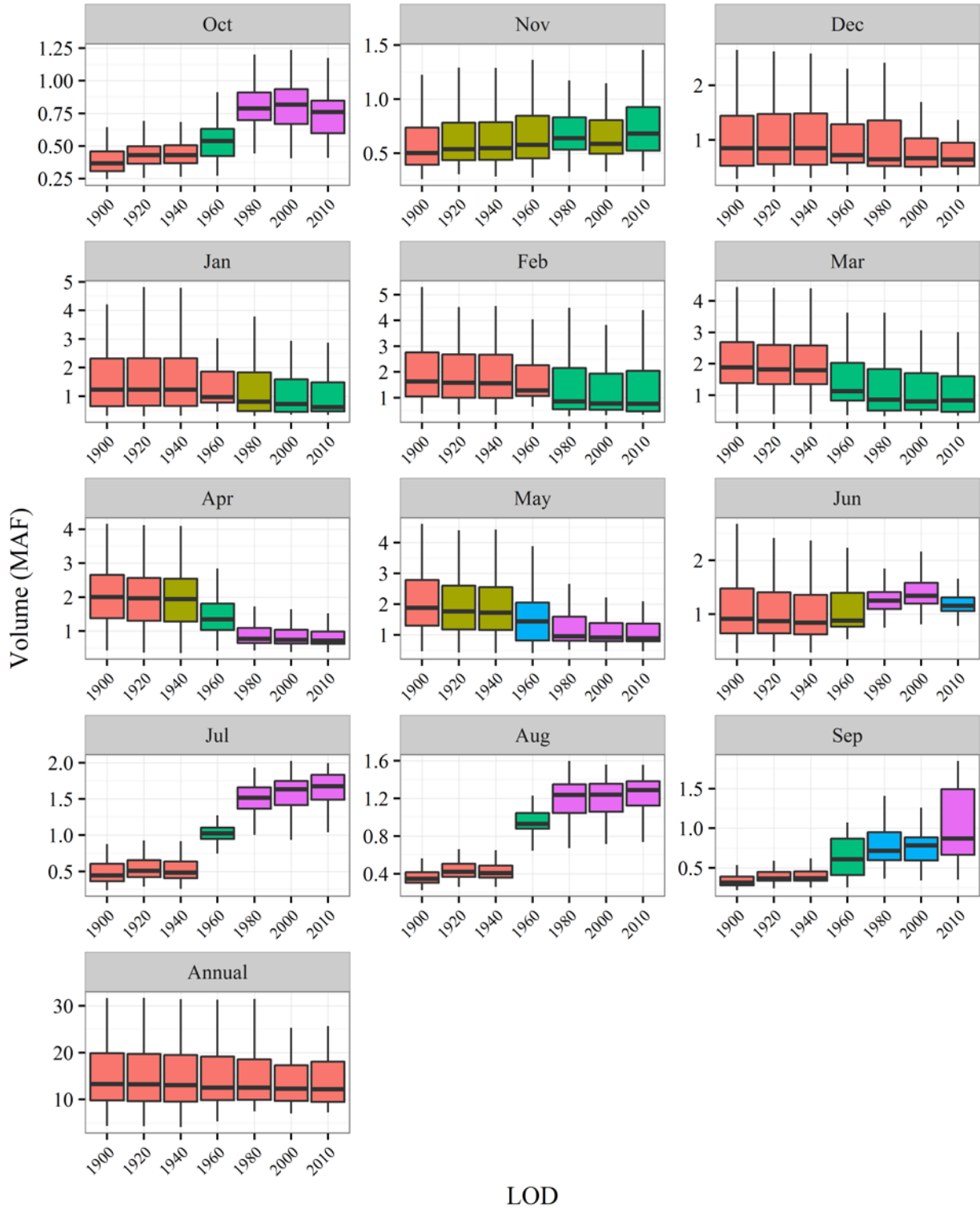


Figure 5-28 Multiple Kruskal-Wallis procedure for Four River Inflow. Boxplots filled with the same color indicate samples that were not found to differ significantly in location by a multiple comparisons Kruskal-Wallis procedure.

## 6 DISCUSSION

---

The statistical analysis of Delta outflow and its component flows provides insight into the significance of changes that occurred over the past nine decades. Because natural variability over time is such a dominant feature of flows in this system, careful testing is needed to parse out true significant anthropogenic change in any of the identified variables. Importantly, the changes are not uniform over the course of the year and even across years. For this reason we performed the analysis of the data by month, by year, and by water year type. For any flow component, e.g., the Sacramento Valley inflow to the Delta, this approach provides a robust assessment of how the flows have changed; whether the flows have changed in certain months, or across the entire year, and whether the change has been pronounced in a certain part of the study period of 1922-2009. These analyses are presented as time series plots and as Mann-Kendall (MK) and Sen tests of significance and magnitudes of slope. The statistical analysis answers the “how have the flows changed?” question posed in Chapter 1. Some key observations related to the changes are as follows:

- The pre-Project period (1922-1967) saw significant increases in late summer and fall (August–November) Delta outflows. In the post-Project period (1968-2009), the pre-Project trends were largely reversed, with net Delta outflows trending downward in September–November. The significance of the downward trend in September is ambiguous, as results varied depending on the assumed method of estimating Delta net channel depletions. Over the entire period of record, the MK test suggests a nominally upward trend in July–September and a nominally downward trend in the remaining months. Specifically, the upward trends in July and August are statistically significant while the upward trend in September is ambiguous (again dependent on the assumed method of estimating Delta net channel depletions). Downward trends in February, April, May and November are statistically significant, while the downward trend in October is ambiguous for the same reason noted for September.
- Because of the importance of Delta outflow in this analysis, and the uncertainty related to net channel depletions within the Delta, the outflow used in the analysis was either that reported in DAYFLOW, or adjusted to account for net channel depletions computed using the DICU model. This comparative analysis showed that the assumption used for net channel depletions has some bearing on the findings of statistical significance, especially in the summer months. For example, October shows a significant decrease in flow using DAYFLOW, but the difference is not significant using the DICU model-based estimate.
- Similar to Delta outflow, the pre-Project period (1922-1967) saw significant increases in summer and fall (July-November) total Delta inflows. In the post-Project period (1968-2012), the pre-Project trends in October and November were partially reversed. Over the entire period of record, the MK test suggests statistically

significant upward trends July-October and statistically significant downward trends in April and May.

- X2 behavior corresponds closely with Delta outflow trends. The pre-Project period (1922-1967) saw significant decreases in X2 position from late summer through the beginning of winter (August-December). In the post-Project period (1968-2012), the pre-Project trends were somewhat reversed. Over the entire period of record, the MK test suggests statistically significant downward trends in August and September and statistically significant upward trends in April, May, November and December. The supporting patterns are important, because the historical X2 values used in this analysis were obtained entirely independently of the flow data (Hutton et al., 2015).
- The MK test consistently suggests significant increases in summer and early fall flows over the pre-Project period and the entire period of record for Sacramento Valley inflow, Four River inflow and Minor Rim inflow. For the spring months in the pre-Project period, the nominal directions of the trend lines are consistent with the decreases discussed above (negative values of Sen's slope), but the changes are not large enough to be statistically significant.
- The evaluation of low frequency variation and non-monotonic changes in the data was performed using the STL approach. The analysis shows a very small non-monotonic trend in the net Delta outflow, with a small increase through about 1960 and a decrease thereafter, but the trend was swamped by the remaining variability in the system. Based on this information, it appears that our use of the MK trend test is not unreasonable and that there are no other major time trends that should be investigated more formally with an MK analysis. The STL affirms the major role of variability compared to the effects of water management that has been noted in previous work (Knowles, 2002; Enright and Culberson 2009).

The second part of our analysis related to the question “why have the flows changed?” posed in Chapter 1. We used two approaches to answer this question of attribution. In the first approach, we constructed a water balance with component flows (for the Delta and for the Sacramento Valley) through a series of annual and monthly scatter plots showing inflow components on the x-axis and outflow components on the y-axis. On the x-axis, we incrementally added component flows to see how well the outflows could be explained by the inflows, i.e. when the points on the scatter-plot fall in proximity to a 1:1 line. The premise of the approach is that, if the inflow and outflow components match up well, we can explain the drivers of the outflow patterns. The second approach used to answer the attribution question relied on modeled data (based on a physical and operations model of flows in the Bay-Delta watershed) provided under separate contract (MWH, 2015). The model was run several times, driven each time by the same 88-year climatic time series, but with watershed development (land use, reservoir construction and operation, and withdrawals for irrigation and municipal use) and Delta water quality regulations set at levels corresponding to 1900, 1920, 1940, 1960, 1980, 2000, and 2010. Each of these is termed a level of development, or LOD, scenario, and each resulted in an 88-year time series of modeled flows at various points through the Central Valley watershed. For a given LOD, the model scenarios provide the response to a wide range of climatic inputs. For example, the 1960 LOD run provides the response to the full record of climatic inputs, whereas the actual system may have received only the inputs associated with the years around 1960, with a much narrower range than the full record. This approach allows the separation of hydrology and underlying watershed

conditions. When patterns in modeled flows—created by imposing various infrastructural, operational, and regulatory conditions—are in agreement with observations of the actual system, we can reasonably infer that the observed patterns are explained by the imposed changes. The modeling can thus allow interpretation of the causes of the observed trends.

Modeled results from the LOD scenarios were broadly consistent with the observations over the entire period of record. A more detailed examination, however, shows that all of the observed trends are not matched. For example, monthly trends, particularly relating to dry weather flows in the first half of the record are not matched (observed flows suggest increases, the LOD scenarios indicate no significant change or decreases).

A flow balance showed the relevance of multiple individual contributors to the Sacramento Valley inflow to the Delta including Four River inflows, Minor Stream inflows, runoff from valley floor precipitation, Trinity River imports, and runoff from groundwater pumping and surface water diversions. The effect of individual surface water flows and valley precipitation are more apparent in wet months, but consideration of these surface flows still indicated a mismatch in the dry months. This could be explained by adding runoff from agriculture, originating from surface water and groundwater irrigation, as a contributor to the water balance. Allowing for variable or “optimized” runoff factors—where the runoff factors were obtained by fitting to the Sacramento Valley inflow data to the Delta—improved the overall explanatory power of the constituent flows. The resulting monthly flow balance fit most of the data, but a residual remained with a trend in time suggesting an increase of Sacramento Valley inflow to the Delta over the study period of roughly 2 MAF per year. This finding suggests the existence of a “sink” or loss term in the earlier part of the data record that is less apparent in the more recent data. It is quite reasonable to assume that this finding is related to the reduced evapotranspirative loss of water in the floodplain, as the rivers in the Sacramento Valley became more channelized over time. The observed error increases as a function of time for most months of the year, i.e., the error increases when all October flows from 1922-2009 are considered, and so on for other months (with the exception of February and April). This analysis, largely driven by the data, is also consistent with the modeling analysis in MWH (2015), where a fixed amount of flow was removed from the modeled value of Sacramento Valley inflow to the Delta in the early part of the record to better match flow observations at the Freeport station in Sacramento River, the main inflow location from the Sacramento Valley to the Delta.

Because of the reasonable correspondence between modeled and observed Delta inflow trends on an annual and monthly scale (as determined through the flow balance and LOD modeling approaches), changes in Delta inflow can be explained by a combination of upstream drivers, each of which has acted over different time horizons. These upstream drivers include: reservoir construction and operation, decreased groundwater accretions to nearby rivers, surface water diversion for agriculture and evapotranspirative loss of a fraction of this volume, additional surface water imports from the Trinity River basin, channelization and reduced evapotranspirative loss in the floodplain, and contribution of drainage water from deeper groundwater pumped for irrigation and municipal use. These are largely anthropogenic changes, because the underlying precipitation did not show statistically significant changes over this period.

Combining the insight from the Delta water balance, where inflows and exports were the main contributors, with the above summary for the Sacramento Valley, allows for the development of an explanation of the overall changes that have occurred in the Delta outflow

on an annual and monthly basis. Slopes in the flow terms are used in the discussion below, and it is noted when they are statistically significant or non-significant. While statistically significant changes are clearly of greater weight, non-significant changes are also considered in the evaluation, because from a water balance standpoint, they can have downstream effects, albeit not as strong as statistically significant changes.

- **Annual flows:** Beginning upstream, the Four River inflow and Minor Rim inflow data suggest an increase in the annual flows in the pre-Project period, which is associated with an increase in the Sacramento Valley inflows to the Delta, and to a small increase in Delta outflows (of these, only the Four River inflow increase is significant). In the post-Project period, there is a decrease in the Four River annual flow, a decrease in the Sacramento Valley inflows to the Delta, and a small decrease in Delta outflows. None of these changes are significant, but may be considered related. The upstream changes may be attributable to an increase in the precipitation over the pre-Project period and a decrease in the post-Project period, which is reflected in the Four River Index (both are non-significant). Over the full record, there are increases in the Four River inflow, Minor Rim inflow, and Sacramento Valley inflow, but a decrease in the Delta outflow (although all these changes are non-significant). The decrease in the Delta outflow may be indicative of the effect of exports and net channel depletions.
- **Winter flows (December through February):** The Four River inflows and the Minor Rim inflows indicate increases in the pre-Project period, which is associated with a similar increase in the Sacramento Valley inflows to the Delta, and Delta outflows (none of these changes is significant). In the post-Project period, there are decreases in the Four River annual flow, Minor Rim inflows, Sacramento Valley inflows to the Delta, and Delta outflows (none of these changes are significant). Over the full record, the upstream flow trends are mixed, with non-significant increases and decreases, but the Delta outflow shows decreases in all months, including a significant decrease in February.
- **Spring flows (March through May):** The Four River inflow data indicate mixed results and the Minor Rim inflows indicate increases in the pre-Project period. The Sacramento Valley inflows to the Delta show mixed slopes and Delta outflows show decreases in the pre-Project period (these changes are not significant). Decreases in the Delta outflow in this period may be indicative of net channel depletions. In the post-Project period, there are mixed results in the Four River annual flow, Minor Rim inflows, Sacramento Valley inflows to the Delta, and Delta outflows (none of these changes is significant). Over the full record, there are statistically significant decreases in the Four River inflow, and mixed results in the Minor Rim inflows. The Sacramento Valley flows to the Delta, however, show significant decreases, as do the Delta outflows.
- **Summer flows (June through August):** The Four River inflow data and the Minor Rim inflows both indicate strong statistically significant increases in the pre-Project period. The Sacramento Valley inflows to the Delta and Delta outflows also show statistically significant increases in this period. Importantly, these changes predate the completion of the CVP and SWP but may indicate the continuing addition of reservoir capacity. In the post-Project period, there are mixed results in the Four River annual flow, Minor Rim inflows, Sacramento Valley flows to the Delta, and Delta outflows (almost no significant changes). Over the full record, the effect of the pre-

Project period on the trends is apparent and there are statistically significant positive trends in all of the flow components discussed here, particularly for July and August.

- **Fall flows (September through November):** The Four River inflow data indicate significant increases in the pre-Project period, which are also observable in the Sacramento Valley inflows to the Delta and in the Delta outflows. In the post-Project period, there are significant decreases in the Four River annual flow, Minor Rim inflows, Sacramento Valley inflows to the Delta, and Delta outflows (significant changes in two of three months). Over the full record, the Four River inflows indicate significant increases in all three months, which are apparent in the Sacramento Valley inflows to the Delta as well. However, Delta outflows show negative trends (in October and November based on DAYFLOW estimates). The decreases, even as inflows show some increases, may be related to exports and net channel depletions occurring in the Delta.

The above discussion highlights trends in the key surface water flows which have the greatest year to year variability, although it can be seen from the scatterplots developed for the water balance in the Delta and Sacramento Valley that a full picture needs to consider additional flow terms, including the Trinity Imports, groundwater-surface water exchange, surface water diversions and resulting runoff, groundwater irrigation and drainage to surface water, and valley floor precipitation and resulting runoff. These scatterplots were shown to provide a reasonably complete attribution of flows by month and on an annual basis across the WY 1922-2009 study period.

Some effects of climate change are apparent in the Four River Index data, indicative of earlier peak runoff over the study period. However, the effect of this change is completely masked downstream by the reservoir operations which determine the Four River inflow. Although future climate change may be more consequential in terms of the effect on runoff in the Sacramento River watershed, it is important that the effects of the small temperature change in the past century are discernible in selected observations we have. It should be emphasized that the flow trends seen downstream of the reservoirs, i.e., in most stations in this study, have not meaningfully been affected by global temperature change to this point.

This work built upon a robust database of hydrologic data from different sources and allowed application of a formal statistical methodology to evaluate changes across time and at various points in the watershed. A reasonably clear picture emerges from this analysis. Statistically significant changes in monthly flows have taken place in the major flows including Delta outflows, Sacramento Valley inflows to the Delta, and Four River inflow (particularly increases in the summer and early fall months, and decreases in spring flows). However, for these same flow terms we found few statistically significant *annual* flow trends. This can be explained by the movement of flows among seasons (from spring to summer), and because the flows in summer are small, a change in summer flows may have a small effect on annual flows. More broadly, the finding of a lack of trends in annual streamflows is counterintuitive because water demands throughout the basin have increased over the study period used here. A closer look at the trend test results shows that the trends in some of the annual flows, especially the Delta outflow and the Sacramento Valley inflow to the Delta, as reported through the Sen Slope, are indeed negative, but not statistically significant. In other words, the large natural variability in the key flows masks the relatively small decline that has occurred over the period of record. Despite the absence of significant annual trends, from the standpoint of regulation and water resources management, trends in individual monthly

flows are important with consequences for salinity intrusion in the San Francisco Estuary. The modeling framework developed under separate contract provided an independent approach to understand the causes of the observed trends and was especially helpful for interpreting the Sacramento Valley water balance.

This page intentionally left blank.



## 7 REFERENCES

---

- Abghari, H., Tabari, H. and Talaei, P.H. (2013). River flow trends in the west of Iran during the past 40 years: Impact of precipitation variability, *Global and Planetary Change*, Vol. 101, pp. 52–60. DOI: 10.1016/j.gloplacha.2012.12.003.
- Arnell, N.W. (2011). Uncertainty in the relationship between climate forcing and hydrological response in UK catchments. *Hydrology and Earth System Sciences* 15, 897–912. doi:10.5194/hess-15-897-2011.
- Bawden, A.J., Linton, H.C., Burn, D.H., Prowse, T.D. (2014). A spatiotemporal analysis of hydrological trends and variability in the Athabasca River region, Canada, *Journal of Hydrology*, Vol. 509, 333–342. doi:10.1016/j.jhydrol.2013.11.051.
- Boé, J., and Habets, F., (2014). Multi-decadal river flow variations in France. *Hydrology and Earth System Sciences*, Vol. 18, 691–708. doi:10.5194/hess-18-691-2014.
- Brush, C. F., Dogrul, E. C. and Kadir, T. N. (2013). Development and Calibration of the California Central Valley Groundwater-Surface Water Simulation Model (C2VSim), version 3.02-CG. Tech. rep. California Department of Water Resources.
- California Department of Water Resources (1995). Estimation of Delta Island Diversions and Return Flows. Tech. rep. URL: [http://www.calwater.ca.gov/Admin\\_Record/C-032892.pdf](http://www.calwater.ca.gov/Admin_Record/C-032892.pdf).
- Cayan, D. R., Dettinger, M. D., Diaz, H. F., and Graham, N. E. (1998). Decadal variability of precipitation over western North America. *Journal of Climate*, 11(12), 3148-3166.
- Chen, J., Wu, X., Finlayson, B. L., Webber, M., Wei, T., Li, M., and Chen, Z. (2014). Variability and trend in the hydrology of the Yangtze River, China: Annual precipitation and runoff, *Journal of Hydrology*, Vol. 513, pp. 403–412. DOI: 10.1016/j.jhydrol.2014. 03.044.
- Chen, Z. and Grasby, S.E. (2009). Impact of decadal and century-scale oscillations on hydroclimate trend analyses,” *Journal of Hydrology*, Vol. 365.1, pp. 122–133. DOI: 10.1016/j.jhydrol.2008. 11.031.
- Cleveland, R.B., Cleveland, W.S., McRae, J.E., Terpenning, I., (1990). STL: A seasonal-trend decomposition procedure based on loess. *Journal of Official Statistics*, Vol. 6, 3–73.
- Déry, S. J., Hernández-Henríquez, M. A., Owens, P. N., Parkes, M. W., & Peticrew, E. L. (2012). A century of hydrological variability and trends in the Fraser River Basin, *Environmental Research Letters*, Vol. 7.2, p. 024019. DOI: 10.1088/1748-9326/7/2/024019.
- Dettinger, M. D and Cayan, D.R. (2003). Interseasonal covariability of Sierra Nevada streamflow and San Francisco Bay salinity,” *Journal of Hydrology*, Vol. 277.3–4, pp. 164–181. DOI: 10.1016/S0022-1694(03)00078-7.
- Enright, C. and Culberson, S.D. (2009). Salinity trends, variability, and control in the northern reach of the San Francisco Estuary, *San Francisco Estuary and Watershed Science*, Vol. 7.2. URL: <http://escholarship.org/uc/item/0d52737t>.

- Fox, J. P., Mongan, T R., and Miller, W.J. (1990). Trends in freshwater inflow to San Francisco Bay from the Sacramento-San Joaquin Delta, *Journal of the American Water Resources Association*, Vol. 26.1, pp. 101–116.
- Fox, P., Hutton, P. H., Howes, D. J., Draper, A. J., and Sears, L. (2015). Reconstructing the natural hydrology of the San Francisco Bay-Delta watershed. *Hydrology and Earth System Sciences*, Vol. 19, 4257-4274, doi:10.5194/hess-19-4257-2015.
- Gudmundsson, L., Tallaksen, L.M., Stahl, K., Fleig, A.K. (2011). Low-frequency variability of European runoff, *Hydrology and Earth System Sciences* Vol. 15, 2853–2869. doi:10.5194/hess-15-2853-2011.
- Hannaford, J. (2015). Climate-driven changes in UK river flows: A review of the evidence, *Progress in Physical Geography*, Vol. 39.1, pp. 29–48. DOI: 10.1177/0309133314536755.
- Hannaford, J., Buys, G., Stahl, K., & Tallaksen, L. M. (2013). The influence of decadal-scale variability on trends in long European streamflow records, *Hydrology and Earth System Sciences* Vol. 17.7, pp. 2717–2733. DOI: 10.5194/hess-17-2717-2013.
- He, Bin, Miao, C., and Shi, W. (2013). Trend, abrupt change, and periodicity of streamflow in the mainstream of Yellow River, *Environmental Monitoring and Assessment*, Vol. 185.7, pp. 6187–6199. doi: 10.1007/s10661-012-3016-z.
- Helsel, D. R. and Hirsch, R.M. (2002). *Statistical methods in water resources*. Vol. 323. Reston, VA: US Geological Survey. URL: <http://pubs.usgs.gov/twri/twri4a3/pdf/twri4a3-new.pdf>.
- Hidalgo, H.G., Das, T., Dettinger, M.D., Cayan, D.R., Pierce, D.W., Barnett, T.P., Bala, G., Mirin, A., Wood, A.W., Bonfils, C. and Santer, B.D. (2009). Detection and Attribution of Streamflow Timing Changes to Climate Change in the Western United States, *Journal of Climate*, Vol. 22.13, pp. 3838–3855. doi: 10.1175/2009JCLI2470.1.
- Hirsch, R. M, Slack, J.R., and Smith, R.A. (1982). Techniques of trend analysis for monthly water quality data, *Water Resources Research* 18.1, pp. 107–121. doi: 10.1029/WR018i001p00107.
- Hutton, P.H., Rath, J.S., Chen, L., Unga, M.J., and Roy, S.B. (2015) Nine Decades of Salinity Observations in the San Francisco Bay and Delta: Modeling and Trend Evaluation. *ASCE Journal of Water Resources Planning and Management*. doi: [http://dx.doi.org/10.1061/\(ASCE\)WR.1943-5452.0000617](http://dx.doi.org/10.1061/(ASCE)WR.1943-5452.0000617).
- Jassby, A.D., Kimmerer, W.J., Monismith, S.G., Armor, C., Cloern, J.E., Powell, T.M., Schubel, J.R., and Vendlinski, T.J. (1995). Isohaline Position as a Habitat Indicator for Estuarine Populations. *Ecological Applications*, Vol. 5: 272–289.
- Jiang, T., Su, B., and Hartmann, H. (2007). Temporal and spatial trends of precipitation and river flow in the Yangtze River Basin, 1961–2000, *Geomorphology*, Vol. 85.3, pp. 143–154. doi: 10.1016/j.geomorph.2006.03.015.
- Karlsson, I. B., Sonnenborg, T. O., Jensen, K. H., & Refsgaard, J. C. (2014). Historical trends in precipitation and stream discharge at the Skjern River catchment, Denmark, *Hydrology and Earth System Sciences* 18.2, pp. 595–610. doi: 10.5194/hess-18-595-2014.
- Kelly, M.H., Gore, J.A. (2008). Florida river flow patterns and the Atlantic multidecadal oscillation. *River Research and Applications* 24, 598–616. doi:10.1002/rra.1139.
- Kendall, M. G. (1938). A New Measure of Rank Correlation, *Biometrika*, Vol 30.1/2, pp. 81–93. doi: 10.2307/2332226.

- Knowles, N. (2002). Natural and management influences on freshwater inflows and salinity in the San Francisco Estuary at monthly to interannual scales, *Water Resources Research*, Vol. 38.12, pp. 25–1.
- Koutsoyiannis, D. (2003). Climate change, the Hurst phenomenon, and hydrological statistics. *Hydrological Sciences Journal* 48, 3–24. doi:10.1623/hysj.48.1.3.43481.
- Lorenzo-Lacruz, J., Vicente-Serrano, S. M., López-Moreno, J. I., Morán-Tejeda, E., & Zabalza, J. (2012). “Recent trends in Iberian streamflows (1945–2005)”. In: *Journal of Hydrology* 414, pp. 463–475. doi: 10.1016/j.jhydrol.2011.11.023.
- Mann, H. B. (1945). Nonparametric Tests Against Trend, *Econometrica*, Vol. 13.3, pp. 245–259. doi: 10.2307/1907187.
- Massei, N., Fournier, M. (2012). Assessing the expression of large-scale climatic fluctuations in the hydrological variability of daily Seine river flow (France) between 1950 and 2008 using Hilbert-Huang Transform. *Journal of Hydrology*, Vol. 448, 119–128. doi:10.1016/j.jhydrol.2012.04.052
- MWH Global (2015). *Evolution of river flows in the Sacramento and San Joaquin Valleys*. Tech. rep. Metropolitan Water District of California.
- Pal, I., Lall, U., Robertson, A.W., Cane, M.A., Bansal, R. (2012). Predictability of Western Himalayan River flow: melt seasonal inflow into Bhakra Reservoir in Northern India. *Hydrology and Earth System Sciences Discussions*, Vol. 9, 8137–8172. doi:10.5194/hessd-9-8137-2012.
- Sen, P.K., 1968. Estimates of the regression coefficient based on Kendall’s tau. *Journal of the American Statistical Association* 63, 1379–1389. doi:10.1080/01621459.1968.10480934.
- Shamsudduha, M., Chandler, R.E., Taylor, R.G., Ahmed, K.M. (2009). Recent trends in groundwater levels in a highly seasonal hydrological system: The Ganges-Brahmaputra-Meghna delta. *Hydrology and Earth System Sciences*, Vol. 13, 2373–2385. doi:10.5194/hess-13-2373-2009.
- Sharif, M., Archer, D. R., Fowler, H. J., and Forsythe, N. (2013). “Trends in timing and magnitude of flow in the Upper Indus Basin”. In: *Hydrology and Earth System Sciences* 17.4, pp. 1503–1516. doi: 10.5194/hess-17-1503-2013.
- Siegel, S. and N.J. Castellan (1988). *Nonparametric Statistics for the Behavioral Sciences*. McGraw-Hill International, pp. 213–214.
- Viviroli, D., Schädler, B., Schmocker-Fackel, P., Weiler, M., Seibert, J. (2012). On the risk of obtaining misleading results by pooling streamflow data for trend analyses. *Water Resources Research*, Vol. 48. doi:10.1029/2011WR011690.
- Wood, S. (2006). *Generalized additive models: an introduction with R*. CRC press.
- Zhang, Y., Shao, Q., Xia, J., Bunn, S.E., Zuo, Q. (2011). Changes of flow regimes and precipitation in Huai River Basin in the last half century. *Hydrological Processes*, Vol. 25, 246–257. doi:10.1002/hyp.7853